DISSERTATIONES
CHIMICAE
UNIVERSITATIS
TARTUENSIS
170

HEDI RAHNEL

ARC-inhibitors: from reliable biochemical assays to regulators of physiology of cells

DISSERTATIONES CHIMICAE UNIVERSITATIS TARTUENSIS
170

DISSERTATIONES CHIMICAE UNIVERSITATIS TARTUENSIS
170

HEDI RAHNEL

ARC-inhibitors: from reliable biochemical assays to regulators of physiology of cells

UNIVERSITY OF TARTU
Press

Institute of Chemistry, Faculty of Science and Technology, University of Tartu, Estonia

Dissertation is accepted for the commencement of the degree of *Doctor philosophiae* in Chemistry on 29th of March, 2018 by the Council of Institute of Chemistry, Faculty of Science and Technology, University of Tartu

Supervisors: Asko Uri, PhD
Institute of Chemistry, University of Tartu, Estonia

Kaido Viht, PhD
Institute of Chemistry, University of Tartu, Estonia

Opponent: Maria Ruzzene, associate professor
Department of Biomedical Sciences, University of Padova, Italy

Commencement: June 11th, 2018 at 14:00, room 1020, 14A Ravila St., Institute of Chemistry, University of Tartu

ISSN 1406-0299
ISBN 978-9949-77-736-5 (print)
ISBN 978-9949-77-737-2 (pdf)

University of Tartu Press
www.tyk.ee

TABLE OF CONTENTS

LIST OF ORIGINAL PUBLICATIONS

1. M. Kriisa, **H. Sinijärv**, A. Vaasa, E. Enkvist, S. Kostenko, U. Moens, A. Uri, Inhibition of CREB Phosphorylation by Conjugates of Adenosine Analogues and Arginine-Rich Peptides, Inhibitors of PKA Catalytic Subunit, ChemBioChem. 16 (2015) 312–319. doi:10.1002/cbic.201402526.
2. K. Viht, S. Saaver, J. Vahter, E. Enkvist, D. Lavogina, **H. Sinijärv**, G. Raidaru, B. Guerra, O.G. Issinger, A. Uri, Acetoxymethyl Ester of Tetrabromobenzimidazole-Peptoid Conjugate for Inhibition of Protein Kinase CK2 in Living Cells, Bioconjug. Chem. 26 (2015) 2324–2335. doi:10.1021/acs.bioconjchem.5b00383.
3. **H. Sinijarv**, S. Wu, T. Ivan, T. Laasfeld, K. Viht, A. Uri, Binding Assay for Characterization of Protein Kinase Inhibitors Possessing Sub-Picomolar to Sub-Millimolar Affinity, Anal. Biochem. 531 (2017) 67–77. doi:10.1016/j.ab.2017.05.017.
4. **H. Rahnel,** K. Viht, D. Lavogina, O. Mazina, T. Haljasorg, E. Enkvist, A. Uri, Selective Biligand Inhibitor of CK2 Increases Caspase-3 Activity in Cancerous Cells and Inhibits Platelet Aggregation, ChemMedChem. 12 (2017) 1723–1236. doi:10.1002/cmdc.201700457

Author's contribution:

Paper 1: The author performed the viability assays, participated in data analysis and writing of the manuscript.

Paper 2: The author performed the viability assays, participated in data analysis and writing of the manuscript.

Paper 3: The author designed the experiments, performed data analysis, designed the online toolbox, and wrote the manuscript.

Paper 4: The author participated in the design of the compounds, purified and analysed the compounds, designed the experimental setup, performed the experiments, and wrote the bulk of the manuscript.

ABBREVIATIONS

$[I]_{50}$	concentration of the *free* inhibitor at 50% inhibition; also, concentration of the *free* inhibitor that reduces the TGLI of the probe:PK complex by half; also, the concentration the *free* inhibitor when 50% displacement has occurred
ARC	biligand inhibitor or probe for protein kinases designed in Asko Uri´s research group at the University of Tartu
ARC(Photo)	ARC labelled with a fluorescent dye; photoluminescent probe, including ARC-Fluo and ARC-Lum(Fluo) probes
ARC-Fluo	ARC-probe comprising a non-phosphorescent heteroaromatic fragment and a fluorescent dye
ARC-Lum(Fluo)	ARC-probe incorporating a phosphorescent heteroaromatic fragment and fluorescent dye; the probe possesses protein binding-induced photoluminescence with microsecond-scale decay time
ATB	4-(2-amino-1,3-thiazol-5-yl)benzoic acid
CASP3	cysteine-aspartic acid protease caspase 3
CHO cells	Chinese hamster´s ovary cells
CPP	cell-penetrating peptide
CREB	cAMP response element-binding transcription factor
GPCR	G-protein coupled receptor
FA	fluorescence anisotropy
FACS	fluorescence-activated cell sorting
FCS	fluorescence correlation spectroscopy
FI	fluorescence intensity
FRET	Förster resonant energy transfer
HeLa cells	cervical cancer cells from Henrietta Lacks
HTS	high-throughput screening
IC_{50}	the *total* concentration of the inhibitor that reduces the TGLI of the probe:PK complex by half; also, the *total* concentration the inhibitor when 50% displacement has occurred
Ida	iminodiacetic acid
K_d	dissociation constant
LoK_d	limit of dissociation constant determination
LoQ	limit of quantification
MA	maximum aggregation
MALDI-TOF MS	matrix-assisted laser desorption/ionization time-of-flight mass spectrometer
MDCK cells	Madin-Darby canine kidney cells
PC-3 cells	human prostate cancer cells
PK	protein kinase
PPC-1 cells	human prostate cancer cells

RP-HPLC-FL	reverse phase HPLC with a fluorescence detector
RSD	relative standard deviation
SD	standard deviation
TBBz	4,5,6,7-tetrabromo-1*H*-benzimidazole
TGLI	time-gated measurement of luminescence intensity [luminescence intensity as measured in a defined period of time (time gate) after excitation of the luminophore with a pulse electromagnetic radiation]

1. INTRODUCTION

Human cell is a complex biological system comprising a wide variety of molecules, each playing its own role in the life cycle of a cell. Members of 540-protein kinase (PK) superfamily catalyse the transfer of a small phosphoryl group from ATP to the target protein. This minor change in the chemical structure of the target protein affects most of the signalling pathways and, consequently, vital processes in the cell.

Aberrant activity of PKs is the cause or result of several diseases: from cardiovascular diseases and different cancers to Alzheimer´s disease. Although PKs were considered to be potential drug targets already since their discovery in the 1950-s, the related research started to widen rapidly in the 1990-s and has not shown signs of extinction. During the years, the knowledge on the structure of PKs has supported the design of new inhibitors – regulators of the activity of PKs. Recently, the biligand approach of the design of inhibitors has gained attractiveness due to concurrent higher affinity and selectivity.

Request for inhibitors regulating the activity of PKs and photoluminescent probes for studying signalling cascades mediated by PKs has driven the development of reliable analysis techniques. In this thesis, we introduce two methods. The first method is a binding assay for characterization of PK inhibitors possessing affinities in a wide range. The assay is based on the application of a non-metal PK binding-responsive photoluminescent ARC-Lum(Fluo) probe with unique photoluminescent properties. The second, HPLC-based method was used for determination of the concentration of potent biligand inhibitors and probes of PKs in cells. Unlike most cellular assays, the HPLC method described here affords the presentation of cellular uptake as concentration of the inhibitor in molar units that makes possible the comparison of analytical results for different cells and the data originating from different research groups.

Besides the development of aforementioned analysis techniques, our other aim was the design of selective and potent biligand inhibitors for regulation and examination of signalling pathways that proceed with participation of CK2 or PKAc. Various strategies to enhance the cellular uptake of inhibitors were compared by the means of achieved intracellular concentration of inhibitor and intracellular availability. The inhibitory potency of the internalized biligand inhibitor was demonstrated by its effect on the phosphorylation levels of substrate proteins or on the signalling pathways related to the target kinase. The results support the applicability of biligand inhibitors for the development of drug candidates or research tools for studying the role of PKs in signalling pathways.

2. LITERATURE OVERVIEW

2.1. PROTEIN KINASES

The discovery of a PK in 1954 revealed the feasibility of enzyme-catalysed phosphorylation of proteins in cells (Burnett and Kennedy 1954). The following identification of several PKs made possible the establishment of their participation in signal transduction pathways and disease mechanisms (Hunter 2000). The transfer of a small structural fragment, the γ-phosphoryl group from ATP (or GTP in rare cases, *e.g.*, CK2-catalysed reactions) to the substrate protein plays an important role in, *e.g.*, the regulation of activity and trans-localisation of the protein, and therefore, guidance of various cellular processes. The importance of PKs could be also illustrated by the incidence of corresponding genes: more than 500 genes encoding PKs (Manning *et al.* 2002) make up approximately 2.6% of the whole human genome. Here, we will concentrate on two remarkable kinases. CK2 – the earliest PK that was discovered and the PK responsible for phosphorylating speculatively 20% (Salvi *et al.* 2009) among 13000 phosphorylateable proteins in human (Vlastaridis *et al.* 2017). Second, protein kinase A (PKA) – PK of which the first three-dimensional structure was determined (Knighton *et al.* 1991) and which has been also the most thoroughly studied PK since its discovery. Both of these PKs exist in a tetrameric complex and they are also ubiquitous, nevertheless, their roles and mechanisms are rather different.

2.1.1. PKA

PKA, also known as cAMP-dependent PK, belongs to the AGC group of PKs (Manning *et al.* 2002). AGC kinases are mostly basophilic enzymes as they catalyse phosphorylation of substrate proteins comprising basic amino acid residues (Arg and Lys) near the phosphorylatable Ser or Thr residue (Pearce *et al.* 2010). The inactive PKA exists as a tetrameric holoenzyme comprising a dimer of two regulatory subunits (PKAr, with four isoforms: rIα, rIβ, rIIα, and rIIβ) and two catalytic subunits (PKAc, with three main isoforms: α, β, γ). Whereas, the proteins PKAcα and PKAcβ are the most extensively studied isoforms of PKAc possessing the highest catalytic activity in human cells (Søberg *et al.* 2013). There are two other, less studied, kinases related to PKA: protein kinase X (PRKX) and Y-linked protein kinase (PRKY) (Pearce *et al.* 2010). The function of both proteins has yet to be established.

The substrate consensus sequence of the PKAc is Arg-Arg-X-Ser-X, where X is any amino acid residue (Poteet-Smith *et al.* 1997). PKAc (often α isoform) is a protein that is simple to produce and it is often used as a model for other PKs (Taylor *et al.* 2012).

The classical activation mechanism of PKAc is prompted when extracellular stimulation induces the formation of cAMP. Thereafter, four molecules of this

second messenger bind to the PKAr dimer leading to the release of PKAc (Skålhegg and Taskén 1997). Active PKAc can diffuse to different cellular compartments and modify functions of various proteins. For example, phosphorylating cAMP response element-binding transcription factor (CREB) regulates gene transcription [Figure 1, (Shabb 2001)]. The specificity of PKA signalling is also affected by the subcellular localization of PKA. The compartmentalization of PKA is largely regulated by A-kinase anchoring proteins (AKAPs) (Wong and Scott 2004; Pidoux and Taskén 2010).

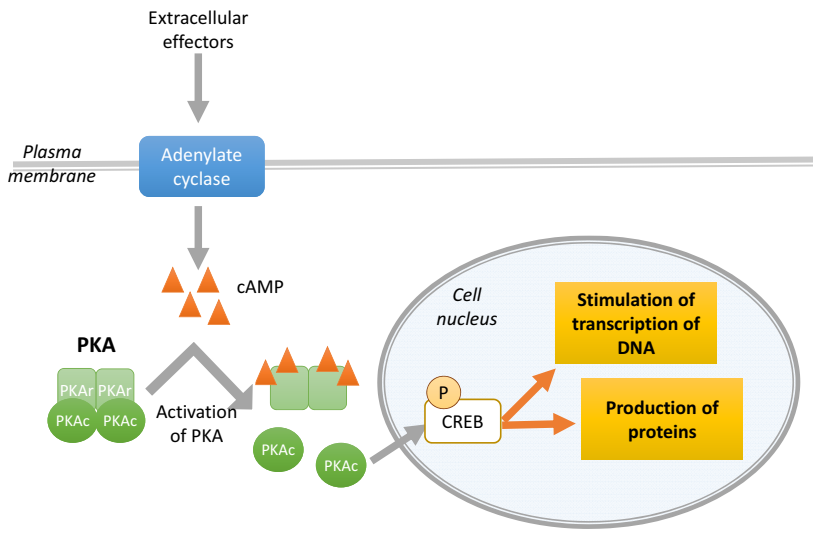

Figure 1. Classical scheme of activation of PKAc and phosphorylation of CREB at Ser133. Phosphorylation activates CREB which induces the transcription of DNA and production of proteins.

Due to the salient role of PKAc in normal physiology, it is expected that dysregulation of PKAc in disease has been also an interest of research (Esseltine and Scott 2013). For example, progressive and congestive heart failure, also onset of certain arrhythmias have been linked to dysregulated phosphorylation by PKA (Chen *et al.* 2008; McKinsey and Olson 2005). Besides cardio diseases, PKA has been also linked to other conditions, *e.g.* the Cushing´s disease, which is caused by excess of glucocorticoid production in adrenocortical tumours (Lacroix *et al.* 2015). Studies have revealed that in case of the Cushing´s disease the reason for higher basal activity of PKA is caused by the mutation of the gene encoding PKAcα (Di Dalmazi *et al.* 2014).

Higher levels of PKA activity in blood serum of cancer patients (*e.g.,* breast, colon, renal, rectal, prostate, lung, adrenal carcinoma, and lymphoma) has been reported (Cho *et al.* 2000; Cvijic *et al.* 2000; Kita *et al.* 2004; Wang *et al.* 2007; Moody *et al.* 2014). These instances reveal that PKA can be used as a drug target for various diseases, but also as a biomarker for cancer (Moody *et al.*

2014). A successful example is an anti-cancer drug AT13148 that inhibits PKA and other AGC-group PKs, and which has been taken into clinical trials (Yap *et al.* 2012).

2.1.2. CK2

Similarly to PKA, CK2 is also composed of two catalytic subunits (α or α') and two regulatory (β) subunits, and the formula of heterotetramer could be either $\alpha_2\beta_2$, $\alpha'_2\beta_2$, or $\alpha'\alpha\beta_2$. Unlike PKAc, CK2α (and CK2α') is enzymatically active separately and also within the tetrameric complex. Furthermore, although the phosphorylation of enzymes often acts as an on/off switch, the activity of catalytic subunit of CK2 is not related to its phosphorylation status. Thereby, not activity, but the selection of substrate of CK2 is regulated by the means of its localization, phosphorylation, and protein-protein interactions. For example, the phosphorylation of the subunits of CK2 by Cdk1 in a cell cycle-dependent manner controls the functional specificity of CK2 due to different protein-protein interactions (Litchfield *et al.* 1991).

In 2009 it was estimated that *circa* 20% of protein phosphorylations are performed by CK2 (Salvi *et al.* 2009). However, a recent study postulates that this evaluation may be an over-estimation. The results of comparative SILAC (stable isotope labeling with amino acids in cell culture) phosphoproteomics analyses indicated that only 10% of the phosphosites were reduced by CK2α or CK2α' negative cells, consistent with their generation by CK2 (Franchin *et al.* 2017a). Nevertheless, the role of CK2 in overall phosphoproteome could not be overemphasized.

Analysing the possibility for such pleiotropy leads to the structure of the substrate binding pockets. The nucleotide-binding pocket makes CK2 eminent in many ways. First of all, CK2 is currently known to be the only PK capable of efficient transferring of the γ-phosphoryl group of ATP and GTP (Rodnight and Lavin 1964; Becher *et al.* 2013). Secondly, due to the presence of larger amino acid residues in the nucleotide binding site, the pocket is slightly more open yet smaller compared to most PKs (Niefind *et al.* 1999; Cozza *et al.* 2010). The protein/peptide binding pocket affects negatively charged proteins and peptides. Namely, CK2 is an acidophilic serine/threonine kinase that catalyses phosphorylation of proteins with a consensus sequence of S/T-X-X-D/E/pS/pY, where X is any amino acid residue, and it also exhibits tyrosine kinase activity in mammalian cells (Vilk *et al.* 2008). The consensus sequence is usually complemented with additional acidic residues (Marin *et al.* 1986; Salvi *et al.* 2009). The small consensus sequence present in a large number of phosphorylatable proteins relates the kinase to almost every signalling pathway in a cell. For example, CK2-catalysed phosphorylation of Hsp90 and Cdc37 regulates protein folding (Figure 2.A), MAP2K2 and MEN1 dictate cell growth and proliferation, MDC1 and RAD51 have been related to DNA damage response, and cysteine-aspartic acid protease caspase 3 (CASP3) and PTEN to apoptosis [Figure 2.B (Rabalski *et al.* 2016)]. Notably, upon activation of caspases

approximately 14% of the kinome is cleaved (Duncan *et al.* 2011; Lüthi and Martin 2007). Although it was known earlier that CK2 regulates the activity of CASP3, it was just recently demonstrated that CK2α′ plays the most important role in regulation of activity of the protease (Turowec *et al.* 2013).

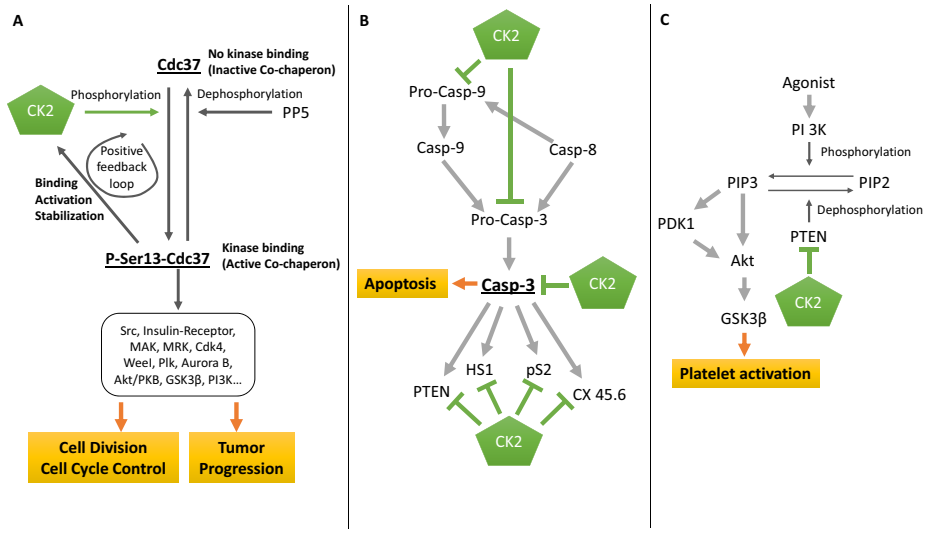

Figure 2. Role of CK2 in signalling pathways. **A)** Phosphorylation of kinase-specific co-chaperone Cdc37 is critical for binding of PKs and for activity of chaperone. Active Cdc37 cooperates with Hsp90 (heat shock protein 90) to assist in the correct folding and functions of many signalling PKs. CK2 itself is also a client of Cdc37, and Cdc37 is required for optimal activity of CK2, thus these proteins together are forming a positive regulatory feedback loop. In conclusion, CK2 mediated regulation of the activity of Cdc37 has an important role in cell division, cell cycle control, but also tumour progression. The scheme is adapted from Ref. (Pinna 2013). **B)** The role of CK2 in the control of cell survival/apoptosis via caspase pathways. First, the phosphorylation of procaspase-3/9 (Pro-CASP3, Pro-CASP9) protects them from cleavage by caspase-8 (CASP8); phosphorylation of procaspase-9 (Pro-CASP9) prevents the formation of CASP9. These events, in turn, prevent the activation of CASP3. Second, the phosphorylation of CASP3 directly inactivates it. Third, the phosphorylation of the targets of CASP3 [e.g., HS1 (actin-regulatory adaptor protein), CX 45.6 (gap junction-forming protein, connexin 45.6), pS2 (estrogen inducible protein), and PTEN (phosphatase and tensin homolog)] prevents the cleavage of these prosurvival proteins by CASP3 (Pinna 2013; Turowec et al. 2013). **C)** CK2 plays an important role in agonist-induced platelet activation through the regulation of PI 3K (phosphatidylinositol-4,5-bisphosphate 3-kinase) pathways. CK2-mediated inhibition of PTEN leads to activation of downstream targets of the PI 3K pathways including PDK1 (3-phosphoinositide-dependent protein kinase-1), Akt (protein kinase B), and GSK3β (glycogen synthase kinase 3 beta). The scheme is adapted from Ref. (Ryu and Kim 2013).

CK2 is a pleiotropic, constitutive active PK that plays important roles in many cellular processes [reviewed in (Guerra and Issinger 2008)]. Aberrant CK2 activity has been associated with a number of diseases. Most often, the role of CK2 in progression of cancer has been acknowledged (Ortega *et al.* 2014). The latter is not unanticipated, first because CK2 regulates numerous processes that are essential for cancer development (Rabalski *et al.* 2016). Second, cancerous cells express high level of CK2 of which they are addicted to (Ruzzene and Pinna 2010). As a significant proportion of substrates of CK2 is involved in cell death and survival, CK2 is a potential target for treatment of cancer (Trembley *et al.* 2017; Ahmad *et al.* 2007).

CK2 also plays a role in the non-cancer diseases. For example, CK2 is a regulator of thrombus formation, affecting multiple interactions of platelets, leukocytes and endothelial cells (Ampofo *et al.* 2015). Nakanishi *et al.* reported in 2008 that stimulation of platelets with PAR1-activating peptide and thrombin resulted in an increase in the activity of CK2. Ryu *et al*. confirmed the role of CK2 in platelet aggregation by regulating the expression level of phosphorylated PTEN, and, in turn, PI 3K-dependent signalling (Figure 2.C). Inhibition of CK2 leads to down-regulation of P-selectin and GPIIb/IIIa (Ampofo *et al.* 2015). As CK2 regulates multiple interaction mechanisms that mediate the activity of platelets, inhibition of CK2 may also contribute to the future treatment of diseases which accompany thrombosis.

2.2. PROTEIN KINASE INHIBITORS

PKs could be both, biomarkers for diagnosis of diseases in their early stages and targets for treatment of diseases. Evidently, there is an unmet need for methods and probes that enable comparative and quantitative analysis of blood samples for determination of abnormal levels of proteins. Equally important to aforementioned is to balance PKs in disease. PKs are well druggable, *i.e*., they possess protein folds that favour interactions with drug-like chemicals. 45 years after the discovery of first PK in 1954, the first PK inhibitor Trastuzumab was approved by the FDA (Baselga *et al.* 1998). This monoclonal antibody targeting receptor kinase ERBB2 is used for the treatment of ERBB2-overexpressed breast cancer, but also for gastric and gastroesophageal cancer (Okines and Cunningham 2012; Roukos 2010). Around twenty large molecule PK inhibitors have been approved by the FDA since (Gharwan and Groninger 2015). Two years after the approval of Trastuzumab, FDA also approved the first small molecule PK inhibitor Imatinib for treating chronic myelogenous leukaemia by targeting mainly tyrosine kinase BCR-Abl (Roskoski). More than 35 small-molecule PK inhibitors have received NDA approval as drugs in recent 16 years (Wu *et al.* 2015; Fabbro *et al.* 2015; Sharma *et al.* 2016; Rask-Andersen *et al.* 2014b).

According to PubMed database, the number of studies related to “PK drugs” have increased almost linearly during the past 30 years (Figure 3). PKs form the

largest category of drug candidates in clinical trials (Rask-Andersen *et al.* 2014b), which explains the continuous interest into this field by academic research groups. These results of PK studies were compared to these of G protein–coupled receptor research (GPCRs), as both account for approximately 20% of the established drug targeted portion of the genome (Rask-Andersen *et al.* 2014a). Despite similar druggability, the number of FDA approved drugs targeting GPCRs is approximately 15-fold larger, approaching 500 (Hauser *et al.* 2017), whereas nearly half of these were accepted before 1990 and less than 7% within past 6 years (Santos *et al.* 2016). The distinctive difference in the number of accepted drugs could be somewhat linked with the escalation of interest in GPCRs as drug targets approximately ten years before PKs. However the level of GPCR-related academic research has remained on the same level for the last 15 years according to PubMed search (Figure 3), which also coincides with the decreased number of approved drugs per year. The comparison of druggability of GPCRs and PKs as target proteins with the number of approved drugs and also with the number of related studies indicates that there is potential and space for more PK inhibitors in pharmaceutical industry and in academic research (Berndt *et al.* 2017).

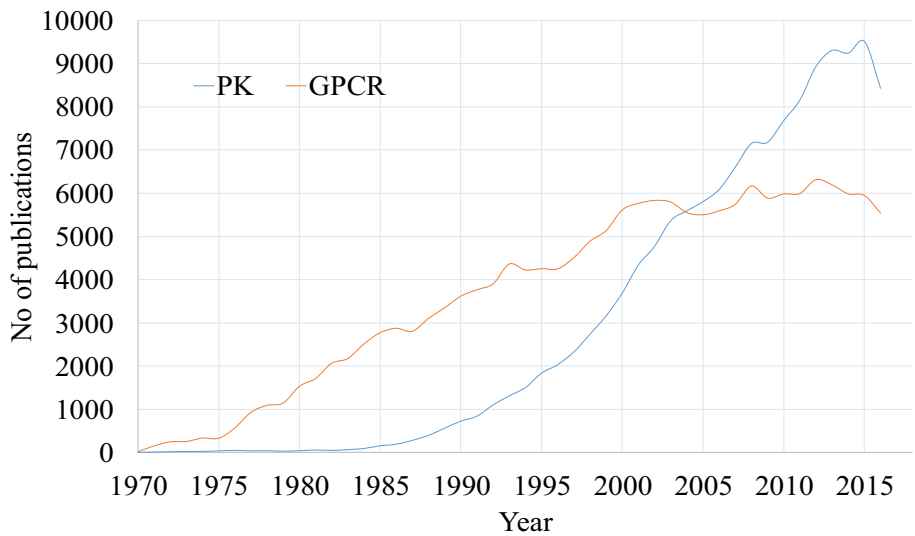

Figure 3. Number of publications related to phrase "protein kinase drug" and "G protein-coupled receptor drug" found in PubMed search engine.

The construction of inhibitors of PKs has been mainly focussed to nucleotide-competitive inhibitors. These small molecules mostly fulfil requirements of the Lipinski´s "Rule-of-five" (Lipinski *et al.* 1997), possess satisfactory inhibitory potency, and hold cell plasma membrane penetration properties. However, the

disadvantage of nucleotide-competitive inhibitors is the similarity of binding sites of the target kinase and more than other 3000 purine-binding proteins, which may lead to poor selectivity of the drug (Knapp *et al.* 2006; Haystead 2006). For example, the study by Karaman *et al.* demonstrated that Staurosporine inhibited 87% of tested PKs with binding constant value below 3 μM (Karaman *et al.* 2008). Nevertheless, there were also successful examples of ATP-competitive inhibitors disclosed in the paper, *e.g.,* Lapatinib whose main target is ERBB2, inhibited 1% of tested PKs (K_d < 3 μM). Lack of high selectivity against a specific target may be also beneficial for a kinase inhibitor that aims to become a useful drug. For instance, an inhibitor targeting simultaneously several PKs that regulate the survival of cancerous cells can be an effective tool to treat cancer. However, non-selective inhibitors could possibly give rise to undesirable side-effects and are not suitable for analysing the biological function of the given PK (Klaeger *et al.* 2017).

Structure of substrate protein binding pocket of PKs is less conserved, therefore construction of substrate-competitive inhibitors would lead to selective inhibitors. Structurally these inhibitors are usually peptides, therefore they often possess bad cellular uptake, intracellular instability, and low affinity for the target protein. For higher affinity peptide-type inhibitors should have large contact area with the target PK, therefore such peptides have higher molecular weight than small organic compounds binding to the ATP pocket of the kinase. For example, PKA inhibitor peptide alpha (PKIα), a 75 amino acid long peptide, inhibits PKAc with K_i value of 0.20 nM (Dalton and Dewey 2006). Several technologies (see paragraph 2.2.2) have been worked out for improving cellular uptake and stability of peptidic inhibitors (Bogoyevitch *et al.* 2005).

Bisubstrate analogue (biligand) inhibitors could overcome the selectivity and specificity issues related to two aforementioned inhibitor types (Cozza *et al.* 2015; Lavogina *et al.* 2010a; Parang and Cole 2002). The moieties of these inhibitors mimic two natural substrates that are conjugated into a single molecule via a suitable linker. Simultaneous association with two regions of the target kinase leads to synergistic effect on affinity, as the binding free energy could be equal to the sum of the free energies for each component and an additional energetic factor deriving from entropy or enthalpy decrease (Jencks 1981; Parang and Cole 2002). Various successful biligand inhibitors have been constructed, *e.g.,* conjugate of ATP-γS and a peptide substrate (Lys-Lys-Lys-Leu-Pro-Ala-Thr-Gly-Asp) possesses K_i value of 370 nM towards the core tyrosine kinase domain of the insulin receptor, cIRK (Parang *et al.* 2001); conjugate of isoquinoline sulfonamide-based H9 and $(L\text{-}Arg)_6$ peptide with IC_{50} of 3 nM towards PKAc (Ricouart *et al.* 1991); and currently the most potent inhibitor of PKAc, the conjugate of 4-(piperazin-1-yl)-7H-pyrrolo[2,3-d]pyrimidine, and $(D\text{-}Arg)_6$ peptide with K_d of 3 pM (Ivan *et al.* 2016).

2.2.1. ARC-Inhibitors

In recent years medicinal chemistry research group at the University of Tartu has focussed its research activities to the development of biligand inhibitors and probes (called ARC-inhibitors and ARC-probes, respectively) for PKs (Enkvist *et al.* 2006; Vahter *et al.* 2017). The design of inhibitors has been guided by extensive structure-affinity studies and X-ray analysis of inhibitor:PK co-crystals (Lavogina *et al.* 2009; Kestav *et al.* 2015). As a result, the affinity of several ARC-inhibitors towards PKs lies in the nanomolar to picomolar range (Ivan *et al.* 2016).

The biligand inhibitors of basophilic PKs are bifunctional compounds (Figure 4.A) that according to results of X-ray analysis of ARC:PK co-crystals associate simultaneously with binding sites of both substrates of the PK. On one hand, each fragment of the molecule is contributing to the total binding affinity of the compound. On the other hand, the oligo-arginine fragment acts as a cell-penetrating peptide (CPP; see paragraph 2.2.2) dragging the compound inside the cellular milieu (Uri *et al.* 2002; Räägel *et al.* 2009; Vaasa *et al.* 2010). The negatively charged ARCs targeting acidophilic PKs like CK2, however, require the application of a facilitated transport mechanism to penetrate the plasma membrane (Figure 4.B).

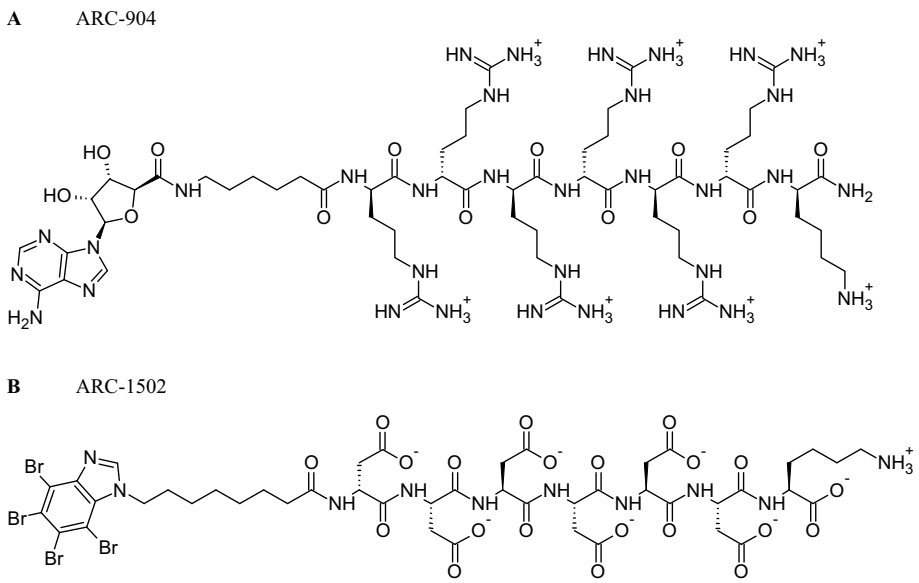

Figure 4. Structures of ARC-type inhibitors targeting **A)** basophilic kinase PKAc and **B)** acidophilic kinase CK2.

The cellular uptake of fluorescently labelled arginine-rich ARCs (ARC-Photo probes) has been demonstrated with microscopy imaging (Uri *et al.* 2002; Viht *et al.* 2003; Räägel *et al.* 2008; Lavogina *et al.* 2010b; Vaasa *et al.* 2009) and the efficacy/functionality of internalized ARC-inhibitors using several assays, *e.g.,* dissociation of cytoskeleton (Räägel *et al.* 2008), effect on parasitemia (Lavogina *et al.* 2014), and intervention in Haspin pathways (Kestav *et al.* 2015). The potential off-targets of basic ARCs are negatively charged proteins, or nucleic acids DNA and RNA, while for acidic ARCs compounds possessing high positive charge could restrict their implementation as specific inhibitors. Thus, the regulation and monitoring of the intracellular concentration and localisation of the compound is of crucial importance for development of inhibitors for cellular studies.

2.2.2. Methods for Cellular and Targeted Delivery

As mentioned earlier, PK inhibitors could be applied as drugs or as probes for studying involvement of PKs in signal transduction pathways or mapping the localization of PKs in cells. However, the cell plasma membrane often limits the uptake of inhibitors/probes. Several technologies have been described for supporting and directing the transport of these compounds into cell interior. For example, the application of CPPs has opened several new avenues for biomedical research and therapy (Frankel and Pabo 1988; Rothbard *et al.* 2000; Guidotti *et al.* 2017). Within 30 years since their discovery, several CPP-conjugated compounds have entered into clinical trials (Vasconcelos *et al.* 2013).

CPPs usually comprise up to 30 amino acid residues, whereas arginine-rich peptides form the most thoroughly studied group of CPPs (Nakase *et al.* 2004; Brooks *et al.* 2005; Futaki 2006; Kosuge *et al.* 2008; Torchilin 2008). Positively charged guanidinium groups of arginines form charge-reinforced hydrogen bonds with carboxylates, phosphates, and/or sulphates on plasma membrane, enabling CPPs to enter the cells using different transport mechanisms (Mai *et al.* 2002; Dom *et al.* 2003; Herce *et al.* 2014; Mitchell *et al.* 2000). The mechanism and efficiency of uptake of arginine-rich CPPs is mostly dependent on the total charge of the compound and concentration of the compound in incubation solution (Ma *et al.* 2012). At lower extracellular concentrations, the main peptide uptake mechanism is endocytosis; if surpassing the critical threshold concentration, arginine-rich peptides directly penetrate the plasma membrane. Clearly, direct penetration mechanism is preferred over the endosomatic pathway, as it is faster and bypasses the possible endosomatic entrapment. The aforementioned critical threshold concentration for peptides comprising D-enantiomers of amino acids is usually lower (1…5 μM) than that for peptides formed of L-enantiomers of amino acids (10 μM) (Ma *et al.* 2012; Vaasa *et al.* 2010; Duchardt *et al.* 2007; Tünnemann *et al.* 2008). Here faster proteolytic degradation of L-peptides in incubation solution and in intracellular milieu may be one factor that affects these results. It has been also proposed, that the reason

for the lower threshold concentration of D-peptides is because the reduction of internalization via endocytosis might accelerate accumulation of peptide at the plasma membrane, which might trigger direct translocation more rapidly (Verdurmen *et al.* 2011).

Second large family of delivery vehicles act through targeting overexpressed receptors on pathological cells. Examples of receptor-targeting molecules include monoclonal antibodies (Lambert 2013), receptor antagonists (Carpenter *et al.* 2009), and oligopeptides (Li and Cho 2012). The conjugation of the ligand to a therapeutic drug helps to facilitate the transport of the drug specifically into the pathological cell. Directed delivery (also called targeted delivery) thus enables to avoid unwanted effect to healthy cells. However, as the drug is transported via receptor-mediated endocytosis, efficiency of which is directly related to the number of receptors available for transport on plasma membrane, only a limited amount of drug is delivered into a cell (Paulos *et al.* 2004). Another disadvantage sometimes related to endocytic mechanism is the low cytosolic release rate (Ma *et al.* 2012). Therefore, the drug must be effective already at very low concentrations.

One of the most thoroughly studied transport ligands is folate which acts through folate receptors (Saul *et al.* 2003; Sudimack and Lee 2000; Vlahov and Leamon 2012; Tyagi 2016). Folic acid is crucial for the proliferation and maintenance of all cells, mainly as it is needed for the synthesis of nucleic acids. Folic acid is transported into the cells via three transport routes: low affinity reduced folate carrier, proton-coupled folate transporter, and folate receptor (Matherly *et al.* 2007; Zhao *et al.* 2009; Kamen and Smith 2004). While the healthy cells ensure their folate supplies mainly with the first two mechanisms, cancerous cells obtain their normal folate levels via highly expressed folate receptors (Ross *et al.* 1993; Parker *et al.* 2005). The latter peculiarities are exploited in the selective transport of drugs. The folate-drug conjugates exhibit no affinity for the reduced folate carrier or proton-coupled folate transporter, yet they bind to folate receptors with high affinity [$K_{d\ (FR\alpha)} \approx 10^{-9}$ M (Parker *et al.* 2005)]. As for other receptor-mediated transport systems, the rate of receptor recycling between cell surface and inside cellular milieu, and the number and accessibility of folate receptors on the cell surfaces are important features in delivery of folate mediated drug. It has been found that it takes approximately 8…12 h for an folate receptor to unload their cargo and recycle, and that an average cancer cell expresses up to 10^7 folate receptors (Paulos *et al.* 2004). Administration of a saturating dose of a folate-drug conjugate more frequently than the recycling rate will result in high concentration of extracellular drug, which can increase the toxicity to surrounding tissue. One promising example of the conjugates in clinical trials is folic acid-Tubulysin conjugate EC1456, which is studied for a treatment of advanced solid tumours (Reddy *et al.* 2009).

While CPPs and conjugation of folate enhances the cell plasma membrane penetration of compounds on a single cell level, peptides called “vascular zip codes” home the compounds into a particular tissue (Teesalu *et al.* 2013). The

structure of these peptides is based on the distinct biochemical signatures expressed on the vasculature in different tissues (Ruoslahti 2002; Ruoslahti and Rajotte 2000). A well-known example of such transporting systems is the iRGD peptide (Figure 5). Upon recognition of the first part (RGD) of the peptide by endothelial receptor specific for cancer vasculature ($\alpha_v\beta_5$ integrin), iRGD is cleaved by proteases (Sugahara *et al.* 2009). As a result, the remaining peptide (called CendR) is recognised by another receptor (Neuropilin-1) which directs the CendR moiety together with the attached cargo insid the cell. The vascular zip code method has been successfully used to facilitate delivery of drugs, imaging agents, viruses and/or nanoparticles to tumour vasculature, acute brain injuries, hippocampus of brain with Alzheimer's disease, and also to uterine vasculature (Paasonen *et al.* 2016; Cureton *et al.* 2017; Simón-Gracia *et al.* 2016; Mann *et al.* 2017; Teesalu *et al.* 2013).

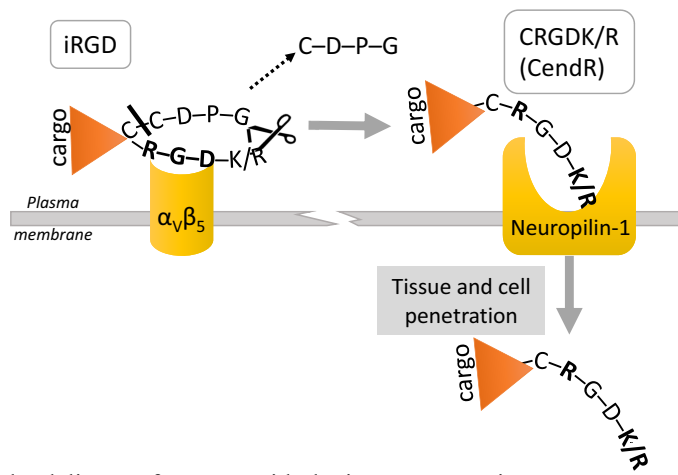

Figure 5. The delivery of a cargo with the iRGD system is a two-step process. First, the cyclic peptide iRGD containing an internal RGD motif binds to a $\alpha_v\beta_5$ integrin on a tumour specific vasculature. The binding supports the proteolytic processing of the iRGD system which results in a linear peptide called CendR, revealing the C-terminus of RGDK/R sequence. Second, the RGDK/R motif binds to Neuropilin-1, inducing the export of CendR-cargo conjugate from blood vessels and import into tissue/cell. The figure is adapted from (Sugahara et al. 2009).

2.3. METHODS FOR CHARACTERISING INHIBITORS

The research on new inhibitors aims to establish how lower doses of the drug can be used and how toxic effect caused by the interaction of drug with non-target PKs and other biomolecules can be reduced. Hence, the design of inhibitors is directed towards high-affinity and selective inhibitors, but also towards effective delivery systems and successful release of the inhibitors into cellular milieu. In order to measure important parameters (binding affinity,

selectivity, intracellular concentration, efficiency of regulation of cell´s physiology, *etc.*) of the constructed inhibitors, there is a need for corresponding analysis methods.

2.3.1. K_d-Values of High-Affinity Compounds

Historically, kinetic inhibition assays have been the most popular choice for characterisation of the inhibitors of PKs. These assays monitor the effect of the inhibitor to the phosphorylation rate of the substrate peptide/protein by a target kinase. A "gold standard" is the radioactive [γ-^{32}P]-ATP method, where the size of the radioisotope is the closest to that of the physiological ATP, compared to other labels, *e.g*. fluorescence dyes (Jia *et al.* 2008). However, the kinetic assays are often expensive, time-consuming, and require special assay components (suitable substrate for phosphorylation, sufficiently catalytically active kinase, and reagents for measuring the phosphorylation reaction).

In recent years different binding/displacement assays have gradually replaced kinetic assays (Davis *et al.* 2011; Fabian *et al.* 2005; Bamborough *et al.* 2008). In the course of binding/displacement assays the displacement of a probe (tracer) from the complex with the PK by the compound under evaluation (*e.g.,* inhibitor, displacer, ligand, binder, or replacer) is monitored. These assays give information about the binding affinity of the inhibitor to the target PK. The binding/displacement assays have many advantages, *e.g.,* simplicity, quickness, amenability for automation, and wider range of resolvable dissociation constants, especially when applying high-affinity probes (Vaasa *et al.* 2009; Huang 2003).

Most of the PK inhibitor-based drugs on the market possess biochemical K_d values in nanomolar range (Karaman *et al.* 2008). However, in cells inhibition of many PKs occurs only at super-micromolar concentrations of these inhibitors. This is due to high concentration of the co-substrate ATP in cells (1...10 mM), substantially up to 1000-fold surpassing K_m values for PKs (1...1000 μM) (Knight and Shokat 2005). The substantially restricted inhibitory potency of inhibitors competing with intracellular ATP leads to the need for highly potent inhibitors possessing picomolar K_d values. By the virtue of the broadened analysis possibilities (*e.g.,* analysis of protein structure and protein-inhibitor complexes), the construction of new inhibitors and higher affinities of the inhibitors towards targets have been achieved (Tal-Gan *et al.* 2010; Xu *et al.* 2009; Zhang *et al.* 2009; Lavogina *et al.* 2009; Noble *et al.* 2004).

Nevertheless, evaluation of compounds with very high affinity towards the target protein is still experimentally challenging (Murphy 2004). As an example, if determining the affinity of the inhibitor by displacing the probe from the complex with PK, one parameter that characterises the precision of interpretation of IC_{50} value from displacement curve is the slope of the curve (also called Hill´s slope). The Hill´s slope is mainly determined by the affinity of both, the inhibitor and the probe towards the protein, and the concentration of

the probe (Figure 6.A). If the K_d of the inhibitor is too low compared to the ratio of the concentration and the K_D of the probe, the Hill´s slope deviates from -1 (thus locating in the so called tight-binding region). In these conditions the correct interpretation of the IC_{50} value is complicated mainly due to high uncertainty accompanying the experimental data.

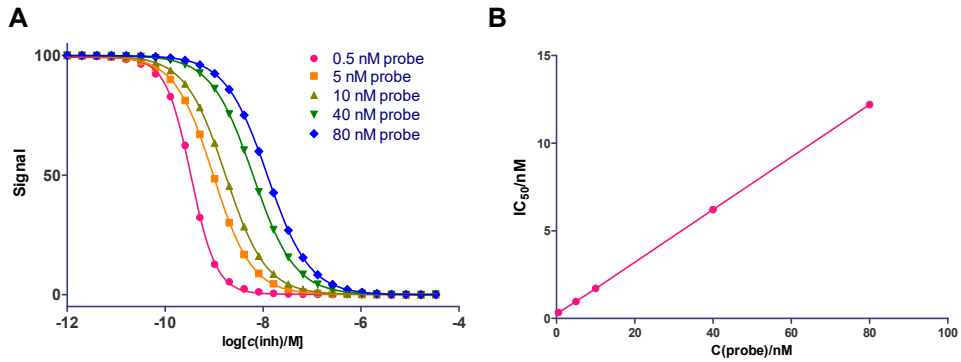

Figure 6. A) Simulation of displacement curves at different concentrations of the probe [c_{PK} = 0.5 nM, $K_{D,probe}$ = 0.02 nM] in the dilution series of high-affinity inhibitor ($K_{d.inhibitor}$ = 0.003 nM). Hill´s slope deviates from -1 if the concentration of the probe is decreased to critical value. **B)** Increase of the concentration of the probe leads to increase of the IC_{50} value.

One possibility to shift the displacement curves away from the tight-binding region is to utilize higher concentrations of the probe (Figure 6) or a higher-affinity probe (Huang 2003). Nevertheless, the applicability of this approach is often restricted because of lack of a suitable probe or strong signal of the free probe that interferes with the signal of the protein-bound probe. Accordingly, in case of analysing high-affinity inhibitors in a displacement assay, the selection of the probe is of crucial importance and sets limits to the range of affinities of inhibitors that can be determined.

Another important aspect of characterization of tight-binding inhibitors is the choice of the parameter that can be used for their comparison. In case of displacement assays, IC_{50} values are usually compared. However, as was demonstrated in Figure 6, IC_{50} values depend on assay conditions: increased concentration of the probe leads to increase in the IC_{50} value. According to the Cheng-Prusoff equation, increase of the ratio of concentration of the applied probe and its affinity towards target kinase leads to bigger difference of IC_{50} and K_d (or K_i) values of the inhibitor (Cheng and Prusoff 1973). K_d, on the contrary, is not dependent on the concentration of PK, affinity or concentration of the probe, and it is directly related to the binding energetics (binding free energy change, $\Delta G_{binding}$) (Copeland 2013; Schwartz and Murray 2011). The IC_{50} value obtained from the displacement curves could be converted to K_d by Cheng-

Prusoff equation or by more exact equation derived by Nikolovska-Coleska (Cheng and Prusoff 1973; Nikolovska-Coleska *et al.* 2004).

2.3.1.1. ARC-Probes

The application of ARC(Photo) photoluminescent probes enabled the determination of low picomolar K_d-values of inhibitors of PKs in binding/displacement assays. The ARC(Photo) probes possess the structure of biligand ARC-inhibitors described in chapter 2.2.1 and additionally comprise a fluorescent dye in the C-terminus of the peptidic moiety. The dissociation constant K_d of compounds determined in binding/displacement assays well coincide with the values of inhibition constants K_i of the same compounds as determined in kinetic/inhibition assays for ATP-competitive, substrate protein-competitive, and biligand inhibitors (Enkvist *et al.* 2011; Vaasa *et al.* 2009). The latter result shows that ARC-probes bind only to active forms of the kinase.

The biligand structure of the probes enables the determination of binding constants for ATP-, substrate protein-competitive, and biligand inhibitors (Viht et al. 2007; Enkvist et al. 2011). Also, the binding equilibrium of probe:PK complex in solution is achieved quickly, which allows the use of short incubation times in displacement assays (Viht et al. 2007; Vaasa et al. 2009; Enkvist et al. 2011).

There are mainly two types of ARC(Photo) probe differing from one another by the photoluminescent properties of the ATP-competitive moiety and the resultant possible applications of the different probes. ARC-Fluo probes are designed for assays with fluorescence anisotropy (FA) readout. Whereas, ARC-Lum(Fluo) probes possess photoluminescent properties that make possible their application in assays with FA readout as well as in assays using time-gated measurement of luminescence intensity (TGLI) (Vaasa et al. 2009; Enkvist et al. 2011; Ligi et al. 2016).

The range of resolvable binding affinities, as determined in assays with FA readout, is limited by the affinity of the probe (Huang 2003). ARC-Lum(Fluo) probes, on the other hand, possess unique photoluminescent properties which greatly expand their applicability in biochemical assays using TGLI (Enkvist *et al.* 2011; Ligi *et al.* 2016). First, upon pulse-excitation with near-UV radiation (between 300...370 nm) the probe reveals characteristic PK binding-responsive photoluminescence with slow (microsecond scale) decay. The latter phenomenon allows the bypass of short-lifetime (nanosecond-scale) background fluorescence of compounds present in the assay system (Enkvist et al. 2011). Second, very weak signal of free probes and high affinity of probes enable their employment for determination of dissociation constants of both tight-binding and low affinity inhibitors (Huang 2003; Vaasa *et al.* 2009; Enkvist *et al.* 2011). The Jablonski diagrams of bound and unbound ARC-Lum(Fluo) probe are presented in Figure 7.

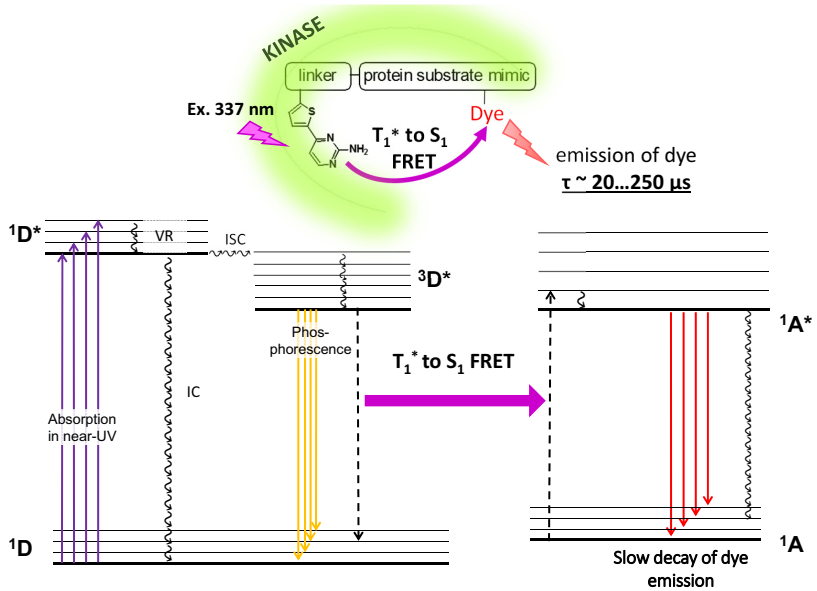

Figure 7. The simplified Jablonski diagram of a PK-bound ARC-Lum(Fluo) probe describing formation of the long lifetime photoluminescence signal at the emission wavelengths of the acceptor fluorescent dye. For clarity, transitions between electronic states leading to short life-time photoluminescence (fluorescence) have been omitted. The donor-luminophore D is excited with a pulse of near-UV radiation. The excited donor-luminophore (^{1}D*) can dissipate its energy via radiative (not shown) and nonradiative processes (curved lines), such as internal conversion (IC) and vibrational relaxation (VR). ^{1}D* can also change its spin by intersystem crossing (ISC) and go into excited triplet state ^{3}D*. Inside the catalytic pocket of a PK the concentration of the quencher, such as dissolved molecular oxygen, is greatly reduced thus the energy is stored in ^{3}D*. In the presence of the acceptor fluorophore in close proximity to donor the energy is released gradually from T^1* to the acceptor fluorophore via FRET. This leads to the relaxation of the donor to the ground singlet state ^{1}D and formation of ^{1}A* that thereafter emits a photon and relaxes to the ground singlet state (^{1}A). To conclude, this type of energy transfer (inter-chromophore triplet-singlet energy transfer) occurs if the tandem probe is bound to a PK and the ^{3}D* state of the phosphor is shielded from dissolved quenchers (*e.g.,* molecular oxygen) and molecular motions are restrained. The emission spectrum of an ARC-Lum(Fluo) probe coincides with the fluorescence spectrum of the attached dye. The emission decay time of the tandem luminophore is defined by the stability of the excited triplet state of the donor phosphor. The rate and efficiency of the transfer also depend on the distance between the chromophores.

ARC-Lum(Fluo) probe library contains compounds that could be applied for analysis of binding affinities for inhibitors of PKAc, ROCKII, PKG, Haspin, AKT3, Pim1, Pim2, CK2, and other PKs (Table 1). The resolvable range of inhibitor affinities if applying a specific probe is discussed in chapter 5.1.1.2. Besides determination of binding constants, the probes could also be used as sensitive tools for determining concentration of the active form of PKs in biochemical assays (Kasari et al. 2012) and mapping the activity of PKs in living cells (Vaasa *et al.* 2010).

Table 1. ARC-probes for assays with TGLI readouts

Probe **(Label)**[1]	K_D/nM[2]					References
ARC-1182 **(PromoFluor-647)** ARC-1063 **(Alexa Fluor 647)** ARC-669 **(5-TAMRA)**	**PKAc** 0.015..0.02	**ROCK II** 0.20	**PKG** 2.7	**Haspin** 9.2…15	**AKT3** 4.9…5.0	(Kasari *et al.* 2013; Ivan *et al.* 2016; Enkvist *et al.* 2011; Kestav *et al.* 2017; Lavogina *et al.* 2014)
ARC-3158 **(PromoFluor-647)** ARC-3159 **(PromoFluor-555)**	**Pim1** 0.4…0.5	**Pim2** 0.7…0.9				(Ekambaram *et al.* 2015)
ARC-3141 **(PromoFluor-647)**	**CK2** 25					(Ekambaram *et al.* 2014)
ARC-1530 **(5-TAMRA)**	**CK2** 0.4					(Vahter)

[1] ARC-1182, ARC-1063, and ARC-669 comprise a different fluorescent label, attached to the same ARC unit; the same applies for ARC-3158 and ARC-3159.

[2] The K_D values are presented either as single values or as a range of K_D values (if the attached label affects the affinity). The average standard deviation of the values is 20%.

2.3.2. Intracellular Concentration: Importance and Determination

Good cellular accumulation of the compound together with its appropriate intracellular compartmentalization are critical factors that pave the way for their successful application as PK inhibitor-based drugs and probes. Determination of the intracellular concentration of these compounds helps to establish amount of the ligand in cells that is necessary for regulation or monitoring of cellular activity of PKs. If used as probes to study the pathways with participation of the target PK, it would be necessary to minimise the intracellular concentration of the active compound in order to reduce the probability of its binding to other proteins and constituents of cells. Nevertheless, in order to cause effective inhibitory effect, often high (micromolar) concentration of the compound in the cell is needed. As an example of successful inhibitor, imatinib (Gleevec) is extensively transported into cells which could explain the remarkable effectiveness of the drug in causing apoptosis of leukemic cells (Widmer *et al.* 2006; Lipka *et al.* 2012).

For several reasons both optimising the intracellular concentration of the inhibitor and knowing its affinity towards the PK are important. First, concentration of the compound lower than 10 μM would be advisable to reduce the probability of its binding to non-target proteins and non-specific binding that increases rapidly at concentrations above 10 μM (Knight and Shokat 2005). Second, the preferences for the concentration of the inhibitor are related to the amount (average concentration) of the target kinase in the cell, as that determines the stoichiometrical amount of the inhibitor needed (Knight and Shokat 2005). Third, in a cell the drug has to compete with high (1…5 mM) concentration of ATP (Kennedy *et al.* 1999; Gribble *et al.* 2000). As the $K_{M,ATP}$ values for most PKs are in the low- to mid-micromolar range, for effective regulation of activity of the PK, the concentration of ATP site-targeting inhibitors in the cell should be about 10- to 100-fold higher than the K_i value of the inhibitor (Knight and Shokat 2005). Therefore, for the development of a successful drug the intracellular molar amount of both the target PK and its inhibitor should be determined.

Several experimental techniques enable the determination of intracellular concentration of compounds. Fluorescent label aids the quantification by high performance liquid chromatography (HPLC) with fluorescence detection (Lucas *et al.* 2016; Palm *et al.* 2006; Aussedat *et al.* 2006), SDS-PAGE (Mussbach *et al.* 2011), fluorescence-activated cell sorting (FACS) (Watkins *et al.* 2009; Nakase *et al.* 2004), fluorescence correlation spectroscopy (FCS) (Verdurmen *et al.* 2011), or the combination of the two (Rezgui *et al.* 2016). However, cellular uptake of a labelled compound (*e.g.*, peptide) can be drastically different of that of the unlabelled counterpart. For unlabelled compounds, HPLC with mass spectrometer (MS) (Kralj *et al.* 2013a) and UV/Vis (das Neves *et al.* 2012) detectors, and matrix-assisted laser desorption/ionization time-of-flight MS (MALDI-TOF MS) (Burlina *et al.* 2005), have been applied.

Molar concentration of inhibitors has been disclosed in relatively rare cases as most of the publications only report the change in the intensity of fluorescence (or some other signal) separately or as normalized to some stable reference indicator (*e.g.,* amount of total protein in the sample) (Lindgren et al. 2004; Aussedat et al. 2006; Balayssac et al. 2006; Kralj et al. 2013a; Palm et al. 2007). These data do not enable the estimation of the molar concentrations of molecules participating in signalling cascades in cells.

There are two aspects complicating the expression of results as molar concentrations that should be considered. First, calculations for molar concentrations require knowledge about the volume of the cell, which is often an approximate value (similarly to the concentration of total protein in a cell). Second, differentiating between the internalised compound and the compound bound to the cell surface could be challenging. Oehlke *et al.* and Aussedat *et al.* solved the obstacle by chemical modification of the extracellular peptide (Aussedat *et al.* 2006; Oehlke *et al.* 1998), and Lindgren *et al.* applied enzymatic digestion (Lindgren *et al.* 2000).

Depending on the specific study area and requirements of the method parameters (*e.g.*, speed, price), a suitable technique can be chosen. As each of the analytical methods has its pros and cons, often different methods are used in parallel – thus a better understanding of the internalisation process could be obtained.

3. AIMS OF THE STUDY

Based on the high demand for PK inhibitors as drugs and as diagnostic agents, the main aims of this study were the development/refinement of methods for characterisation of high-affinity PK inhibitors and the development of biligand ARC-inhibitors for regulation of cell physiology. Accordingly, the following tasks were set for the study.

- Establishment of the applicability of ARC-Lum(Fluo) probes for characterization of high-affinity inhibitors of PKs.
- Elaboration of a HPLC method for determination of intracellular concentration of labelled and unlabelled ARCs.
- Development of a selective and potent biligand inhibitor for CK2.
- Modification of the structure of biligand inhibitors and demonstration of their applicability for regulation of activity of cellular PKs (in particular CK2 or PKA).

4. MATERIALS AND METHODS

4.1. DISPLACEMENT ASSAYS FOR DETERMINATION OF BINDING AFFINITIES

The binding affinities of ligands were determined in displacement assays as described earlier (Vaasa *et al.* 2009; Roehrl *et al.* 2004; Kashem *et al.* 2007; Vahter). The assays with CK2 were carried out in 4-component buffer [50 mM HEPES (Sigma), 150 mM NaCl (Riedel-de Haën), 0.005% Tween® 20 (Sigma), 5 mM DTT (Fluka), pH 7.5] and with PKA in 5-component buffer [additional 1.5 μM or 7.5 μM BSA (Sigma) for higher- and lower-affinity inhibitors, respectively]. Buffer solutions were made in MilliQ ultrapure water (Millipore Corporation).

The concentrations of stock solutions of ligands and probes were determined spectrophotometrically (NanoDrop 2000c, Thermo Scientific) in a buffer or in DMSO (Sigma Aldrich) by the reference to molar extinction coefficients determined previously: unlabelled compounds containing ATB-fragment, ε_{322nm} = 23 000 $M^{-1}cm^{-1}$; unlabelled compounds containing TBBz-fragment, ε_{272nm} = 10 000 $M^{-1}cm^{-1}$; ARC-1504, ARC-1139, ARC-1182, ε_{647nm} = 250 000 $M^{-1}cm^{-1}$; ARC-1530 and ARC-1042, ε_{558nm} = 80 000 $M^{-1}cm^{-1}$; ARC-904, ARC-1411, ARC-1222, and ARC-1012, ε_{260nm} = 15 000 $M^{-1}cm^{-1}$ (Vahter; Enkvist *et al.* 2012; Vaasa *et al.* 2009; Enkvist *et al.* 2011; Kestav *et al.* 2015). For compounds comprising both, ATB and folate moiety (ARC-778), the molar extinction coefficient of ε_{306nm} = 32 000 $M^{-1}cm^{-1}$ was calculated by summarizing the corresponding epsilon values (Vahter; Dántola *et al.* 2010).

Full length human recombinant protein His-CK2α-His (Manoharan 2016) and PKAc (Lavogina *et al.* 2009) were prepared as described previously. The concentration of the PKs was determined before each displacement measurement series in the direct binding assay using FA or TGLI readout as described previously (Vaasa *et al.* 2009; Vahter). The concentration of CK2α was determined by titration of the fixed concentration (20 nM) of PromoFluor-647-labeled fluorescent probe ARC-1504 or 5-TAMRA-labelled luminescent probe ARC-1530 (available from Kinasera OÜ, Estonia) with the solution of the enzyme (2-fold dilutions). The concentration of PKAc was determined by titration of the fixed concentration of 5-TAMRA-labelled fluorescent probe ARC-1042 (20 nM) or PromoFluor-647-labeled luminescent probe ARC-1139 (100 nM) with the solution of the enzyme (2-fold or 3-fold dilutions, respectively).

All assays were performed in the final volume of 20 μL in black 384-well polystyrene microplates with nonbinding surface (Corning #4514 or #3676). Experiments were run in 3…6 parallels with a PHERAstar platereader (BMG Labtech)

The displacement assay was performed by mixing the compounds under evaluation at a single concentration or using a 3-fold dilution series. Before measurements, the microplates were incubated with orbital mixing with 300

rpm at 30 °C for 25…60 min. The difference of the value of fluorescence anisotropy (FA) compared to the FA-value of the free probe was registered on a PHERAstar platereader. For FA measurements, optical modules suitable for fluorescent dyes PromoFluor-647 {FP608B [ex 590(50) nm, em 675(50) nm]} and 5-TAMRA {FP607B [ex 540(20) nm, em 590(20) nm]} were applied. The change in luminescence intensity was measured in time gate (time window) (TGLI) after time delay, upon excitation with a pulse of near-UV radiation. For TGLI measurements with the probe ARC-1530 optical module TRF805B1 [ex 337(300…360) nm, em 590(50) nm] and with ARC-1182 optical module HTRF802D1 [ex 337(50) nm, em 675(50) nm], delay time of 80 µs, and gate time of 400 µs were applied. Assays with the probe ARC-1139 were performed with optical module HTRF802D1 [ex 337(50) nm, em 675(50) nm] and delay time of 50 µs, and gate time of 150 µs.

Single concentration displacement measurements were used for the estimation of IC_{50} values of inhibitors according to Equation (1):

$$IC_{50} = \frac{IC_x}{\frac{100}{x}-1}, \quad (1)$$

where IC_x is concentration of the inhibitor that leads to x% of the retained TGLI signal.

The IC_{50} values were converted into $[I]_{50}$ values (the estimations of the concentration of the *free* inhibitor when 50% displacement has occurred) in case of single concentration and full curve displacement assays, according to Equation (2):

$$[I]_{50} = IC_{50} - [EI]_{50}, \quad (2)$$

where $[EI]_{50}$ is the concentration of the enzyme:inhibitor (PKAc:inhibitor) complex in case of 50% displacement. The gained values were converted to dissociation constants ($K_{d,inh}$) according to the Cheng-Prusoff equation modified by Nikolovska-Coleska *et al.* (Nikolovska-Coleska *et al.* 2004) [Eq. (3)]:

$$K_{d,inh} = \frac{[I]_{50}}{1+\frac{[P]_{50}}{K_{D,probe}}+\frac{[E]_0}{K_{D,probe}}}, \quad (3)$$

where $[P]_{50}$ is the concentration of the free probe at 50% displacement, $[E]_0$ the concentration of the free enzyme at 0% displacement, and $K_{D,probe}$ is the dissociation constant of the complex of the probe and enzyme [see Supplementary Material 3 in Paper III for solution of Equations (2) and (3)].

Data analysis was performed using GraphPad Prism software (version 5.01, GraphPad) and Microsoft Excel 2016 software.

4.2. CELLULAR ASSAYS

The following cell lines were used in this work: human cervical cancer HeLa cells, Madin-Darby canine kidney cells (MDCK), human prostate cancer cells (PC-3), Chinese hamster´s ovary cells (CHO; all from American Type Culture Collection, ATCC), human prostate cancer cells (PPC-1, a kind gift from Dr. Tambet Teesalu, Cancer Biology Laboratory, University of Tartu), MIA PaCa-2 cells (ATCC). The cells were grown on 6-well (Thermo Scientific™ 130184) culture plates (if not mentioned otherwise) in the medium (RPMI, DMEM, or DMEM/Ham's F12, PAA Laboratories) supplemented with 10% FBS, 100 U/mL penicillin, 100 μg/mL streptomycin (PAA Laboratories). Cell cultures were grown and maintained at 37 °C in a humidified 5% CO_2 containing air environment.

4.2.1. Cell Counting, Determination of Viability and Diameter of the Cells

15 μL of the cell suspension in DPBS and 15 μL of 0.4% trypan blue solution were mixed thoroughly. 10 μL of the obtained cell-suspension was added into dual-chamber counting slide (Bio-Rad); measurements with cell counter (TC-10™, Bio-Rad) were performed 4 to 6 times. The cell counter provided the number of cells in 1 mL of cell suspension, percentage of live cells, histograms of diameters of alive and dead cells. The volume of the cells was calculated based on the formula of the volume of a sphere.

4.2.2. Cytotoxicity Assay

In case of cytotoxicity assays described in chapter 5.2.2.1, HeLa cells were grown in a 24-well plate (Nunc) to ~50% confluence. Thereafter, the cells were washed with 2 mL of DPBS and incubated with ARC-1842, CX-4945 (Synkinase), TBBz, or ARC-1859 (all at 0, 1, 5, 10, or 20 μM) in serum-free DMEM high glucose medium containing 1% DMSO and 0.1% Pluronic F-127 (300 μL total volume) for 24 h in triplicate. Cells incubated in culture medium without DMSO and Pluronic F-127 were used as control. Thereafter each well was washed twice with 1 mL of DPBS and the solutions were transferred into a screw-capped tube. The cells were incubated with 0.25% trypsin, 0.1% EDTA (PAA Laboratories, 100 μL) for 2 min, suspended in DPBS (PAA Laboratories, 1 mL), and added to the screw-capped tube. After centrifugation at 100 g for 5 min, the supernatant was removed and the cells were resuspended in the indicator-free RPMI medium (200 μL). Thereafter the viability was determined as described in chapter 4.2.1.

4.2.3. Microscopy Analyses

For microscopy analyses 15 000 cells were seeded on a 12-well microscopy chamber (Ibidi), cultured for 2 days. Thereafter, the medium was removed and the cell layer was washed two times with 200 µL of DPBS. ARC-1042 was diluted in serum- and antibiotics-free medium (total volume 100 µL, final concentration 10 µM). The cells were incubated with ARC-compound for 1 h or for 24 h. After incubation, the solution of ARC was washed off with 200 µL of DPBS. During the microscopy analyses, cells were kept in 100 µL of the indicator-, serum-, and antibiotics-free medium at room temperature.

The cells were imaged with a custom made microscope (TILL Photonics), using light source – oligochrome [excitation filter 520(35) nm, emission filter 605(70) nm], exposure time – 100 µs, 10% of the maximal power of the lamp, and 20x oil objective. Images were analysed with ImageJ software (version 1.46r, Wayne Rasband, National Institutes of Health). The intensities of the images were auto-scaled.

4.2.4. HPLC and Western Blot Analyses

Cells were seeded on 6-well (Thermo Scientific™ 130184; HPLC + Western Blot assays) or 12-well (Nunc; only Western Blot assays) culture plates. After 1 or 2 days, ARC-compound of interest was diluted in serum- and antibiotics-free medium [DMEM High glucose or folate free RPMI (PAA Laboratories)], and added to the cells. The cells analysed with CREB phosphorylation assay were additionally treated with forskolin (Tocris) for 30 min after the treatment with inhibitors. All assays were performed at least in three replicates. After incubation, the cells were detached from the surface by solution of 0.25% trypsin, 0.1% EDTA (PAA Laboratories). After multiple washing steps with DPBS (PAA Laboratories), 15 µL of cell suspension was used for cell counting (see paragraph 4.2.1). The remaining cell suspension was lysed in cell lysis buffer (NP 40, Invitrogen) containing 1% of Triton-X (Sigma), protease inhibitor cocktail (Sigma-Aldrich), 1 mM DTT, and 0.5 mM phenylmethylsulfonyl fluoride (AppliChem). The cell lysate was analysed by Western blot and/or HPLC.

4.2.4.1. HPLC Analyses

For HPLC experiments, the internal standard was added to the lysate and the proteins were precipitated with acetonitrile (lysate:acetonitrile ratio was 1:2 to 1:3). Thereafter, the sample was centrifuged at 20 000 g and 4 °C for 30 min and thereafter the supernatant was dried in the rotational-vacuum-concentrator (RVC 2-25, Christ). Dry sample was re-suspended in 100 µL of buffer (50 mM HEPES, 150 mM NaCl, 0.005% Tween® 20, pH 7.5) or 50% ACN in water and analysed with HPLC. HPLC was equipped with a Kinetex XB-C18 or Luna C18 (Phenomenex) analytical column (5 µm, 250 × 4.6 mm) maintained at 30 °C,

photodiode array detector SPD-M20A, fluorescence detector RF-20A xs, and autosampler SIL-20A. Acetonitrile/water (0.1% TFA) gradient at a flow rate of 1 mL/min was used.

Calibration solutions included the analyte and the internal standard in either buffer [50 mM HEPES, 150 mM NaCl, 0.005% Tween® 20, pH 7.5) or 50% ACN in water. The ratio of the peak area of analyte to that of the internal standard was used as the assay parameter. Peak area ratios were plotted against the corresponding concentration ratios, and standard calibration curves were obtained from least-squares linear regression analysis of the data. The linearity of the method was confirmed *via* evaluation of the calibration y-intercept and correlation coefficients. The intracellular concentration was calculated by the measurement model (4):

$$C_{x\_cell} = \frac{\frac{A_x}{A_s} - b}{a} C_s \cdot V_{final} \frac{1}{N_{ca}\frac{4}{3}\pi\left(\frac{d_{ca}}{2\cdot 1000}\right)^3 + N_{cd}\frac{4}{3}\pi\left(\frac{d_{cd}}{2\cdot 1000}\right)^3} \quad (4)$$

where $C_{\text{x-cell}}$ – intracellular concentration of ARC, A_x – peak area of the analyte, A_s – peak area of the internal standard, b – intercept, a – slope, C_s – concentration of the internal standard, V_{final} - final volume of the sample, N_{ca} – number of living cells, d_{ca} – diameter of a live cell, N_{cd} - number of dead cells, d_{cd} – diameter of a dead cell.

The intracellular concentration of ARC was determined with applying the calibration curve. The calculations were performed with the software Microsoft Excel (2016). All uncertainties given in this thesis are expressed as combined uncertainty (Kragten 1994).

4.2.4.2. Western Blot Analyses

Proteins of cell lysates were separated by gel-electrophoresis and transferred to Western blot membranes. Proteins were identified by developing of the membranes with the following primary antibodies (analyses described in chapters 5.2.1 and 5.2.2.2.2): rabbit monoclonal antiphospho-Cdc37 (Ser13, Cell Signaling Technology Cat# 13248), rabbit monoclonal anti-Cdc37 (Cell Signaling Technology, Cat# 4793), rabbit polyclonal phospho-CREB-1 (Ser133, Santa Cruz Biotechnology, Cat# sc-101663), and mouse monoclonal anti-α-tubulin (Abcam, Cat# DM1A); and secondary antibodies: goat anti-rabbit IgG alkaline phosphatase conjugate (Thermo Fisher Scientific, Cat# T2191), goat anti-rabbit alkaline phosphatase conjugate (AnaSpec, Fremont, CA, Cat# 28178), and goat anti-mouse (Applied Biosystems, Cat# T2129). Analysis of Western blot images was performed with ImageJ software (version 1.46r, Wayne Rasband, National Institutes of Health) and the calculations of band intensities with Microsoft Excel (2016). More detailed procedure is described in Papers I and IV.

Western blot membranes (analyses described in chapter 5.2.2.1) were processed with the following antibodies: rabbit polyclonal antiphospho-NFκB p65 (Ser529, Abcam), rabbit monoclonal anti-NFκB p65, (Cell Signaling Technology), mouse monoclonal anti-Cdc37 (Santa Cruz Biotechnology), mouse monoclonal anti-β-actin (Sigma), and affinity-purified antiphospho-Cdc37 (Ser13) antibody (a kind gift from Dr. I. Miyata, University of Kyoto, Japan). More detailed procedure is described in Paper II.

4.2.5. Caspase-3 Activity Assays

For determining the change in CASP3 activity, a Förster resonant energy transfer (FRET) biosensor (Casper3-GR, Evrogen company) was used combined with the baculovirus-based BacMam transduction system (Rahnel *et al.* 2017). The activation of CASP3 in cells leads to cleavage of the Asp-Glu-Val-Asp sequence between the donor and acceptor fluorophores in the fusion protein and thus to elimination of FRET between the fluorophores. The reaction resulted in decrease of the emission of TagRFP and increase in the emission of TagGFP. Plasmid construction and generation of BacMam viruses was done as described earlier (Mazina *et al.* 2012). The cells were incubated with the virus for 3…4 hours, detached with 0.25% trypsin/0.1% EDTA, and seeded on a black clear-bottom 96-well cell culture plates (Ibidi, 89626) at the density of 50 000…100 000 cells/well in 90 µL of culture medium, supplemented with sodium butyrate (Aldrich) at 10 mM final concentration for enhanced protein expression. The cells were further incubated for 24 h to allow the expression of Casper3-GR fusion protein. Before incubation with inhibitors, the cells were washed with DPBS.

All reactions were carried out in the final volume of 100 µL. 10 µL of the 10× concentrated ligand solution was added to the wells containing 90 µL of serum- and antibiotics-free medium and the image acquisition program was initiated. Autofocus was performed in the donor channel (Tag-GFP) and the acceptor channel (Tag-RFP) used the same focus. At least 4 images per well were captured in both channels, using the fluorescence plate reader mode on Biotek microscope Cytation5 at 37 °C, 5% CO_2. The responses were measured every 30 min for the first 8 h, and every 60 min for the next 16 h.

For excitation 465 nm LED cube was used for both channels, for donor (Tag-GFP) emission 525 nm cube and for acceptor (Tag-RFP) emission 593 nm cube were used. The change in acceptor/donor emission ratios was calculated using the equation 5:

$$Change\ in\ FI\ ratio = \frac{\frac{I_{593_0}}{I_{525_0}} - \frac{I_{593_t}}{I_{525_t}}}{\frac{I_{593_0}}{I_{525_0}}} \quad (5)$$

where I_{593_0}, I_{525_0}, I_{593_t}, and I_{525_t} refer to the mean pixel intensities of fluorescence emission for Tag-RFP and Tag-GFP proteins before and after the ligand treatment, respectively. The calculated values were plotted against time or concentration on the x-axis. Analysis of CASP3 activity images were performed with Gen5 software and the obtained data were analysed using Aparecium software (The GPCR Workgroup (Universtity of Tartu)) running in Matlab environment, and GraphPad Prism (5.04) program. For calculating of EC_{50} values, the average values of Change in FI ratio of 11...16 h data points were used. The highest value of Change in FI ratio was unified for all data sets according to the control compound Staurosporine.

4.2.6. Platelet Aggregation Assays

Platelet samples [4 BC platelet concentrate, platelet content $(180…340)\times10^9$, filtered] originating from healthy volunteer anonymous donors, were obtained from Tartu University Hospital. A general consent of every donor for use of his/her blood in scientific studies was preliminarily obtained. The study was approved by the Research Ethics Committee of the University of Tartu in accordance with The Code of Ethics of the World Medical Association (Declaration of Helsinki; 251/M-1, PI Dr. Asko Uri and Dr. Darja Lavogina).

The measurement of platelet aggregation was performed by monitoring change in light transmission at 590 nm using PheraStar microplate reader. The assay was performed on transparent 96-well plates with flat bottom (Greiner, #655101). The pre-incubation of platelets and incubations during the assay were performed at 30 ^oC. Tyrode's buffer [120 mM NaCl, 5 mM KCl (AppliChem), 3 mM $MgCl_2$ (AppliChem), 2 mM $CaCl_2$ (AppliChem), 45 mM glucose (Sigma), 25 mM HEPES pH 7.4] was used as the main assay buffer. The final total volume in the assay was 120 µL. During the measurement, the following stirring conditions were applied: 1 mm double orbital shaking, shaking time 9 s before each cycle. Each measurement was performed as a triplicate; two independent experiments were performed on two separate days.

Initially, the concentration of ADP (Sigma) suitable for induction of platelet aggregation was identified as follows. 2-fold dilutions of ADP were prepared in the assay buffer and pipetted together with blank solution (Tyrode's buffer) onto the microplate. The measurement was started in the kinetic mode. After 3 cycles (cycle time 27 s), the measurement was paused and platelets or buffer were added to the indicated wells; aggregation of platelets was monitored for 30 min. Based on the results of this assay, we used final total concentration of 10 µM or 25 µM ADP in the following measurements (25 µM was the lowest concentration that consistently induced significant aggregation and sufficient measurement window with low signal to noise ratio, 10 µM concentration was chosen as it has been used most often in platelet aggregation assays).

In order to monitor the effect of CK2 inhibitors on aggregation, the following assay was performed. The solutions of CK2 inhibitors and the

reference compound Forskolin (Tocris, adenylyl cyclase activator) were prepared in the assay buffer and then pipetted together with blank solution (Tyrode's buffer) onto the microplate. The measurement was started in the kinetic mode. After 3 cycles [cycle time 37 s (first experiment) or 73 s (second experiment)], the measurement was paused and platelets or buffer were added to the indicated wells; the microplate was then incubated for the indicated amount of time (30 min or 60 min) and the absorbance at 590 nm was constantly monitored. Finally, solution of ADP or buffer was added to the indicated wells and the measurement was continued for another 30 min.

The final total concentration of inhibitors as well as Forskolin was 10 μM. The platelet count in each well was calculated as $>1.8\times10^7$ according to the initial number of provided platelets and the dilution used. The data were analysed with GraphPad Prism 5.04. For the column diagrams, the absorbance values at ~15 min following addition of ADP were used. Unpaired t-test (two-tailed *p*-value, confidence level of 95%) was used for the analysis of statistical significance of effects.

5. RESULTS AND DISCUSSION

5.1. METHODS FOR CHARACTERIZATION OF PK INHIBITORS

Drug development pipelines are focused on construction of PK inhibitors with the highest possible affinity. This approach leads to the application of lower doses of the drug and thus reduced possibility for toxic effects caused by interactions with non-target PKs and other biomolecules. Nevertheless, accurate evaluation of K_d values of high-affinity inhibitors is challenging. In this chapter we first introduce a high-throughput binding assay for determining affinities of PK inhibitors possessing K_d values in the sub-picomolar to sub-millimolar range. Second, an HPLC method was developed for determination of molar concentration of inhibitors in cells.

5.1.1. Binding Assay for Determination of Affinities of PK Inhibitors (PAPER III)

In the binding/displacement assay described in the paper III, ARC-Lum(Fluo) probes were used for determination of K_d values of PK inhibitors and probes. Unlike several other inhibitor-screening technologies (Lebakken *et al.* 2009), a single probe is used instead of a combination of antibody and fluorescent tracer, making the assay simpler, cheaper, and more accurate. Upon excitation with a flash of UV radiation, the probe in complex with the PK emits long-lifetime luminescence whose intensity is measured after delay in predetermined time window (TGLI measurement mode). Moreover, in case of such measurement conditions the signal from the free probe is negligible. As bound and free ARC-Lum(Fluo) probes possess significant difference in photoluminescence properties, they are well usable in displacement assays for determination of the dissociation constants of competitive inhibitors (Figure 8). The physical background of photoluminescent properties of ARC-Lum(Fluo) probes has been described in chapter 2.3.1.1 and elsewhere (Ligi *et al.* 2016; Enkvist *et al.* 2011).

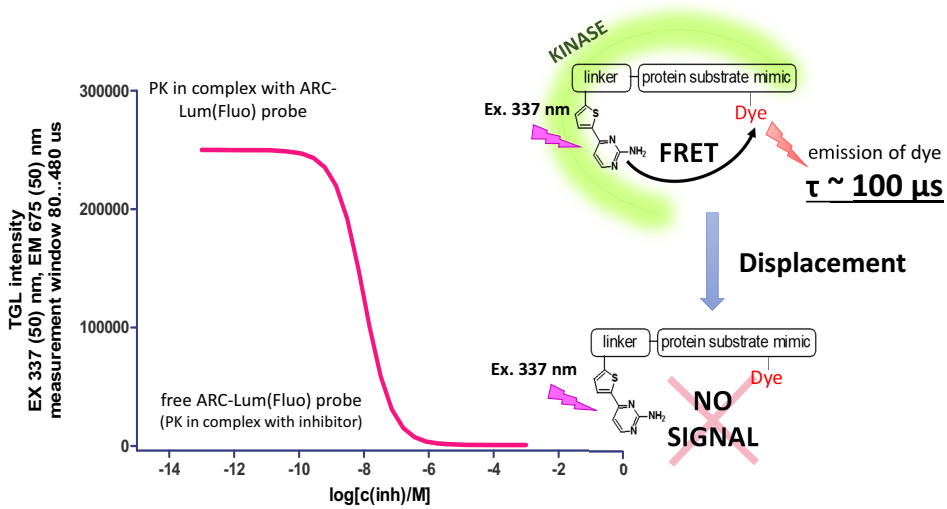

Figure 8. ARC-Lum(Fluo) probe displacement assay based on TGLI. In case of low concentration of the inhibitor, the probe is bound into the binding pocket of the PK, resulting in intramolecular triplet to singlet FRET of ARC-Lum(Fluo) probe and emission of TGLI signal. In case of high concentration of the inhibitor under evaluation, the inhibitor:PK complex is formed. The displaced free probe upon excitation at 337 nm possesses no TGLI signal at the emission wavelengths of the dye.

5.1.1.1. Determination of Optimal Concentrations of the Probe and PK

The cost of high-throughput screening (HTS) measurements is largely comprised of the price of reagents used in the assay system. Suitable measurement conditions should satisfy the economic aspects of the assay [low concentration of assay components (PK, probe, and inhibitor)], but also result in accurate and precise outcome.

We chose the enzyme PKAc, the probe ARC-1182, and three inhibitors [ARC-904, K_d (SD) = 0.22 (0.04) nM; ARC-1012, K_d (SD) = 2.5 (0.8) nM; ARC-1411, K_d (SD) = 0.003 (0.001) nM] for demonstration of the applicability range of the binding assay (Lavogina *et al.* 2009; Vaasa *et al.* 2009; Viht *et al.* 2007; Ivan *et al.* 2016; Enkvist *et al.* 2006).

The affinities of inhibitors under investigation dictate the suitable measurement conditions, thus the inhibitors under study were divided into two groups: inhibitors possessing higher-affinity than the probe ($K_{d,inh} < K_{D,probe}$) belonged to the first group and inhibitors with lower-affinity ($K_{d,inh} > K_{D,probe}$) formed the second group. Our first aim was to establish the optimal concentration of the enzyme (PKAc) and probe (ARC-1182, K_d = 0.02 nM with PKAc) for analysis of K_d. Concentrations of aforementioned assay components was varied and the choice of optimal measurement conditions was made according to the values of

the following quality parameters: Z′-factor, SD of data points, and number of outliers.

Taking into account the results of statistical tests and economic considerations, for characterization of a lower-affinity inhibitor (K_d > 0.02 nM) the optimal measurement conditions were established: c_{probe} = 0.5 nM, c_{PKAc} = 0.5 nM. Reliable evaluation of higher-affinity inhibitors should be performed also at c_{PKAc} = 0.5 nM. The choice of the concentration of the probe is dictated by the affinity of the inhibitor, as one key aspect for achieving accuracy is to ensure sufficient shift of IC_{50} value of the tested high-affinity inhibitor away from the tight-binding region. Thus, for evaluation of ARC-1411 it should be 10 nM, but for evaluation of inhibitors possessing even higher affinity (K_d < 0.003 nM) it should gradually higher (c_{probe} ≤80 nM).

5.1.1.2. Simulation of Resolvable Range of Inhibitor Affinities

Herein we propose a method for establishment of the resolvable affinity range of inhibitors using different assay setups. In practice, the K_d value is not directly determined from the measured data, instead it is converted from the IC_{50} value (total concentration of the inhibitor at the 50% displacement). The limit of resolvable K_d (LoK_d) values of the assay system could be determined at the point where the relationship between these two parameters (IC_{50} and K_d) starts to deviate significantly from linearity. According to the classical Cheng-Prusoff equation (Cheng and Prusoff 1973), if the determined IC_{50} value is below $10[E]_T$, the correlation deviates from linearity and IC_{50} values converge to the half-value of total concentration of PK ($1/2\ [E]_T$) in the assay system (Graph 1, blue dashed line). The latter value ($IC_{50} = 1/2[E]_T$) determines LoK_d in case of ideal, error-free measurement. In practice, the application of the classical Cheng-Prusoff equation below $IC_{50} = 10[E]_T$ leads to significant rise in measurement uncertainty. Thus, we suggest the determination of LoK_d at $IC_{50} = 10[E]_T$.

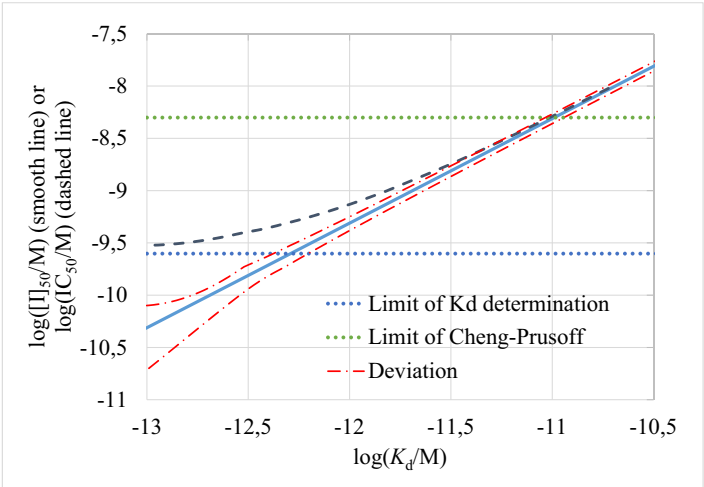

Graph 1. Defining the value of LoK_d. A) The relationship between $logK_d$ and $log[I]_{50}$ – blue smooth line, and between $logK_d$ and $logIC_{50}$ – blue dashed line, assay conditions: c_{PK} = 0.5 nM, c_{probe} = 10 nM, $K_{D,probe}$ = 0.02 nM. Limit of Cheng-Prusoff (green dotted line) indicates the lowest value of IC_{50} which obeys the Cheng-Prusoff equation $\{log[I]_{50}=log(10[E]_T)\}$. Limit of K_d determination (blue dotted line) indicates the limit from where the determination of K_d values is not reasonable due to the sensitivity of the determined values to measurement errors $\{log[I]_{50} =log(1/2[E]_T)\}$. The red dashed line reveals how the 10% deviation of IC_{50} values affects the precision of $log[I]_{50}$ and $logK_d$ values.

Another possibility is to convert IC_{50} to free concentration of the inhibitor at 50% of displacement ($[I]_{50}$) as follows: $[I]_{50} = IC_{50} - [EI]_{50}$, where $[EI]_{50}$ is the concentration of enzyme:inhibitor complex at 50% of the displacement. This conversion enables the linearization of the relationship between $K_{d,inh}$ and $[I]_{50}$ according to the logarithmic presentation of modified Cheng-Prusoff equation (6) (see Supplementary Material 3 of Paper III or paper by Nikolovska-Coleska *et al.*, 2004 for details):

$$log[I]_{50} = logK_{d,inh} + log\left(1 + \frac{[P]_{50}}{K_{D,probe}} + \frac{[E]_0}{K_{D,probe}}\right). \quad (6)$$

Compared to the classical Cheng-Prusoff equation, the modified Cheng-Prusoff equation is less affected by the measurement uncertainty up to $[I]_{50} = 1/2[E]_T$ (Graph 1, red dashed line and blue smooth line). Accordingly, we propose the application of the modified (and more precise) Cheng-Prusoff formula and the determination of LoK_d at $log[I]_{50} = log(1/2[E]_T)$ (Graph 1, blue dotted line).

Next, we plotted the results of the linearized and modified Cheng-Prusoff Equation (6) and determined LoK_d values at different assay conditions. The concentration of the probe applied in the displacement assay *mainly* pre-

determined the value of LoK_d. The difference in LoK_d values was 200-fold, from 12 pM (at 0.5 nM PKAc and 0.5 nM probe) to 60 fM (at 0.5 nM PKAc and 80 nM probe), simultaneously preserving good quality of the assay (Z' > 0.5). The upper threshold of the resolvable range of affinities, on the other hand, is limited by the artefacts (change in viscosity, optical interference, non-specific binding, solubility issues, *etc.*) related to required high concentration of inhibitor under investigation.

The wide dynamic range makes ARC-1182 an excellent photoluminescent probe for determination of affinity of PKAc inhibitors possessing widely variable binding properties. As a comparison, the LoK_d for commercially available LanthaScreen™ Eu Kinase Binding Assay applying time-resolved FRET measurements was calculated to be 20 pM (0.2 nM PKA, 100 nM probe) (Lebakken *et al.* 2009; Invitrogen). The main reason for much higher LoK_d value, compared to our method, was low affinity of the probe "Kinase Tracer 236" ($K_{D,PKA}$ = ~30 nM).

The public toolbox (http://www.ut.ee/medchem/toolbox-fluorescence-probes) can be used for creating the map of resolvable affinities (including LoK_d) for a variety of competitive probes at defined assay conditions.

5.1.1.3. Single Concentration and Full Displacement Curve Analysis

The single-concentration measurement is a rational, quick, and inexpensive method for screening compounds. Instead of construction of a full displacement curve, these measurements yield only one value corresponding to the displacement percentage of the probe from its complex with the PK at fixed concentration of the inhibitor. The obtained values could be converted to IC_{50} values according to equation (1). For reliability and accuracy reasons, the IC_x of the single-concentration measurement should remain between 0.1 × IC_{50} to 10 × IC_{50} corresponding to 9% to 91% displacement of the probe from the complex with the PK (Copeland 2013).

In order to compare the single concentration and full displacement curve assay, a random selection of inhibitors was analysed with both methods in similar conditions. Good correlation between the IC_{50} values obtained with these methods was demonstrated by R^2 = 0.97 (Graph 2). The latter result confirms the rationality behind the use of single concentration measurements at initial screening of compounds and assessment of affinity of inhibitors.

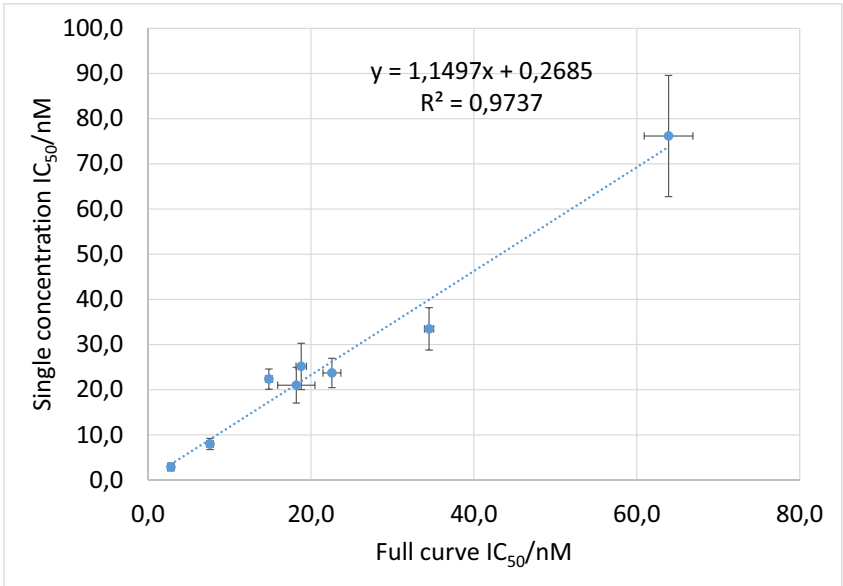

Graph 2. Correlation of IC_{50} values determined in a single concentration and full curve displacement assays.

Nevertheless, more precise K_d values of the selected inhibitors should be determined from full displacement curves. The previously discussed "map" facilitates a quick selection of the probe that possesses suitable concentration to affinity ratio and the concentration of the compound under evaluation (Fig. 10 in Paper III). The details of the full analysis can reveal additional information about the compound-PK interaction and errors made during the experimentation. For example, deviation from the steepness of the displacement from the expected value of -1 could point to possible pipetting errors, multiple binding sites of PK, nonspecific or tight-binding inhibition, aggregation or insolubility of the inhibitor (Copeland 2013).

To summarise, we introduced a method applying a non-metal photoluminescent protein binding-responsive probe [ARC-Lum(Fluo) probe] for determination of dissociation constants of competitive inhibitors of protein kinases. High affinity (K_d = 20 pM) and low background signal of the free probe supports the determination of dissociation constants of tight-binding as well as low affinity inhibitors. The lowest K_d value of 60 fM can be accurately determined with the method. We also introduced the graphical presentation of the linearized Cheng-Prusoff equation in Paper III and showed multiple possibilities for its application. Highlighting the quality and economic aspects of performing the measurements, the graphical presentation supports the decision making by reference to the assay conditions, calculation of LoK_d values, and convenient conversion of IC_{50} values to K_d values.

5.1.2. HPLC-UV/Vis Based Method for Quantifying the Intracellular Concentration of Biligand Probes and Inhibitors

There are several important properties of inhibitors that should be established for their successful implementation for cellular studies and drug development. Cellular uptake efficiency has gained less attention compared to inhibitory potency, selectivity, and cellular compartmentalization. Despite the importance, only a few papers quantify the uptake efficiency of inhibitors (Lucas *et al.* 2016; Kralj *et al.* 2013b).

In some cases, introduction of inhibitors to cells at lower concentrations is needed – for example, if applying inhibitors as optical probes (indicators) for mapping of concentration of PKs in cells. In this case, the intracellular concentration of the probe should be lower than concentration of PKs in cells. For application as drugs, often higher concentration is needed. In both cases, the probe/inhibitor has to compete with high (millimolar) concentration of cellular ATP, at the same time avoiding nonspecific interactions (Knight and Shokat 2005).

We developed a HPLC method for measuring the molar concentration of biligand inhibitors and probes of PKs in cells. The studied probe ARC-1042 comprised of ATP-site targeted fragment, a linker, a hexa-arginine moiety, and a fluorescent dye 5-TAMRA (Figure 9).

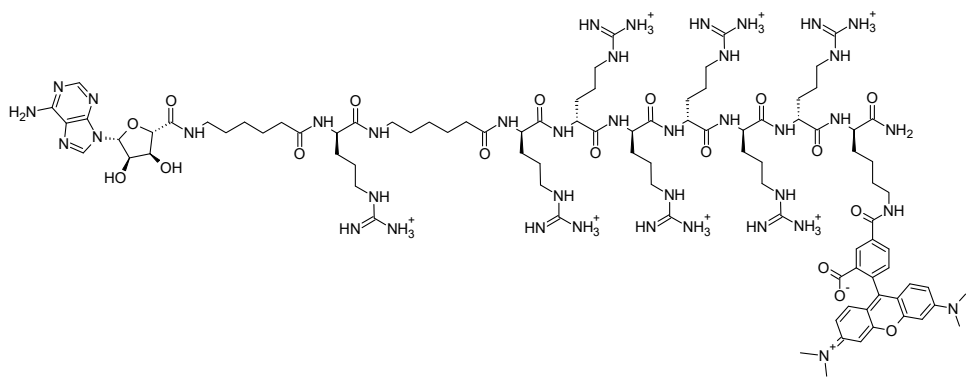

Figure 9. Structure of the biligand probe ARC-1042.

5.1.2.1. Intracellular Compartmentalization

We performed microscopy analysis of intracellular distribution of ARC-1042 for two reasons. First, we wanted to clarify the localization of the compound in cells. Second, it was necessary to establish that the internalised compound is not substantially bound to cell plasma membrane, as this could add complexity to reliable determination of its intracellular concentration.

Microscopy analyses revealed that ARC-1042 mostly localized in the cell nucleoli and cytoplasm, and less efficiently in the nucleoplasm of the tested

HeLa, MDCK, and PC-3 cells after 1 h incubation [Figure 10.A and Figure 7 in Ref. (Sinijarv 2013)]. Upon 24 h incubation period, ARC-1042 was perceptibly concentrated in nucleoli (Figure 10.B). In both cases, the images revealed low concentration of ARC-1042 in the plasma membrane – supporting the quantitative HPLC analysis of the compound in cells. Similar results have been obtained by the studies about uptake efficiency of arginine-rich-CPPs and other ARCs (Vaasa *et al.* 2010; Kasari *et al.* 2012; Ma *et al.* 2012; Tünnemann *et al.* 2008; Melikov *et al.* 2015). Previous studies suggest that the uptake mechanism of CPPs at 10 μM concentration is mainly direct penetration through the plasma membrane (Ma *et al.* 2012). The studies with a PK binding-responsive ARC-probe [ARC-Lum(Fluo) probe, see chapter 2.3.1.1] revealed that the signal from nucleoli and partially from cytoplasm could be related to ARC:PK complex. The cytoplasmic ARC was partially either freely in the cytoplasm or bound to other cellular proteins (Vaasa *et al.* 2012). As the reference compound ARC-1042 is structurally analogous to the particular ARC-Lum(Fluo) probe, similar behaviour could be expected.

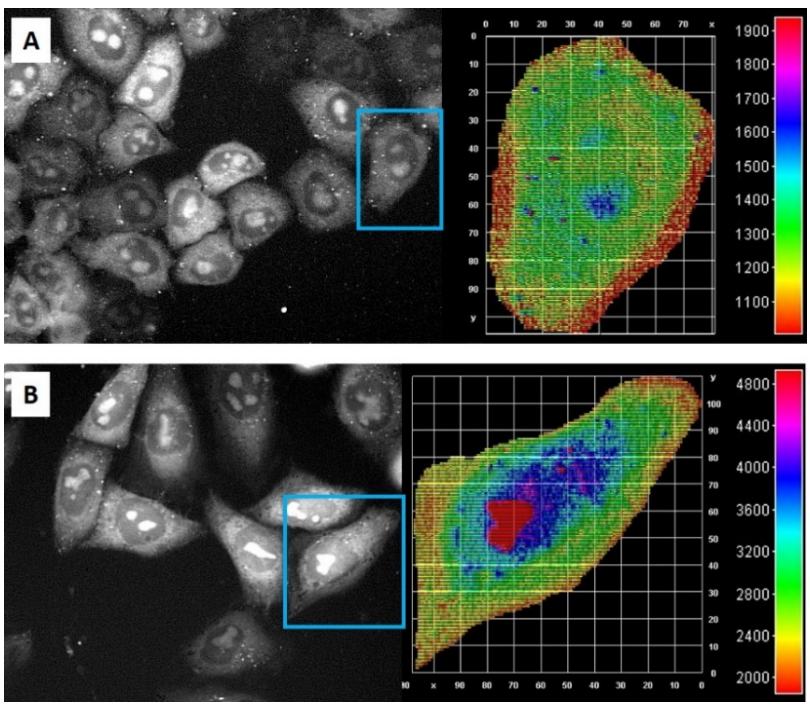

Figure 10. Fluorescence microscopy images of localisation of ARC-1042 in HeLa cells and corresponding colour intensity plots. **A)** Incubation with 10 μM ARC-1042 for 1 h. **B)** Incubation with 10 μM ARC-1042 for 24 h.

Strong fluorescence intensity apparent in all cells pointed to efficient cellular uptake of ARC-1042 by all cells, whereby the average integrated fluorescence intensity (FI) was rather similar in different cells [FI(1 h) = (1400 ± 200) AU; FI(24 h) = (3100 ± 300) AU; n(cells) = 31, Figure 11]. The increase in the FI of cells incubated for 24 h compared to that of cells incubated only for 1 h points to substantial (two-fold) increase of intracellular concentration of the compound. The colour plot (Figure 10.B) demonstrates at least two-fold higher concentration in the nucleoli compared to that of cytoplasm after a 24-hour incubation period in certain cells. Yet, this kind of contrast between distinct cellular compartments is not valid in case of all cells.

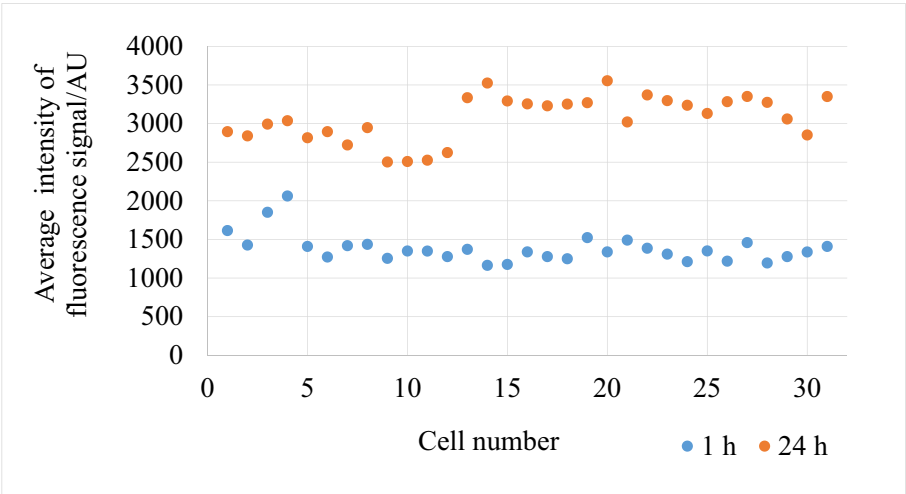

Figure 11. Average integrated intensity of fluorescence signal of a single cell incubated for 1 h (blue) or 24 h (orange) with 10 µM ARC-1042.

5.1.2.2. Determination of Intracellular Concentration

The developed HPLC-UV methodology took into account the number, size, and viability of the cells to present the intracellular molar concentration of the compounds (Figure 12, Equation 4). The control over loss of analyte during sample preparation was achieved by applying an internal standard [detailed information in Ref. (Sinijarv 2013)]. The limit of quantification (LoQ) of ARC-1042 in the analytical sample with the developed HPLC-UV method was 9.7 pmol.

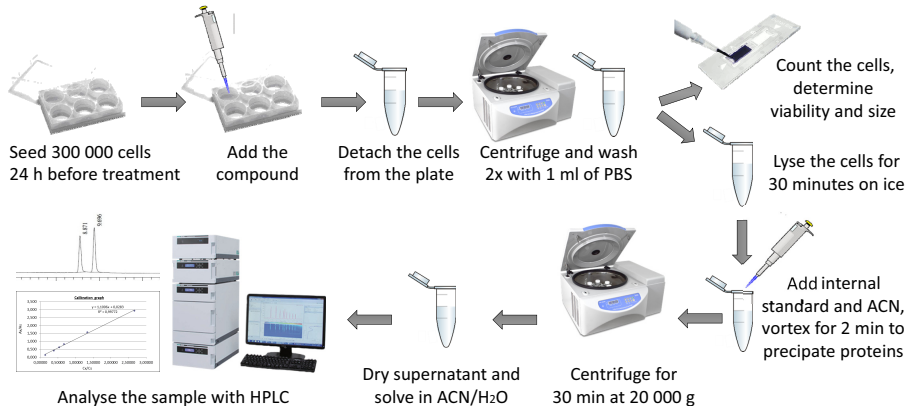

Figure 12. Methodology for determination of intracellular concentration of ARCs.

The method was implemented to check how the intracellular concentration depends on the incubation time and concentration of the compound in the incubation solution. MDCK, HeLa, and PC-3 cells were incubated with 10 μM ARC-1042 for 1 h to 96 h (Figure 13.A). The uptake trends were similar in case of MDCK and HeLa cells, PC-3 cells revealed slightly different concentrations of the compound in the cells. The highest intracellular concentration of ARC [(352 ± 41) μM] was found in MDCK cells (72 h incubation).

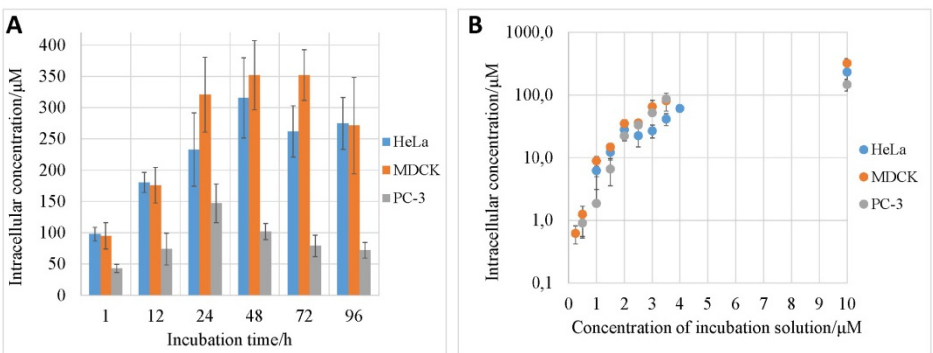

Figure 13. A) Intracellular concentration of ARC-1042 after various incubation times. Concentration of ARC-1042 in incubation solution was 10 μM. **B)** Uptake of ARC-1042 at different concentrations of incubation solution, incubation time 24 h. Analyses were performed on three different days with three replicates each day. Data are expressed as average values of these measurements with combined uncertainty.

Results of HPLC and fluorescence microscopy analyses were in good concurrence. The ratio of integrated FI values of 24 h and 1 h incubation in HeLa cells from microscopy experiments was 2.2, while the ratio of corresponding intracellular concentrations was 2.4. Approximate information about the concentration distribution within different cellular compartments could be also given by comparing the FI values with the average intracellular concentration of the compound. The average intracellular concentration after 24-hour incubation with 10 μM ARC-1042 in HeLa cells was (233 ± 58) μM, and the corresponding average FI was (3100 ± 300) AU (Figure 10.B). As the FI in nucleoli of the chosen cell was more than 4800 AU, the particular concentration of the compound in nucleoli could be (in case of linear relationship between the concentration and FI) more than 360 μM, simultaneously the FI in the cytoplasm was approximately 2400 AU, pointing to 180 μM concentration.

The cells were next incubated with 0.25…10 μM ARC-1042 for 24 h which led to 1.8…25-fold higher concentration of the compound in cells compared to that in the incubation solution (Figure 13.B). The shape of the graph could indicate increased proportion of directly penetrated (over endosomatically internalized) ARC-1042 as the concentration of incubation solution increases. This result is in concurrence with the general understanding of the dependence of uptake mechanism and extent on applied concentration of the arginine-rich compound (see section about CPPs in paragraph 2.2.2). Overall, the results of experiments with ARC-1042 demonstrated the possibility of regulation of the intracellular concentration of the probe in wide range, based on varying the concentration of the probe in the incubation medium and incubation time. The developed method could be also applied for analyses of intracellular concentration of various other inhibitors and probes.

5.2. BIOLOGICAL EFFECT OF CELL-PENETRATING BILIGAND INHIBITORS OF PKS

Recently, we showed that the *in vitro* potency and selectivity of PK inhibition can be remarkably increased by the biligand inhibitor approach (Lavogina *et al.* 2010a), *i.e.*, construction of conjugates that simultaneously occupy the binding sites of both the phospho-donor nucleotide and phospho-acceptor protein substrate of the PK. In this study, we developed two types of high-affinity and cell plasma membrane permeable biligand inhibitors: targeting either basophilic (*e.g.,* PKA) or acidophilic kinases (*e.g.,* CK2). Our aim was to establish the effectiveness of biligand inhibitors to suppress the phosphorylation of proteins in cells and to affect the viability of cells.

5.2.1. Biligand Inhibitors of Basophilic PKs (PAPER I)

Biligand inhibitors targeting basophilic protein kinases usually comprise positively charged amino acids in the peptide-mimicking moiety. Besides contributing to binding affinity, arginines support the uptake of these compounds. HPLC-based analysis according to the method described in chapter 5.1.2 demonstrated that previously developed ARC-type biligand inhibitors of basophilic PKs are intensively taken up by cells – a ten-fold higher intracellular concentration of the compound compared to their concentration in the incubation medium was achieved. In earlier studies it was demonstrated that myristoylated oligo-arginines possess even better cellular uptake than their non-acylated arginine-rich peptide counterparts (Lee and Tung 2010). In this regard, *N*-myristylation of ARCs was used for further improvement of the cellular uptake of the conjugates (Figure 14).

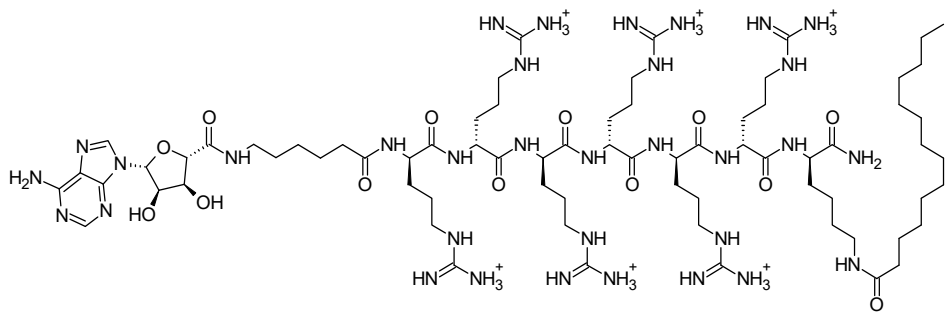

Figure 14. Structure of ARC-1222, comprising a myristoyl group conjugated via the C-terminal lysine residue.

The biochemical affinity (K_d) of the developed compounds towards PKAc was determined with ARC-Lum-based assay described in Papers I and III using the selenophene-comprising probe ARC-1139 (Figure 1 in Paper I). The K_d of non-myristoylated compound ARC-904 was approximately 10-fold lower (0.4 nM) compared to the myristoylated ARC-1222 (3.7 nM), both still remaining in the high-affinity range. Also, the acylated ARC bound to PKAc three-fold more tightly than H89 – a well-characterised commercially available ATP-competitive inhibitor of PKAc (K_d = 10 nM) (Davies *et al.* 2000).

HPLC-analyses demonstrated that the uptake of myristoylated ARC-1222 by the CHO cells was approximately 3-fold more efficient compared to its non-myristoylated counterpart ARC-904. 1 h incubation with 10 μM ARC-1222 lead to 300 μM intracellular concentration. High affinity towards PKAc, high rate of cellular accumulation, and the great structural stability of ARCs in cellular milieu (Enkvist *et al.* 2006) pointed to the applicability of ARCs for regulation of intracellular protein phosphorylation balances. Several important cellular

signalling cascades are started by activation of PKA. For instance, CREB induces gene transcription after being phosphorylated at Ser133 by PKA or other PKs (Johannessen *et al.* 2004).

We monitored how inhibitors of PKA affect phosphorylation of CREB (Figure 1) with an immunoblot-based protein phosphorylation assay. While H89 and ARC-1222 (each at 10 μM) suppressed forskolin-induced phosphorylation of CREB, ARC-904 caused no significant change in CREB phosphorylation balance (Figure 15.A). The inhibitory potency of ARC-1222 was higher probably due to better cell membrane penetrative properties and despite the lower binding affinity towards PKAc compared to ARC-904. More efficient inhibition of the cAMP/PKA pathway by H89 relative to its three fold lower affinity compared to ARCs may be (partially) due to its better internalization into cells and localisation to the cell nucleus where it can act on a target PK, PKAc.

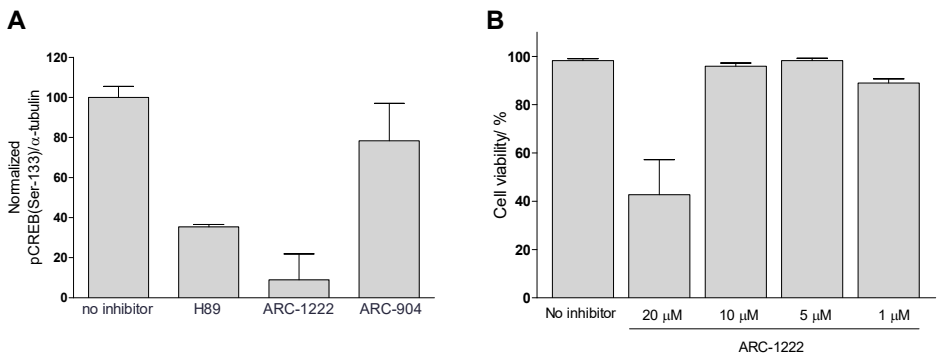

Figure 15. **A)** The effect of H89, ARC-1222, and ARC-904 on the phosphorylation of CREB in CHO cells. Cells were treated with 10 μM compound for 1 h, and then stimulated with 10 μM forskolin for 30 min. The data concerning inhibitor-treated cells was normalised relative to the ratio of integrated intensities of the bands of phospho-CREB and α-tubulin of non-treated cells (n = 3, average ± SDM). **B)** Cell viability determined by trypan blue exclusion test. The CHO cells were incubated with 1… 20 μM ARC-1222 for 1 h and then treated with 0.4% trypan blue stain (n = 4, average ± SDM).

To test the cytotoxic effect of the compound, cell viability was determined in assays with Trypan Blue (Figure 15.B). After 1 h incubation with ARC-1222 at 1…10 μM, the viability of the cells varied from 100% to 80%. At 20 μM ARC-1222 the viability was substantially reduced (<50% of the control). The effect of myristoylated compound on the cell viability at high concentration might be the result of membrane destruction (Brock 2014; Shai *et al.* 2006). However, the relatively high cell viability over 1…10 μM ARC-1222 shows that the change in the luciferase activity and CREB phosphorylation is likely to be caused by the inhibition of PKAc and not by cytotoxicity of the compound.

As demonstrated in the present study, the improvement of cellular inhibitory potency of ARCs targeting basophilic PKs could be achieved with simple structural modification of the conjugates, *N*-myristoylation of ARCs. This result points to the importance of further research on structural modifications of ARCs that could lead to their better intracellular targeting, improved availability by nuclear PKs, and inhibition of PKs.

5.2.1. Biligand Inhibitors of CK2 (Paper II and IV)

As for other PKs, the development of inhibitors of CK2 has been mainly focused to nucleotide-competitive inhibitors. ATP-competitive CX-4945, the only CK2 inhibitor that has reached clinical trials, is the most successful example. Development of substrate protein competitive or biligand inhibitors of CK2 has not been popular as the acidophilic nature of CK2 dictates the need for negatively charged peptide sequences, making these compounds poorly plasma membrane permeable. Nevertheless, we aimed to develop cell plasma membrane permeable biligand inhibitors as they are potentially more selective and potent compared to ATP-competitive inhibitors.

5.2.2.1. Acetoxymethyl Ester of Tetrabromobenzimidazole-Peptoid Conjugate for Inhibition of CK2 in Living Cells

We had previously developed selective high-affinity (K_d <1 nM) biligand inhibitors (ARCs) for CK2 that were suitable for biochemical studies, but due to poor proteolytic stability and plasma membrane permeability, the compounds were not suitable for cellular studies (Ekambaram *et al.* 2014; Enkvist *et al.* 2012). Here, the structure of CK2-targeted ARCs was modified for the application in live cells. The oligo-aspartate moiety present in previously reported structures (Vahter *et al.* 2017; Enkvist *et al.* 2012) was replaced with the corresponding carboxylate-rich peptoid chain comprising *N*-carboxymethylglycine (iminodiacetic acid, Ida) residues. Proteolytically stable achiral oligoanionic peptoid conjugates of 4,5,6,7-tetrabromo-1*H*-benzimidazole (TBBz) were constructed and ARC-1842 [$K_{d,CK2}$ = (8.7 ± 0.7) nM] was chosen for further studies on cells. The oligocarboxylic acid part of the inhibitor was modified for increasing its stability in biofluids (Miller *et al.* 1995) and for enabling its loading into cell in the form of per-acetoxymethyl (AM) ester prodrug (Figure 16).

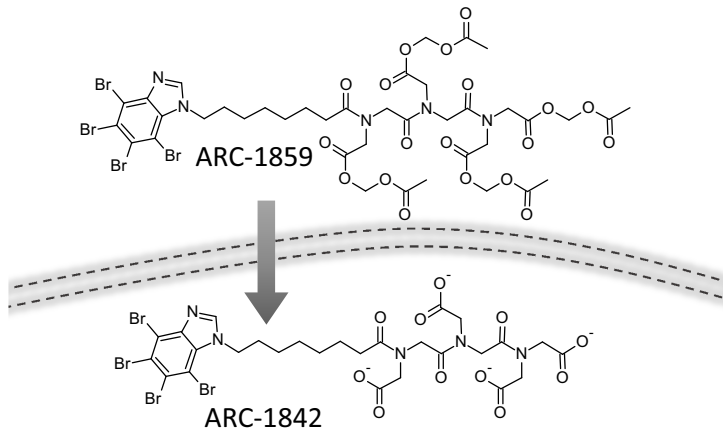

Figure 16. Schematic presentation of cellular uptake of per-esterified compound ARC-1859 that is hydrolysed to ARC-1842 by esterases in cells.

The inhibition potency of CK2 inhibitors was investigated in MIA PaCa-2 cells. Western blot analysis was performed for determination of the phosphorylation status of two CK2 substrates: Cdc37 and NFκB. Treatment of cells with 10 μM ARC-1859 (AM-form of ARC-1842, Figure 17.A) decreased the phosphorylation level of the substrates by the same extent as the control inhibitor CX-4945 at the same concentration. Controversially, ARC-1842 did not have significant influence on the phosphorylation balance as expected because of poor uptake of the non-esterified conjugate.

As inhibition of CK2 in cells leads to activation of CASP3 and thereafter to apoptosis [Figure 2.B (Turowec *et al.* 2013; Duncan *et al.* 2011)], the effect of CK2 inhibitors on the viability of HeLa and MIA PaCa-2 cells was studied. ARC-1859 showed concentration-dependent reduction of viability for both types of cells (Figure 17.B, Supporting Information Figure S5 in Paper II). There were about 60% of viable cells after 24 h treatment with 10 μM ARC-1859 and 50% after 48 h treatment. On the contrary, no effect with ARC-1842 was observed in the course of the experiments (Figure 17.B, Supporting Information Figure S5 in Paper II). The effect of CX-4945 on cell viability was similar to that of ARC-1859 in HeLa cells. TBBz was used as the reference compound in HeLa cell line that at 10 μM concentration caused about 20% of loss of viability after 24 h incubation and 50% after 48 h incubation (Figure 17.B, Figure 5.B in Paper II). Although TBBz has more than 70-fold lower affinity towards CK2 compared to the conjugate of TBBz and oligoanionic peptoid (Table 1 in Paper II), it induces cellular death to a similar extent. The latter phenomenon could be explained by nonspecific interactions of TBBz with other ATP-binding proteins that are essential for cell viability (Duncan *et al.* 2008).

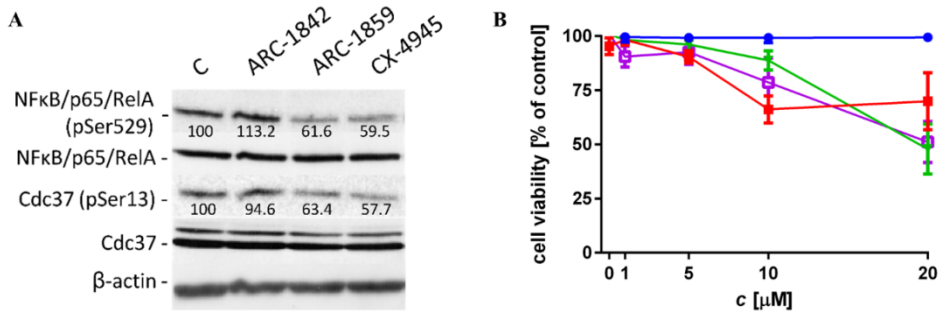

Figure 17. A) Western blot analysis of whole lysates from MIA PaCa-2 cells. Control (C) experiment refers to cells treated with vehicle (0.1% DMSO v/v). β-actin measurement was used as the control for equal loading. Values beneath protein bands refer to the results of densitometric analysis of integrated band intensities expressed in percentage values. Cells were incubated with 10 μM ARC-1842, ARC-1859, or CX-4945 for 5 h. **B)** Cytotoxic effect of ARC-1842 (blue ●), ARC-1859 (red ■), CX-4945 (green ▼) or TBBz (purple □) in HeLa cells (trypan blue test). Control experiment (c = 0) refers to cells treated with vehicle (DMSO and Pluronic F-127). HeLa cells were treated for 24 h with increasing concentrations of compounds, as indicated. The reported values represent the means ± SD from three parallel experiments.

To the best of our knowledge, this is the first study of the application of AM ester loading technique to enhance the bioavailability of compounds comprising an oligoanionic peptoid backbone. This technique also represents a general approach for designing cell-permeable prodrugs of highly potent and selective biligand inhibitors of CK2.

5.2.2.2. Construction of Selective and Cell-Penetrating Biligand Inhibitors of CK2

Although TBBz and its biligand conjugates revealed good inhibitory potency, the moiety also accompanies several disadvantages (selectivity, solubility, and non-specific binding issues). Thus, our next aim was to change the fragment targeting the nucleotide binding pocket of CK2 to a more promising hetero-aromatic moiety. 4-(2-amino-1,3-thiazol-5-yl)benzoic acid (ATB) moiety possesses several outstanding properties for the construction of biligand inhibitors. First, it is less hydrophobic compared to TBBz. Second, it has remarkable affinity towards CK2 and its cellular activity has been demonstrated (Hou *et al.* 2012). Third, the moiety possesses good fluorescence properties, which enables its sensitive quantification with HPLC (Figure S. 1 in Paper IV).

Length of the linker connecting ATB moiety to the peptoid composed of *N*-carboxymethylglycine (iminodiacetic acid, Ida) residues was optimized for gaining high affinity of the inhibitor. Based on the affinity analysis (Table 1, compounds 1…6 in Paper IV) the linker comprising succinic acid and 12-

aminododecanoic acid residues connected via *N*-carboxymethylated amide bond was chosen for further studies. As for other previously reported biligand inhibitors of CK2 (Viht *et al.* 2015), binding affinity increased with the number of Ida-residues in the peptoid chain. Among the constructed inhibitors, conjugate with 5 Ida residues reached the lowest K_d value of 40 pM. However, taking into account molecular weight, structural complexity, and binding affinity, the compound comprising 3 Ida residues [ARC-772, $K_{d,CK2}$ = (0.3 ± 0.1) nM, Figure 18] was considered structurally more promising for cellular experiments in the present study.

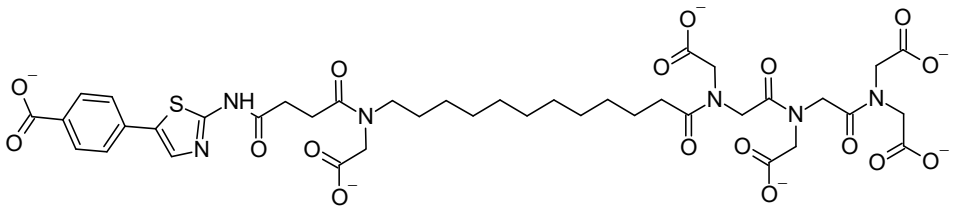

Figure 18. Structure of ARC-772.

The inhibition selectivity of ARC-772 was tested in a commercial panel of 140 PKs to discover the off-targets of the inhibitor (Figure 19, Table 2 in Paper IV). ARC-772 revealed Gini coefficient of 0.752 and hit rate of 0.05, which highlighted the good selectivity of the compound. The hit rate demonstrated that among the tested PKs only 5% (including CK2, 3 PKs of the DYRK family, BRSK1, BRSK2, and TAO1) were inhibited more than 50%.

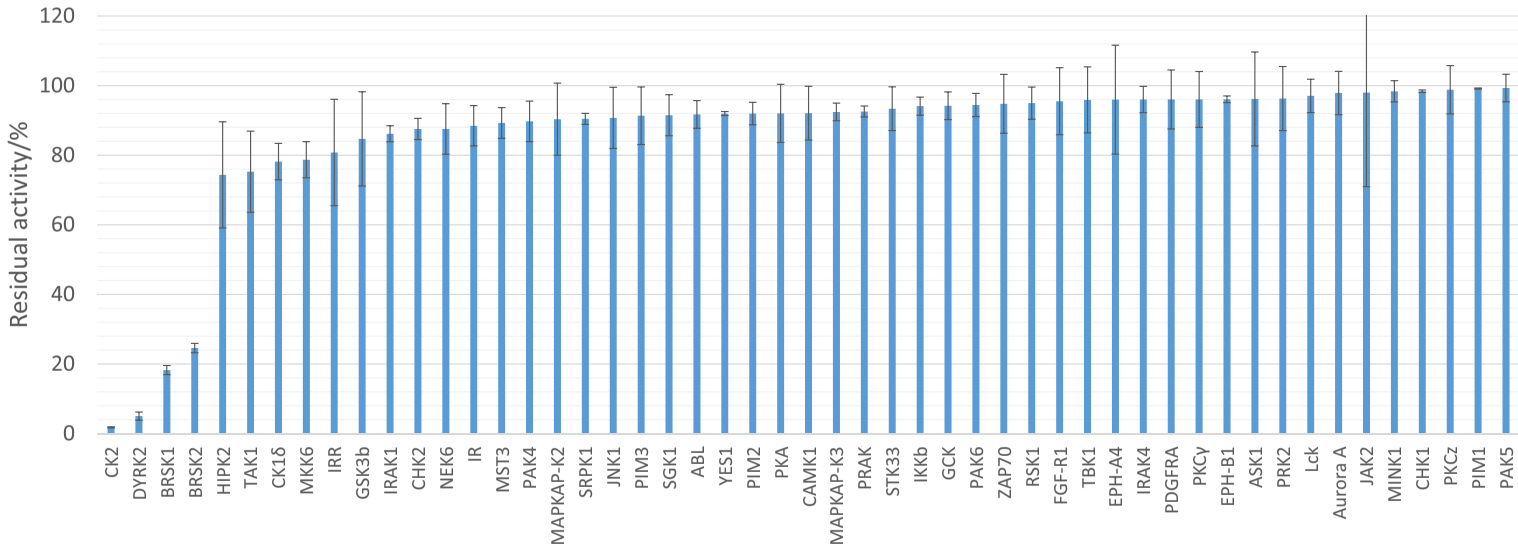

Figure 19. Inhibition selectivity of ARC-772 (c = 100 nM) presented in the percentage scale of residual activities of PKs (a selection from 140 tested PKs).

5.2.2.2.1. Intracellular Delivery

Similarly to our previously developed biligand CK2 inhibitor ARC-1842 (described in Paper II and chapter 5.2.2.1), ARC-772 possessed properties like good affinity and selectivity, accompanied with low cellular accumulation. Although the per-esterification technique applied in Paper II supported the plasma membrane penetration of the negatively charged compound, it was in our interest to compare the efficiency of other technologies for transport of ARC-772 into cells. Five different technologies were tested for the delivery of ARC-772 into cells (Figure 20): conjugation of the ligand with folic acid (Sudimack and Lee 2000), RPARPAR (Simón-Gracia *et al.* 2016), or $(L\text{-}Arg)_9$ moiety (Trabulo *et al.* 2010); masking the negatively charged carboxyl groups as esters (Viht *et al.* 2015); and encapsulating ARC-772 into micelles of the transfection reagent TurboFect. In order to enable attachment of various transporters to ARC-772, a sulfhydryl group was added to the C-terminus of the peptoid [Scheme S. 1.E, compound 11 (ARC-772-SH) in Paper IV]. Two of the applied delivering techniques have been used for specific targeting of cancerous cells; the uptake mechanisms included receptor-mediated endocytosis. First, folate receptor-mediated delivery of the folate conjugated compound (ARC-778) and, secondly, neuropilin-1 receptor (NRP-1) mediated delivery of the compound conjugated with RPARPAR peptide (ARC-791).

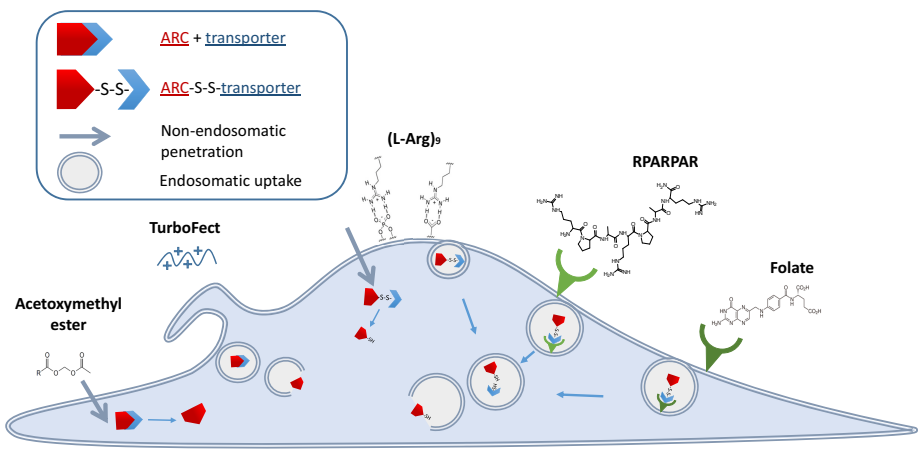

Figure 20. Scheme of delivery systems used for the transport of ARC-772 into cells.

The efficiency of uptake techniques was compared by determining the intracellular concentration of the compound after 12 h incubation with HeLa cells. We applied the HPLC method described in chapter 5.1.2, with the difference of detecting fluorescence intensity derived from the ATB moiety. The limit of quantification (LoQ) of the RP-HPLC-FL methodology was 5.1 fmol.

ARC-772 without any transporter penetrated the cell plasma membrane poorly, leading to low micromolar intracellular concentration (Figure 21). Despite the overexpression of folate receptors (Sudimack and Lee 2000; Paulos *et al.* 2004; Saul *et al.* 2003) as well as NRP-1 receptors (Bagri *et al.* 2009; Pellet-Many *et al.* 2008) in cancerous cells, these receptor-mediated transport techniques did not enhance the uptake efficiency of the compound. Similarly, no significant uptake enhancement was gained with conjugation of transport peptide $(L\text{-}Arg)_9$ to ARC-772-SH (code of conjugate:ARC-783). The latter could be explained by both, inefficient endosomatic uptake (Ma *et al.* 2012) and masking of positively charged guanidinium groups of $(L\text{-}Arg)_9$ with the negatively charged carboxyl groups of ARC-772-SH. Commercially available transfection reagent TurboFect is mostly used for introducing nucleic acids into eukaryotic cells. Despite the numerous positive charges of the transfection reagent suitable for forming charge-charge interactions with ARC-772, it did not substantially enhance the uptake of ARC-772 upon 12 h incubation.

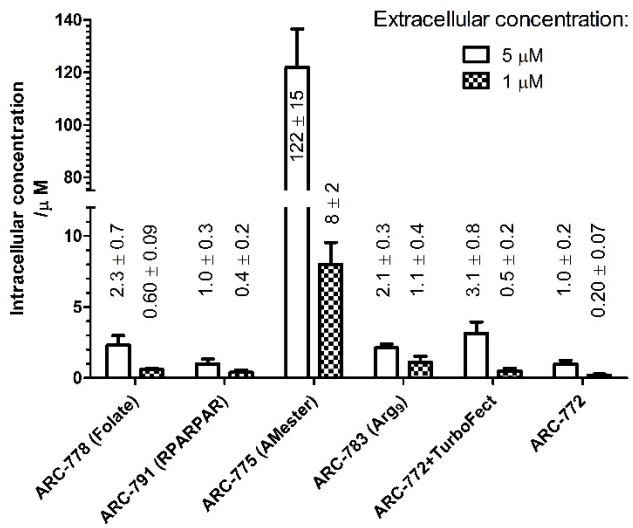

Figure 21. Comparison of the efficiency of different internalization methods on basis of the intracellular concentration of ARC-772 in HeLa cells (n = 3) as determined with HPLC analysis. Incubation solution containing the compound at 5 μM or 1 μM concentration (extracellular concentration) was applied on the cells for 12 hours.

Remarkably efficient uptake of the inhibitor ARC-772 was achieved if it was used in the form of per-acetoxymethyl ester prodrug of the compound, ARC-775. The treatment of cells with 5 μM solution of ARC-775 led to more than 100 μM intracellular concentration of ARC-772. Inside cellular milieu, the ester groups of ARC-775 are hydrolysed by esterases within less than an hour. Hydrolysed compound is thereafter trapped in cells and possesses full activity for its interaction with CK2 (Viht *et al.* 2015).

We explain the modest uptake efficiency of the tested techniques [conjugation of folate, RPARPAR or $(L\text{-}Arg)_9$, or micellization with TurboFect] with the following hypothesis. All of these technologies used different types of endocytosis mechanisms for uptake and the bonds between inhibitor and transport system or receptor and transport system were destabilised in the acidic environment of the endosome (pH 5.5…6.5, depending on the development stage of the endosome). First, in case of charge-charge interactions [*e.g.,* between TurboFect and ARC-772, or folate and RPARPAR with corresponding receptors] the acidic environment affected the binding affinity. Second, when a disulphide bridge was applied to connect transport system and inhibitor, the acidic environment enhanced the enzymatic reduction of disulphide bond (Arunachalam *et al.* 2000). Once the bond between the transporter and inhibitor is destabilised, it is highly likely, that the negatively charged ARC-772 (or ARC-772-SH) does not effectively escape to the cytosol. In case of folate and RPARPAR technologies the limiting factor is also the recycling efficiency and the number of the corresponding receptors.

The cellular accumulation of per-esterified compound ARC-775 was further tested upon 1 h, 5 h, and 12 h incubation period (Figure 22). Approximately 20-fold increase of concentration of ARC-772 was recorded in cells, compared to concentration of the prodrug ARC-775 in incubation solution (tested at extracellular concentrations of 0.5 μM, 1.0 μM, and 5.0 μM; 5 h incubation). The concentration in cells was somewhat reduced at 12 h time point that may point to activation of apoptotic or other processes leading to cell death and export of ARC-772 from cells. Moreover, as the difference in intracellular concentration after 5 h and 12 h incubation with 5.0 μM ARC-775 was not significant, ARC-772 is probably excreted as constant, not proportional amounts.

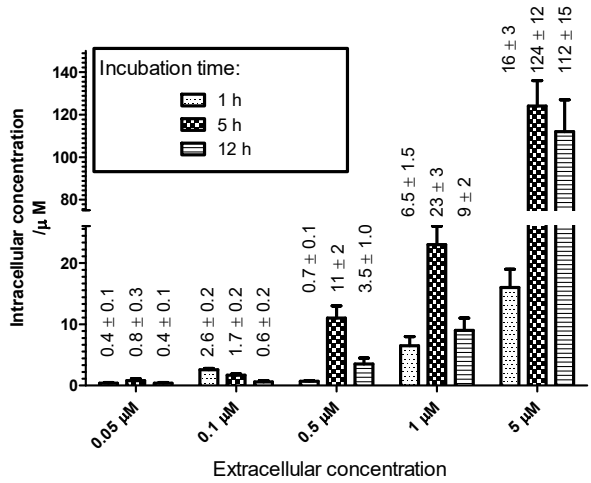

Figure 22. Intracellular concentration of ARC-772 in HeLa cells after treatment of the cells with various concentrations of ARC-775 for 1 h, 5 h, or 12 h, n = 3.

5.2.2.2.2. Regulation of Cell's Physiology

In case of negatively charged ARCs the prodrug approach leads to very high intracellular concentration as after hydrolysis of ester groups the drug is trapped in cells. The functionality of ARC-772 as an inhibitor was demonstrated in three types of assay: determination of the phosphorylation level of a CK2 substrate protein Cdc37; determination of activity of CASP3 (by monitoring the cleavage of FRET probe GFP-Asp-Glu-Val-Asp-RFP); and measurement of the effect on platelet aggregation (Figure 23).

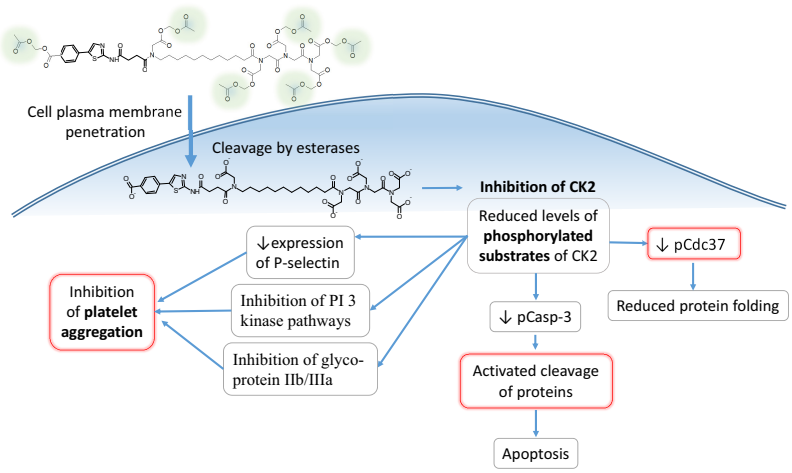

Figure 23. Upon penetration of cell plasma membrane, the prodrug ARC-775 is modified by esterases into its active form ARC-772. The efficiency of the inhibitor in the cellular milieu is demonstrated by three assays (written in bold).

Inhibition of Phosphorylation of Substrate-Protein Cdc37

CK2 mediated phosphorylation of kinase-specific co-chaperone Cdc37 is critical for binding of PKs and activity of chaperone Hsp90 [Figure 2.A (MacLean and Picard 2003)]. Active Cdc37 assists the correct folding and functions of many signalling PKs. Cdc37 also plays a role in mediating the development of cancer by stabilizing the compromised structures of oncogenic kinases (Pearl 2005; Gray *et al.* 2008). Accordingly, inhibition of CK2 may result in numerous benefits.

We tested the efficiency of developed prodrug ARC-775 and compared its effect with the efficiency of well-known control compound, CK2 inhibitor CX-4945. Treatment of cancerous HeLa cells with ARC-775 or CX-4945 resulted in efficient inhibition of CK2-catalyzed phosphorylation of Cdc37 at Ser13. The average pCdc37/Cdc37 ratio (compared to that of control) of ARC-775 (5 μM) treated cells was (44 ± 8)% after 5 h and (36 ± 7)% after 12 h incubation, CX-4945 revealed phosphorylation level of (72 ± 10)% after 5 h and (55 ± 8)% after 12 h incubation (Figure 24). It was recently shown that even in case of full exclusion of CK2 activity in cells does not lead to full disappearance of pCdc37 from cells (Franchin *et al.* 2017b), meaning that other PKs can to some extent replace CK2 as phosphorylation catalysts. In conclusion, the results support the use of oligoanionic biligand inhibitors in the form of per-esterified prodrug for targeting CK2 in cells to affect the activity of Cdc37.

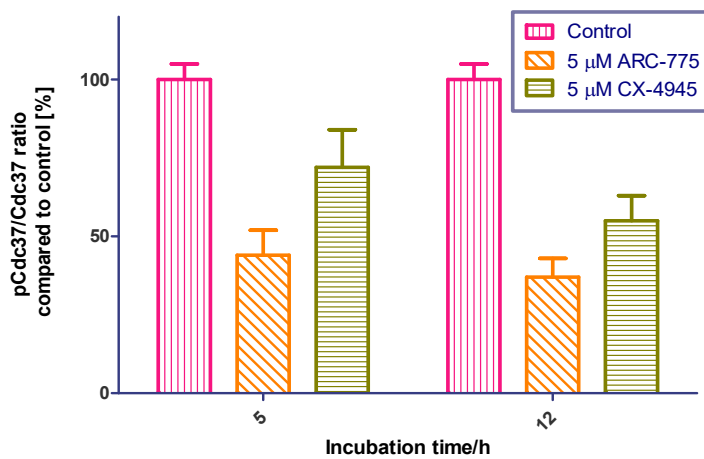

Figure 24. Average pCdc37/Cdc37 ratio results of HeLa cells (n = 3). Control is the pCdc37/Cdc37 ratio in untreated cells.

Affecting the Activity of CASP3

Activation of CASP3 induces apoptosis, thus the former process can be used to characterise molecular regulators of programmed cell death. The role of caspases in apoptosis is regulated by the CK2-dependent phosphorylation in many

ways (Turowec *et al.* 2013; Duncan *et al.* 2011). First, phosphorylated target proteins are not cleaved by CASP3. Second, phosphorylated procaspase-3 is protected from cleavage by CASP8 and CASP9, which, in turn, prevents the activation of CASP3. Third, the phosphorylation of CASP3 by CK2 directly inactivates it (Figure 2.B). Therefore we studied the effect of three inhibitors on activity of CASP3. While CX-4945 and ARC-775, probably, affect the activity of CASP3 as CK2 inhibitors, effect of Staurosporine on CASP3 is complex as it inhibits many PKs simultaneously (Belmokhtar *et al.* 2001; Karaman *et al.* 2008).

The activation of CASP3 upon treatment of cells with PK inhibitors is clearly seen in case of both, cancerous HeLa cells and noncancerous CHO cells. However, the kinetic profiles were substantially dependent on type of the cell line and origin of the tested compound. The maximal activity of CASP3 was achieved upon 12 h treatment of HeLa cells with ARC-775, whereas CX-4945 and Staurosporine showed faster effect – it took 8 h and 4 h to achieve maximal activity of CASP3, accordingly (Figure 25.A). In case of noncancerous CHO cells, the activation kinetics of CASP3 was substantially slower for all compounds (Figure 25.B). As it has been reported previously, the time-scale of induction of apoptosis for Staurosporine is dependent on the particular apoptotic pathway – the caspase dependent pathway was quicker (3 h), and caspase independent pathway slower (>12 h) (Belmokhtar *et al.* 2001). In case of CK2 inhibitors CX-4945 and ARC-775, the apoptosis should be induced by caspase-dependent pathway, nevertheless the activation of CASP3 was delayed. The non-compliance for ARC-775 could be partly explained by the extra time needed for the de-esterification of the prodrug [up to an hour (Viht *et al.* 2015)], but the reason(s) of the overall slow kinetics is unclear and needs further investigation.

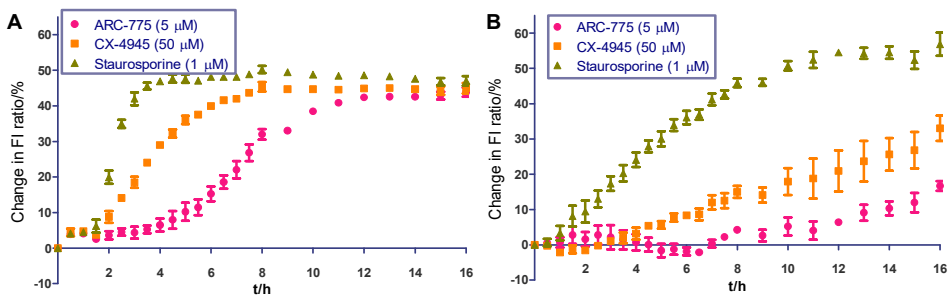

Figure 25. Kinetics of CASP3 activity during treatment with ARC-775 (5 µM), CX-4945 (50 µM), and Staurosporine (1 µM) in HeLa (**A**) and CHO cells (**B**), n = 2…4.

The comparison of EC_{50} values of caspase activation (Table 2) for cancerous HeLa cells and noncancerous CHO cells confirms the previous knowledge: the viability of cancerous cells is more reliant on the activity of CK2 than that of non-cancerous cells (Siddiqui-Jain *et al.* 2010; Ruzzene and Pinna 2010). Thus the effect of ARC-775 on CASP3 activation in cancerous HeLa cells is more conspicuous than that of CX-4945 and Staurosporine. The ratio in the EC_{50} values found for these compounds in HeLa and CHO cells was 53-, 5.5-, and 3-fold, respectively. These results support further investigation of ARC-775 as a cancer cell-selective prodrug.

Table 2. EC_{50} values determined from the dose–response curves of ARC-775, CX-4945, and staurosporine for HeLa and CHO cells

Cell line	Compound	(EC_{50} ± SD)/μM
CHO	ARC-775	~16
	CX-4945	36 ± 2
	Staurosporine	0.09 ± 0.01
HeLa	ARC-775	0.3 ± 0.1
	CX-4945	6.5 ± 1.1
	Staurosporine	0.03 ± 0.01

Inhibition of Aggregation of Platelets

Previous findings indicate that CK2 regulates multiple interaction mechanisms that mediate the activity of platelets (Nakanishi *et al.* 2008; Ryu and Kim 2013; Ampofo *et al.* 2015; Hoyt *et al.* 1994). Therefore, inhibition of CK2 may contribute to the future treatment of diseases which accompany thrombosis. Here, the effect of CK2 inhibitors and Forskolin on the ADP-induced aggregation of human platelets was studied. CK2 inhibitors lower the expression of P-selectin, inhibition of glycoprotein IIb/IIIa (Ampofo *et al.* 2015) and downstream targets of the PI 3-kinase pathways (Figure 2.C). Forskolin, on the other hand, inhibits platelet aggregation by activating adenylyl cyclase, production of cAMP, and, in consequence, activation of PKA (Kariya *et al.* 1985; Insel *et al.* 1982).

In our experiments platelets were pre-treated with compounds of interest for 30 min or 60 min; thereafter, aggregation was initiated by the addition of ADP. Choice of the compound initiating the aggregation process for studying the effect of was made based on the knowledge that activation of platelets by ADP results in inhibition of the PKA pathway and utilization of the intrinsically active CK2-catalyzed pathways. The optimal concentration of ADP that consistently induced significant aggregation and sufficient measurement window with high signal to noise ratio was 25 μM (Figure 8.A in paper IV). The addition of ADP induced aggregation quickly, reaching the maximal effect within 5…6 min.

The results of experiments with human platelets (Figure 26) demonstrated good efficiency of ARC-775 in inhibition of ADP-induced platelet aggregation. While the platelets pre-treated for 30 min with ARC-775 resulted in (16 ± 3)% of maximum aggregation (MA), the platelets pre-treated for 60 min demonstrated even negative aggregation percent [MA = (-56 ± 11)%], pointing to decrease from the basal level of aggregation. The improved influence of ARC-775 over time could be clearly related to the effect of increased proportion of de-esterified prodrug. Another prodrug of a biligand inhibitor (ARC-1859) did not show significantly different results for 30 min and 60 min incubation period. Despite lower affinity of the de-esterified form of ARC-1859 ($K_{d,ARC\text{-}1842\text{-}CK2}$ = 8.7 nM) compared to ARC-772 ($K_{d,ARC\text{-}772\text{-}CK2}$ = 0.3 nM) as well as to CX-4945 [$K_{d,CX\text{-}4945\text{-}CK2}$ = 0.56 nM (Enkvist *et al.* 2012)], ARC-1859 and CX-4945 revealed comparable efficiency for inhibition of aggregation. Pre-treatment of the platelets with Forskolin resulted in significant suppression of aggregation. Moreover, the effect of Forskolin was more pronounced after 30 min pre-incubation as compared to 60 min pre-incubation.

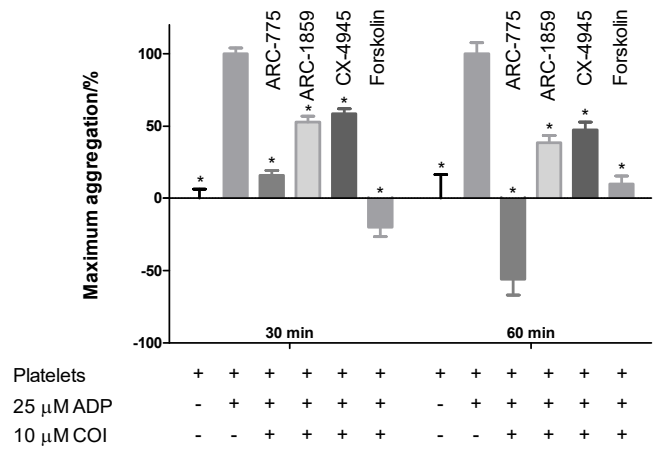

Figure 26. ADP-induced aggregation of platelets. The platelets were pre-incubated for 30 min or 60 min with a compound of interest (COI): ARC-775, ARC-1859, CX-4945, or Forskolin (n = 3). The aggregation of platelets was initiated with 25 μM ADP. * $p < 0.05$ compared to active platelets (platelets + ADP).

To sum up, three different assays were used to demonstrate the capability of ARC-772 prodrug ARC-775 to regulate the activity of CK2 in cells. First, inhibition of CK2 with ARC-772 resulted in lowered proportion of phosphorylated Cdc37 in HeLa cell lysate at similar or slightly lower level than in the presence of CX-4945, the first CK2 inhibitor in clinical trials. This change in phosphorylation balance could affect the proper folding of client proteins of Cdc37 and thus influence many processes in cells. Next, it was studied how inhibition of CK2 regulates the activity of CASP3. A distinctive specificity

between cancerous HeLa cells and non-cancer CHO cells was achieved with ARC-775. Despite similar CK2-binding affinities of ARC-772 and CX-4945, ARC-775 possessed 20-fold lower EC_{50} value for CASP3 activation in HeLa cells that may be caused by trapping ARC-772 at high concentration in cells. Finally, it was demonstrated for the first time that effective suppression of platelet aggregation is possible by their treatment with prodrugs of biligand inhibitors of CK2.

6. CONCLUSIONS

The present thesis focussed on the development of methods for characterising of PK inhibitors in biochemical assays and on the design and cellular application of biligand inhibitors of basophilic and acidophilic PKs for regulation of cell physiology. The main results of the current thesis can be summarised as follows.

- The methodology of applying a non-metal photoluminescent protein-binding-responsive probe [ARC-Lum(Fluo) probe] for determination of dissociation constants of competitive inhibitors of PKs was worked out. High affinity (K_d = 20 pM) and low background signal of the free probe supported the determination of dissociation constants of tight-binding as well as low affinity inhibitors. The lowest resolvable K_d value (K_d = 60 fM) was ~300-fold lower than that value reported for commercially available LanthaScreen™ Eu Kinase Binding Assay.
- A graphical presentation of the linearized Cheng-Prusoff equation was introduced and multiple possibilities for its application in determining affinities of PK inhibitors were presented. Quality and economic aspects of performing the measurements were disclosed, which together with the graphical presentation aids the decision making upon choosing the assay conditions, calculation of LoK_d values, and convenient conversion of IC_{50} values to K_d values.
- An HPLC based method for determination of intracellular concentration of ARCs with a fluorescent label (probes) and without it (inhibitors) was developed. It was demonstrated, that by regulating the extracellular concentration and incubation time, it was possible to gain very high (~350 μM), but also low (~600 nM) intracellular concentration of the compounds. Combining fluorescence microscopy analysis with HPLC analysis enabled the prediction of the concentration of probes in particular cellular compartments.
- The improvement of cellular uptake efficiency of biligand inhibitors (ARCs) targeting basophilic PKs was achieved with N-myristoylation of the conjugates. Good PKAc inhibitory properties were demonstrated without causing cytotoxic effect to the cell.
- The acetoxymethyl ester loading technique was applied to enhance the bioavailability of ARCs targeting acidophilic PKs. The method resulted in significantly higher cellular uptake compared to other techniques (conjugation of folate, RPARPAR, Arg_9, or applying transfection reagent TurboFect).
- High selectivity and affinity of the developed biligand inhibitor ARC-772 towards CK2 led to discriminating activation of apoptosis of cancerous HeLa cells compared to inhibitors CX-4945 and Staurosporine.
- Effective suppression of ADP-induced platelet aggregation upon their treatment with prodrugs of biligand inhibitors of CK2 was demonstrated.

REFERENCES

Ahmad K. A., Harris N. H., Johnson A. D., Lindvall H. C. N., Wang G., Ahmed K. (2007) Protein kinase CK2 modulates apoptosis induced by resveratrol and epigallocatechin-3-gallate in prostate cancer cells. *Mol. Cancer Ther.* **6**, 1006–1012.

Ampofo E., Müller I., Dahmke I. N., Eichler H., Montenarh M., Menger M. D., Laschke M. W. (2015) Role of protein kinase CK2 in the dynamic interaction of platelets, leukocytes and endothelial cells during thrombus formation. *Thromb. Res.* **136**, 996–1006.

Arunachalam B., Phan U. T., Geuze H. J., Cresswell P. (2000) Enzymatic reduction of disulfide bonds in lysosomes: characterization of a gamma-interferon-inducible lysosomal thiol reductase (GILT). *Pnas* **97**, 745–750.

Aussedat B., Sagan S., Chassaing G., Bolbach G., Burlina F. (2006) Quantification of the efficiency of cargo delivery by peptidic and pseudo-peptidic Trojan carriers using MALDI-TOF mass spectrometry. *Biochim. Biophys. Acta* **1758**, 375–383.

Bagri A., Tessier-Lavigne M., Watts R. J. (2009) Neuropilins in tumor biology. *Clin. Cancer Res.* **15**, 1860–1864.

Balayssac S., Burlina F., Convert O., Bolbach G., Chassaing G., Lequin O. (2006) Comparison of penetratin and other homeodomain-derived cell-penetrating peptides: interaction in a membrane-mimicking environment and cellular uptake efficiency. *Biochemistry* **45**, 1408–1420.

Bamborough P., Drewry D., Harper G., Smith G. K., Schneider K. (2008) Assessment of Chemical Coverage of Kinome Space and Its Implications for Kinase Drug Discovery. 7898–7914.

Baselga J., Norton L., Albanell J., Kim Y., Mendelsohn J. (1998) Recombinant Humanized Anti-HER2 Antibody (Herceptin^{TM}) Enhances the Antitumor Activity of Paclitaxel and Doxorubicin against HER2/neu Overexpressing Human Breast Cancer Xenografts. *Cancer Res.* **58**, 2825–2831.

Becher I., Savitski M. M., Savitski M. F., Hopf C., Bantscheff M., Drewes G. (2013) Affinity profiling of the cellular kinome for the nucleotide cofactors ATP, ADP, and GTP. *ACS Chem. Biol.* **8**, 599–607.

Belmokhtar C. A., Hillion J., Ségal-Bendirdjian E. (2001) Staurosporine induces apoptosis through both caspase-dependent and caspase-independent mechanisms. *Oncogene* **20**, 3354–3362.

Berndt N., Karim R. M., Schönbrunn E. (2017) Advances of small molecule targeting of kinases. *Curr. Opin. Chem. Biol.* **39**, 126–132.

Bogoyevitch M. a, Barr R. K., Ketterman A. J. (2005) Peptide inhibitors of protein kinases-discovery, characterisation and use. *Biochim. Biophys. Acta* **1754**, 79–99.

Brock R. (2014) The uptake of arginine-rich cell-penetrating peptides: Putting the puzzle together. *Bioconjug. Chem.* **25**, 863–868.

Brooks H., Lebleu B., Vivès E. (2005) Tat peptide-mediated cellular delivery: back to basics. *Adv. Drug Deliv. Rev.* **57**, 559–577.

Burlina F., Sagan S., Bolbach G., Chassaing G. (2005) Quantification of the cellular uptake of cell-penetrating peptides by MALDI-TOF mass spectrometry. *Angew. Chem. Int. Ed. Engl.* **44**, 4244–4247.

Burnett G., Kennedy E. P. (1954) The Enzymatic Phosphorylation of Proteins. *J. Biol. Chem.* **211**, 969–980.

Carpenter R. D., Andrei M., Aina O. H., Lau E. Y., Lightstone F. C., Liu R., Lam K. S., Kurth M. J. (2009) Selectively Targeting T- and B-Cell Lymphomas: A Benzothiazole Antagonist of α4 β1 Integrin. *NIH Public Access* **52**, 14–19.

Chen K. Y., Li Y. J., Huang T. G., Li Y. M. (2008) Neural remodeling may partly contribute to the abnormality of excitation-contraction coupling in heart failure. *Med. Hypotheses* **70**, 112–116.

Cheng Y., Prusoff W. H. (1973) Relationship between the inhibition constant (K1) and the concentration of inhibitor which causes 50 per cent inhibition (I50) of an enzymatic reaction. *Biochem. Pharmacol.* **22**, 3099–108.

Cho Y. S., Park Y. G., Lee Y. N., Kim M. K., Bates S., Tan L., Cho-Chung Y. S. (2000) Extracellular protein kinase A as a cancer biomarker: its expression by tumor cells and reversal by a myristate-lacking Calpha and RIIbeta subunit overexpression. *Proc. Natl. Acad. Sci. U. S. A.* **97**, 835–840.

Copeland R. A. (2013) *Evaluation of Enzyme Inhibitors in Drug Discovery*. Wiley.

Cozza G., Bortolato A., Moro S. (2010) How Druggable is Protein Kinase CK2? *Med. Res. Rev.* **20**, 419–462.

Cozza G., Zanin S., Sarno S., Costa E., Girardi C., Ribaudo G., Salvi M., Zagotto G., Ruzzene M., Pinna L. A. (2015) Design, validation and efficacy of bisubstrate inhibitors specifically affecting ecto-CK2 kinase activity. *Biochem. J.* **471**, 415–430.

Cureton N., Korotkova I., Baker B., Greenwood S., Wareing M., Kotamraju V. R., Teesalu T., et al. (2017) Selective targeting of a novel vasodilator to the uterine vasculature to treat impaired uteroplacental perfusion in pregnancy. *Theranostics* **7**, 3715–3731.

Cvijic M. E., Kita T., Shih W., Dipaola R. S. (2000) Extracellular Catalytic Subunit Activity of the cAMP-dependent Protein Kinase in Prostate Cancer Extracellular Catalytic Subunit Activity of the cAMP-dependent Protein Kinase in Prostate Cancer 1. **6**, 2309–2317.

Dalmazi G. Di, Kisker C., Calebiro D., Mannelli M., Canu L., Arnaldi G., Quinkler M., et al. (2014) Novel somatic mutations in the catalytic subunit of the protein kinase a as a cause of adrenal Cushing's syndrome: A European multicentric study. *J. Clin. Endocrinol. Metab.* **99**, E2093–E2100.

Dalton G. D., Dewey W. L. (2006) Protein kinase inhibitor peptide (PKI): a family of endogenous neuropeptides that modulate neuronal cAMP-dependent protein kinase function. *Neuropeptides* **40**, 23–34.

Dántola M. L., Denofrio M. P., Zurbano B., Gimenez C. S., Ogilby P. R., Lorente C., Thomas A. H. (2010) Mechanism of photooxidation of folic acid sensitized by unconjugated pterins. *Photochem. Photobiol. Sci.* **9**, 1604–1612.

Davies S. P., Reddy H., Caivano M., Cohen P. (2000) Specificity and mechanism of action of some commonly used protein kinase inhibitors. *Biochem. J* **351**, 95–105.

Davis M. I., Hunt J. P., Herrgard S., Ciceri P., Wodicka L. M., Pallares G., Hocker M., Treiber D. K., Zarrinkar P. P. (2011) Comprehensive analysis of kinase inhibitor selectivity. *Nat. Biotechnol.* **29**, 1046–1051.

Dom G., Shaw-Jackson C., Matis C., Bouffioux O., Picard J. J., Prochiantz A., Mingeot-Leclercq M.-P., Brasseur R., Rezsohazy R. (2003) Cellular uptake of Antennapedia Penetratin peptides is a two-step process in which phase transfer precedes a tryptophan-dependent translocation. *Nucleic Acids Res.* **31**, 556–561.

Duchardt F., Fotin-Mleczek M., Schwarz H., Fischer R., Brock R. (2007) A comprehensive model for the cellular uptake of cationic cell-penetrating peptides. *Traffic* **8**, 848–866.

Duncan J. S., Gyenis L., Lenehan J., Bretner M., Graves L. M., Haystead T. A., Litchfield D. W. (2008) An Unbiased Evaluation of CK2 Inhibitors by Chemoproteomics. *Mol. Cell. Proteomics* **7**, 1077–1088.

Duncan J. S., Turowec J. P., Duncan K. E., Vilk G., Wu C., Luscher B., Li S. S.-C., Gloor G. B., Litchfield D. W. (2011) A Peptide-Based Target Screen Implicates the Protein Kinase CK2 in the Global Regulation of Caspase Signaling. *Sci. Signal.* **4**, 1–11.

Ekambaram R., Enkvist E., Manoharan G. B., Ugandi M., Kasari M., Viht K., Knapp S., Issinger O.-G., Uri A. (2014) Benzoselenadiazole-based responsive long-lifetime photoluminescent probes for protein kinases. *Chem. Commun.* **50**, 4096–4098.

Ekambaram R., Manoharan G. babu, Enkvist E., Ligi K., Knapp S., Uri A. (2015) PIM kinase-responsive microsecond-lifetime photoluminescent probes based on selenium-containing heteroaromatic tricycle. *RSC Adv.* **5**, 96750–96757.

Enkvist E., Lavogina D., Raidaru G., Vaasa A., Viil I., Lust M., Viht K., Uri A. (2006) Conjugation of adenosine and hexa-(D-arginine) leads to a nanomolar bisubstrate-analog inhibitor of basophilic protein kinases. *J. Med. Chem.* **49**, 7150–7159.

Enkvist E., Vaasa A., Kasari M., Kriisa M., Ivan T., Ligi K., Raidaru G., Uri A. (2011) Protein-induced long lifetime luminescence of nonmetal probes. *ACS Chem. Biol.* **6**, 1052–1062.

Enkvist E., Viht K., Bischoff N., Vahter J., Saaver S., Raidaru G., Issinger O.-G., Niefind K., Uri A. (2012) A subnanomolar fluorescent probe for protein kinase CK2 interaction studies. *Org. Biomol. Chem.* **10**, 8645–8653.

Esseltine J. L., Scott J. D. (2013) AKAP signaling complexes: Pointing towards the next generation of therapeutic targets? *Trends Pharmacol. Sci.* **34**, 648–655.

Fabbro D., Cowan-Jacob S. W., Moebitz H. (2015) Ten things you should know about protein kinases: IUPHAR Review 14. *Br. J. Pharmacol.* **172**, 2675–2700.

Fabian M. A., Biggs W. H., Treiber D. K., Atteridge C. E., Azimioara M. D., Benedetti M. G., Carter T. A., et al. (2005) A small molecule-kinase interaction map for clinical kinase inhibitors. *Nat. Biotechnol.* **23**, 329–336.

Franchin C., Borgo C., Cesaro L., Zaramella S., Vilardell J., Salvi M., Arrigoni G., Pinna L. A. (2017a) Re-evaluation of protein kinase CK2 pleiotropy: new insights provided by a phosphoproteomics analysis of CK2 knockout cells. *Cell. Mol. Life Sci.*, 1–16.

Franchin C., Borgo C., Zaramella S., Cesaro L., Arrigoni G., Salvi M., Pinna L. (2017b) Exploring the CK2 Paradox: Restless, Dangerous, Dispensable. *Pharmaceuticals* **10**, 1–8.

Frankel A. D., Pabo C. O. (1988) Cellular uptake of the tat protein from human immunodeficiency virus. *Cell* **55**, 1189–1193.

Futaki S. (2006) Oligoarginine Vectors for Intracellular Delivery: Design and Cellular-Uptake Mechanisms. *Biopolym. (Peptide Sci.* **84**, 241–249.

Gharwan H., Groninger H. (2015) Kinase inhibitors and monoclonal antibodies in oncology: clinical implications. *Nat. Rev. Clin. Oncol.* **13**, 209–227.

Gray P. J., Prince T., Cheng J., Stevenson M. A., Calderwood S. K. (2008) Targeting the oncogene and kinome chaperone CDC37. *Nat. Rev. Cancer* **8**, 491–495.

Gribble F. M., Loussouarn G., Tucker S. J., Zhao C., Nichols C. G., Ashcroft F. M. (2000) A novel method for measurement of submembrane ATP concentration. *J. Biol. Chem.* **275**, 30046–30049.

Guerra B., Issinger O. (2008) Protein Kinase CK2 in Human Diseases. *Curr. Med. Chem.* **15**, 1870–1886.

Guidotti G., Brambilla L., Rossi D. (2017) Cell-Penetrating Peptides: From Basic Research to Clinics. *Trends Pharmacol. Sci.* **38**, 406–424.

Hauser A. S., Misty A., Mathias R.-A., Schiöth H. B., Gloriam D. E. (2017) Trends in GPCR drug discovery: new agents, targets and indications. *Nat Rev Drug Discov* **16**, 829–842.

Haystead T. A. J. (2006) The Purinome, a Complex Mix of Drug and Toxicity Targets. *Curr. Top. Med. Chem.* **6**, 1117–1127.

Herce H. D., Garcia A. E., Cardoso M. C. (2014) Fundamental molecular mechanism for the cellular uptake of guanidinium-rich molecules. *J. Am. Chem. Soc.* **136**, 17459–17467.

Hou Z., Nakanishi I., Kinoshita T., Takei Y., Yasue M., Misu R., Suzuki Y., et al. (2012) Structure-based design of novel potent protein kinase CK2 (CK2) inhibitors with phenyl-azole scaffolds. *J. Med. Chem.* **55**, 2899–2903.

Hoyt C., Oh C., Beekman J., Litchfield D., Lerea K. (1994) Identifying and Characterizing Casein Kinase-Ii in Human Platelets. *Faseb J.* **8**, A1389–A1389.

Huang X. (2003) Fluorescence Polarization Competition Assay: The Range of Resolvable Inhibitor Potency Is Limited by the Affinity of the Fluorescent Ligand. *J. Biomol. Screen.* **8**, 34–38.

Hunter T. (2000) Signaling-2000 and beyond. *Cell* **100**, 113–127.

Insel P. A., Stengel D., Ferry N., Hanoune J. (1982) Regulation of adenylate cyclase of human platelet membranes by forskolin. *J. Biol. Chem.* **257**, 7485–7490.

Invitrogen *LanthaScreen ™ Eu Kinase Binding Assay for PRKACA*.

Ivan T., Enkvist E., Viira B., Manoharan G. B., Raidaru G., Pflug A., Alam K. A., Zaccolo M., Engh R. A., Uri A. (2016) Bifunctional Ligands for Inhibition of Tight-Binding Protein-Protein Interactions. *Bioconjug. Chem.* **27**, 1900–1910.

Jencks W. P. (1981) On the attribution and additivity of binding energies. *Proc. Natl. Acad. Sci. U. S. A.* **78**, 4046–4050.

Jia Y., Quinn C. M., Kwak S., Talanian R. V (2008) Current in vitro kinase assay technologies: the quest for a universal format. *Curr. Drug Discov. Technol.* **5**, 59–69.

Johannessen M., Delghandi M. P., Moens U. (2004) What turns CREB on? *Cell. Signal.* **16**, 1211–1227.

Kamen B. A., Smith A. K. (2004) A review of folate receptor alpha cycling and 5-methyltetrahydrofolate accumulation with an emphasis on cell models in vitro. *Adv. Drug Deliv. Rev.* **56**, 1085–1097.

Karaman M. W., Herrgard S., Treiber D. K., Gallant P., Atteridge C. E., Campbell B. T., Chan K. W., et al. (2008) A quantitative analysis of kinase inhibitor selectivity. *Nat. Biotechnol.* **26**, 127–132.

Kariya T., Morito F., Sakai T., Takahata K., Yamanaka M. (1985) Effect of forskolin on platelet deaggregation and cyclic AMP generation. *Naunyn. Schmiedebergs. Arch. Pharmacol.* **331**, 119–121.

Kasari M., Ligi K., Williams J. A. G., Vaasa A., Enkvist E., Viht K., Pålsson L. O., Uri A. (2013) Responsive microsecond-lifetime photoluminescent probes for analysis of protein kinases and their inhibitors. *Biochim. Biophys. Acta - Proteins Proteomics* **1834**, 1330–1335.

Kasari M., Padrik P., Vaasa A., Saar K., Leppik K., Soplepmann J., Uri A. (2012) Time-gated luminescence assay using nonmetal probes for determination of protein kinase activity-based disease markers. *Anal. Biochem.* **422**, 79–88.

Kashem M. A., Nelson R. M., Yingling J. D., Pullen S. S., Prokopowicz A. S., Jones J. W., Wolak J. P., et al. (2007) Three mechanistically distinct kinase assays compared: Measurement of intrinsic ATPase activity identified the most comprehensive set of ITK inhibitors. *J. Biomol. Screen.* **12**, 70–83.

Kennedy H. J., Pouli A. E., Ainscow E. K., Jouaville L. S., Rizzuto R., Rutter G. A. (1999) Glucose Generates Sub-plasma Membrane ATP Microdomains in Single Islet β-Cells. **274**, 13281–13291.

Kestav K., Lavogina D., Raidaru G., Chaikuad A., Knapp S., Uri A. (2015) Bisubstrate inhibitor approach for targeting mitotic kinase Haspin. *Bioconjug. Chem.* **26**, 225–234.

Kestav K., Viht K., Konovalov A., Enkvist E., Uri A., Lavogina D. (2017) Slowly on, Slowly off: Bisubstrate-Analogue Conjugates of 5-Iodotubercidin and Histone H3 Peptide Targeting Protein Kinase Haspin. *ChemBioChem* **18**, 790–798.

Kita T., Goydos J., Reitman E., Ravatn R., Lin Y., Shih W. C., Kikuchi Y., Chin K. V. (2004) Extracellular cAMP-dependent protein kinase (ECPKA) in melanoma. *Cancer Lett.* **208**, 187–191.

Klaeger S., Heinzlmeir S., Wilhelm M., Polzer H., Vick B., Koenig P. A., Reinecke M., et al. (2017) The target landscape of clinical kinase drugs. *Science (80-.).* **358**.

Knapp M., Bellamacina C., Murray J. M., Bussiere D. E. (2006) Targeting Cancer: The Challenges and Successes of Structure-Based Drug Design Against the Human Purinome. *Current*, 1129–1159.

Knight Z. A., Shokat K. M. (2005) Features of selective kinase inhibitors. *Chem. Biol.* **12**, 621–637.

Knighton D. R., Zheng J., Eyck L. F. T. E. N., Ashford V. A., Xuong N., Taylor S. S., Sowadski J. M. (1991) Crystal Structure of the Catalytic Subunit of Cyclic Adenosine Monophosphate-Dependent Protein Kinase. *Science (80-.).* **253**, 407–414.

Kosuge M., Takeuchi T., Nakase I., Jones A. T., Futaki S. (2008) Cellular internalization and distribution of arginine-rich peptides as a function of extracellular peptide concentration, serum, and plasma membrane associated proteoglycans. *Bioconjug. Chem.* **19**, 656–664.

Kragten J. (1994) Calculating Standard Deviations and Confidence Intervals with a Universally Applicable Spreadsheet Technique. *Analyst* **119**, 2161–2165.

Kralj E., Simon Z., Trontelj J., Pajic T., Preloz I., Peter C., Simon Z., Ostanek B., Marc J., Kristl A. (2013a) Monitoring of imatinib targeted delivery in human leukocytes. *Eur. J. Pharm. Sci.* **50**, 123–129.

Kralj E., Žakelj S., Trontelj J., Pajič T., Preložnik Zupan I., Černelč P., Ostanek B., Marc J., Kristl A. (2013b) Monitoring of imatinib targeted delivery in human leukocytes. *Eur. J. Pharm. Sci.* **50**, 123–129.

Lacroix A., Feelders R. A., Stratakis C. A., Nieman L. K. (2015) Cushing's syndrome. *Lancet* **386**, 913–927.

Lambert J. M. (2013) Drug-conjugated antibodies for the treatment of cancer. *Br. J. Clin. Pharmacol.* **76**, 248–262.

Lavogina D., Budu A., Enkvist E., Hopp C. S., Baker D. A., Langsley G., Garcia C. R. S., Uri A. (2014) Targeting Plasmodium falciparum protein kinases with adenosine analogue-oligoarginine conjugates. *Exp. Parasitol.* **138**, 55–62.

Lavogina D., Enkvist E., Uri A. (2010a) Bisubstrate inhibitors of protein kinases: from principle to practical applications. *ChemMedChem* **5**, 23–34.

Lavogina D., Lust M., Viil I., König N., Raidaru G., Rogozina J., Enkvist E., Uri A., Bossemeyer D. (2009) Structural analysis of ARC-type inhibitor (ARC-1034) binding to protein kinase A catalytic subunit and rational design of bisubstrate analogue inhibitors of basophilic protein kinases. *J. Med. Chem.* **52**, 308–321.

Lavogina D., Nickl C. K., Enkvist E., Raidaru G., Lust M., Vaasa A., Uri A., Dostmann W. R. (2010b) Adenosine analogue-oligo-arginine conjugates (ARCs) serve as high-affinity inhibitors and fluorescence probes of type I cGMP-dependent protein kinase (PKGIα). *Biochim. Biophys. Acta - Proteins Proteomics* **1804**, 1857–1868.

Lebakken C. S., Riddle S. M., Singh U., Frazee W. J., Eliason H. C., Gao Y., Reichling L. J., Marks B. D., Vogel K. W. (2009) Development and applications of a broad-coverage, TR-FRET-based kinase binding assay platform. *J. Biomol. Screen.* **14**, 924–935.

Lee J. S., Tung C. (2010) Lipo-oligoarginines as effective delivery vectors to promote cellular uptake. *Mol. Biosyst.* **6**, 2049–2055.

Li Z. J., Cho C. H. (2012) Peptides as targeting probes against tumor vasculature for diagnosis and drug delivery. *J. Transl. Med.* **10**, 1–9.

Ligi K., Enkvist E., Uri A. (2016) Deoxygenation Increases Photoluminescence Life-time of Protein-Responsive Organic Probes with Triplet-Singlet Resonant Energy Transfer. *J. Phys. Chem. B* 120, 4945–4954.

Lindgren M. E., Hällbrink M. M., Elmquist A. M., Langel U. (2004) Passage of cell-penetrating peptides across a human epithelial cell layer in vitro. *Biochem. J.* **377**, 69–76.

Lindgren M., Gallet X., Soomets U., Hallbrink M., Brakenhielm E., Pooga M., Brasseur R., Langel U. (2000) Translocation properties of novel cell penetrating transportan and penetratin analogues. *Bioconjug. Chem.* **11**, 619–626.

Lipinski C. A., Lombardo F., Dominy B. W., Feeney P. J. (1997) Experimental and Computational Approaches to Estimate Solubility and Permeability in Drug Discovery and Develop ment Settings. *Adv. Drug Deliv. Rev.* **23**, 3–25.

Lipka D. B., Wagner M. C., Dziadosz M., Schnöder T., Heidel F., Schemionek M., Melo J. V., et al. (2012) Intracellular retention of ABL kinase inhibitors determines commitment to apoptosis in CML cells. *PLoS One* **7**, 1–16.

Litchfield D. W., Lozeman F. J., Cicirelli M. F., Harrylock M., Ericsson L. H., Piening C. J., Krebs E. G. (1991) Phosphorylation of the β subunit of casein kinase II in human A431 cells. Identification of the autophosphorylation site and a site phosphorylated by p34cdc2. *J. Biol. Chem.* **266**, 20380–20389.

Lucas A. T., Santos C. M., White T. F., Zamboni W. C. (2016) A Sensitive High Performance Liquid Chromatography Assay for the Quantification of Doxorubicin Associated with DNA in Tumor and Tissues. *J Pharm Biomed Anal* **119**, 122–129.

Lüthi A. U., Martin S. J. (2007) The CASBAH: a searchable database of caspase substrates. *Cell Death Differ.* **14**, 641–650.

Ma Y., Gong C., Ma Y., Fan F., Luo M., Yang F., Zhang Y.-H. (2012) Direct cytosolic delivery of cargoes in vivo by a chimera consisting of D- and L-arginine residues. *J. Control. Release* **162**, 286–294.

MacLean M., Picard D. (2003) Cdc37 goes beyond Hsp90 and kinases. *Cell Stress Chaperones* **8**, 114–119.

Mai J. C., Shen H., Watkins S. C., Cheng T., Robbins P. D. (2002) Efficiency of protein transduction is cell type-dependent and is enhanced by dextran sulfate. *J. Biol. Chem.* **277**, 30208–30218.

Mann A. P., Scodeller P., Hussain S., Braun G. B., Mölder T., Toome K., Ambasudhan R., Teesalu T., Lipton S. A., Ruoslahti E. (2017) Identification of a peptide recognizing cerebrovascular changes in mouse models of Alzheimer's disease. *Nat. Commun.* **8**, 1–11.

Manning G., Whyte D. B., Martinez R., Hunter T., Sudarsanam S. (2002) The protein kinase complement of the human genome. *Science* **298**, 1912–1934.

Manoharan G. babu (2016) *Combining chemical and genetic approaches for photoluminescence assays of protein kinases*. University of Tartu.

Marin O., Meggio F., Marchiori F., Borin G., Pinna L. A. (1986) Site specificity of casein kinase-2 (TS) from rat liver cytosol. A study with model peptide substrates. *Eur. J. Biochem.* **160**, 239–244.

Matherly L. H., Hou Z., Deng Y. (2007) Human reduced folate carrier: Translation of basic biology to cancer etiology and therapy. *Cancer Metastasis Rev.* **26**, 111–128.

Mazina O., Reinart-Okugbeni R., Kopanchuk S., Rinken a. (2012) BacMam System for FRET-Based cAMP Sensor Expression in Studies of Melanocortin MC1 Receptor Activation. *J. Biomol. Screen.* **17**, 1096–1101.

McKinsey T. A., Olson E. N. (2005) Toward transcriptional therapies for the failing heart: Chemical screens to modulate genes. *J. Clin. Invest.* **115**, 538–546.

Melikov K., Hara A., Yamoah K., Zaitseva E., Zaitsev E., Chernomordik L. V. (2015) Efficient entry of cell-penetrating peptide nona-arginine into adherent cells involves a transient increase in intracellular calcium. *Biochem. J.* **471**, 221–230.

Miller S. M., Simon R. J., Ng S., Zuckermann R. N., Kerr J. M., Moos W. H. (1995) Comparison of the Proteolytic Susceptibilities of Homologous L-Amino Acid, D-Amino Acid, and N-Substituted Glycine Peptide and Peptoid Oligomers. *Drug Dev. Res.* **35**, 20–32.

Mitchell D. J., Kim D. T., Steinman L., Fathman C. G., Rothbard J. B. (2000) Polyarginine enters cells more efficiently than other polycationic homopolymers. *J. Pept. Res.* **56**, 318–325.

Moody S. E., Schinzel A. C., Singh S., Izzo F., Strickland M. R., Luo L., Thomas S. R., et al. (2014) PRKACA mediates resistance to HER2-targeted therapy in breast cancer cells and restores anti-apoptotic signaling. *Oncogene* **34**, 2061–2071.

Murphy D. J. (2004) Determination of accurate Ki values for tight-binding enzyme inhibitors: an in silico study of experimental error and assay design. *Anal. Biochem.* **327**, 61–67.

Mussbach F., Franke M., Zoch A., Schaefer B., Reissmann S. (2011) Transduction of peptides and proteins into live cells by cell penetrating peptides. *J. Cell. Biochem.* **112**, 3824–3833.

Nakanishi K., Komada Y., Hayashi T., Suzuki K., Ido M. (2008) Protease activated receptor 1 activation of platelet is associated with an increase in protein kinase CK2 activity. *J. Thromb. Haemost.* **6**, 1046–1048.

Nakase I., Niwa M., Takeuchi T., Sonomura K., Kawabata N., Koike Y., Takehashi M., et al. (2004) Cellular uptake of arginine-rich peptides: roles for macropinocytosis and actin rearrangement. *Mol. Ther.* **10**, 1011–1022.

Neves J. das, Sarmento B., Amiji M., Bahia M. F. (2012) Development and validation of a HPLC method for the assay of dapivirine in cell-based and tissue permeability experiments. *J. Chromatogr. B Anal. Technol. Biomed. Life Sci.* **911**, 76–83.

Niefind K., Pütter M., Guerra B., Issinger O. G., Schomburg D. (1999) GTP plus water mimic ATP in the active site of protein kinase CK2. *Nat. Struct. Biol.* **6**, 1100–1103.

Nikolovska-Coleska Z., Wang R., Fang X., Pan H., Tomita Y., Li P., Roller P. P., et al. (2004) Development and optimization of a binding assay for the XIAP BIR3 domain using fluorescence polarization. *Anal. Biochem.* **332**, 261–273.

Noble M. E. M., Endicott J. A., Johnson L. N. (2004) Protein Kinase Inhibitors: Insights into Drug Design from Structure. *Science (80-.).* **303**, 1800–1804.

Oehlke J., Scheller a, Wiesner B., Krause E., Beyermann M., Klauschenz E., Melzig M., Bienert M. (1998) Cellular uptake of an alpha-helical amphipathic model peptide with the potential to deliver polar compounds into the cell interior non-endocytically. *Biochim. Biophys. Acta* **1414**, 127–39.

Okines A. F. C., Cunningham D. (2012) Trastuzumab: a novel standard option for patients with HER-2-positive advanced gastric or gastro-oesophageal junction cancer. *Therap. Adv. Gastroenterol.* **5**, 301–318.

Ortega C. E., Seidner Y., Dominguez I. (2014) Mining CK2 in cancer. *PLoS One* **9**, 1–25.

Paasonen L., Sharma S., Braun G. B., Kotamraju V. R., Chung T. D. Y., She Z. G., Sugahara K. N., et al. (2016) New p32/gC1qR Ligands for Targeted Tumor Drug Delivery. *ChemBioChem* **17**, 570–575.

Palm C., Jayamanne M., Kjellander M., Hällbrink M. (2007) Peptide degradation is a critical determinant for cell-penetrating peptide uptake. *Biochim. Biophys. Acta* **1768**, 1769–1776.

Palm C., Netzereab S., Hällbrink M. (2006) Quantitatively determined uptake of cell-penetrating peptides in non-mammalian cells with an evaluation of degradation and antimicrobial effects. *Peptides* **27**, 1710–1716.

Parang K., Cole P. a (2002) Designing bisubstrate analog inhibitors for protein kinases. *Pharmacol. Ther.* **93**, 145–57.

Parang K., Till J. H., Ablooglu A. J., Kohanski R. A., Hubbard S. R., Cole P. A. (2001) Mechanism-based design of a protein kinase inhibitor. *Nat. Struct. Biol.* **8**, 37–41.

Parker N., Turk M. J., Westrick E., Lewis J. D., Low P. S., Leamon C. P. (2005) Folate receptor expression in carcinomas and normal tissues determined by a quantitative radioligand binding assay. *Anal. Biochem.* **338**, 284–293.

Paulos C. M., Reddy J. a, Leamon C. P., Turk M. J., Low P. S. (2004) Ligand binding and kinetics of folate receptor recycling in vivo: impact on receptor-mediated drug delivery. *Mol. Pharmacol.* **66**, 1406–1414.

Pearce L. R., Komander D., Alessi D. R. (2010) The nuts and bolts of AGC protein kinases. *Nat. Rev. Mol. Cell Biol.* **11**, 9–22.

Pearl L. H. (2005) Hsp90 and Cdc37 - A chaperone cancer conspiracy. *Curr. Opin. Genet. Dev.* **15**, 55–61.

Pellet-Many C., Frankel P., Jia H., Zachary I. (2008) Neuropilins: structure, function and role in disease. *Biochem. J.* **411**, 211–226.

Pidoux G., Taskén K. (2010) Specificity and spatial dynamics of protein kinase a signaling organized by A-kinase-anchoring proteins. *J. Mol. Endocrinol.* **44**, 271–284.

Pinna L. A., ed (2013) *Protein Kinase CK2*. John Wiley & Sons, Inc.

Poteet-Smith C. E., Shabb J. B., Francis S. H., Corbin J. D. (1997) Identification of critical determinants for autoinhibition in the pseudosubstrate region of type Iα cAMP-dependent protein kinase. *J. Biol. Chem.* **272**, 379–388.

Räägel H., Lust M., Uri A., Pooga M. (2008) Adenosine-oligoarginine conjugate, a novel bisubstrate inhibitor, effectively dissociates the actin cytoskeleton. *FEBS J.* **275**, 3608–3624.

Räägel H., Säälik P., Hansen M., Langel Ü., Pooga M. (2009) CPP-protein constructs induce a population of non-acidic vesicles during trafficking through endo-lysosomal pathway. *J. Control. Release* **139**, 108–117.

Rabalski A. J., Gyenis L., Litchfield D. W. (2016) Molecular Pathways: Emergence of Protein Kinase CK2 (CSNK2) as a Potential Target to Inhibit Survival and DNA Damage Response and Repair Pathways in Cancer Cells. *Clin. Cancer Res.* **22**, 2840–2847.

Rahnel H., Viht K., Lavogina D., Mazina O., Haljasorg T., Enkvist E., Uri A. (2017) A Selective Biligand Inhibitor of CK2 Increases Caspase-3 Activity in Cancer Cells and Inhibits Platelet Aggregation. *ChemMedChem* **12**, 1723–1736.

Rask-Andersen M., Masuram S., Schiöth H. B. (2014a) The Druggable Genome: Evaluation of Drug Targets in Clinical Trials Suggests Major Shifts in Molecular Class and Indication. *Annu. Rev. Pharmacol. Toxicol.* **54**, 9–26.

Rask-Andersen M., Zhang J., Fabbro D., Schiöth H. B. (2014b) Advances in kinase targeting: Current clinical use and clinical trials. *Trends Pharmacol. Sci.* **35**, 604–620.

Reddy J. A., Dorton R., Dawson A., Vetzel M., Parker N., Nicoson J. S., Westrick E., et al. (2009) In vivo structural activity and optimization studies of folate-tubulysin conjugates. *Mol. Pharm.* **6**, 1518–1525.

Rezgui R., Blumer K., Yeoh-Tan G., Trexler A. J., Magzoub M. (2016) Precise quantification of cellular uptake of cell-penetrating peptides using fluorescence-activated cell sorting and fluorescence correlation spectroscopy. *Biochim. Biophys. Acta - Biomembr.* **1858**, 1499–1506.

Ricouart A., Gesquiere J. C., Tartar A., Sergheraert C. (1991) Design of Potent Protein Kinase Inhibitors Using the Bisubstrate Approach. *J. Med. Chem.* **34**, 73–78.

Rodnight R., Lavin B. E. (1964) Phosvitin kinase from brain: activation by ions and subcellular distribution. *Biochem. J.* **93**, 84–91.

Roehrl M. H. A., Wang J. Y., Wagner G. (2004) A general framework for development and data analysis of competitive high-throughput screens for small-molecule inhibitors of protein-protein interactions by fluorescence polarization. *Biochemistry* **43**, 16056–16066.

Roskoski R. J. *FDA-approved protein kinase inhibitors*.

Ross J. F., Chaudhuri P. K., Ratnam M., Ph D. (1993) Differential Regulation of Folate Receptor Isoforms in Normal and Malignant Tissues In Vivo and in Established Cell Lines. *Cancer* **73**, 2432–2443.

Rothbard J. B., Garlington S., Lin Q., Kirschberg T., Kreider E., McGrane P. L., Wender P. a, Khavari P. a (2000) Conjugation of arginine oligomers to cyclosporin A facilitates topical delivery and inhibition of inflammation. *Nat. Med.* **6**, 1253–1257.

Roukos D. H. (2010) Targeting gastric cancer with trastuzumab: new clinical practice and innovative developments to overcome resistance. *Ann. Surg. Oncol.* **17**, 14–17.

Ruoslahti E. (2002) Specialization of Tumour Vasculature. *Nat. Rev. Cancer* **2**, 83–90.

Ruoslahti E., Rajotte D. (2000) An Address System in the Vasculature of Normal Tissues and Tumors. *Annu. Rev. Immunol.* **18**, 813–827.

Ruzzene M., Pinna L. A. (2010) Addiction to protein kinase CK2: A common denominator of diverse cancer cells? *Biochim. Biophys. Acta - Proteins Proteomics* **1804**, 499–504.

Ryu S. Y., Kim S. (2013) Evaluation of CK2 inhibitor (E)-3-(2,3,4,5-tetrabromophenyl)acrylic acid (TBCA) in regulation of platelet function. *Eur. J. Pharmacol.* **720**, 391–400.

Salvi M., Sarno S., Cesaro L., Nakamura H., Pinna L. A. (2009) Extraordinary pleiotropy of protein kinase CK2 revealed by weblogo phosphoproteome analysis. *Biochim. Biophys. Acta - Mol. Cell Res.* **1793**, 847–859.

Santos R., Ursu O., Gaulton A., Bento A. P., Donadi R. S., Bologa C. G., Karlsson A., et al. (2016) A comprehensive map of molecular drug targets. *Nat. Rev. Drug Discov.* **16**, 19–34.

Saul J. M., Annapragada A., Natarajan J. V., Bellamkonda R. V. (2003) Controlled targeting of liposomal doxorubicin via the folate receptor in vitro. *J. Control. Release* **92**, 49–67.

Schwartz P. A., Murray B. W. (2011) Protein kinase biochemistry and drug discovery. *Bioorg. Chem.* **39**, 192–210.

Shabb J. B. (2001) Physiological substrates of cAMP-dependent protein kinase. *Chem. Rev.* **101**, 2381–2411.

Shai Y., Makovitzky A., Avrahami D. (2006) Host defense peptides and lipopeptides: modes of action and potential candidates for the treatment of bacterial and fungal infections. *Curr. Protein Pept. Sci.* **7**, 479–486.

Sharma S., Singh J., Ojha R., Singh H., Kaur M., Bedi P. M. S. S., Nepali K. (2016) Design strategies, structure activity relationship and mechanistic insights for purines as kinase inhibitors. *Eur. J. Med. Chem.* **112**, 298–346.

Siddiqui-Jain A., Drygin D., Streiner N., Chua P., Pierre F., O'Brien S. E., Bliesath J., et al. (2010) CX-4945, an orally bioavailable selective inhibitor of protein kinase CK2, inhibits prosurvival and angiogenic signaling and exhibits antitumor efficacy. *Cancer Res.* **70**, 10288–10298.

Simón-Gracia L., Hunt H., Scodeller P., Gaitzsch J., Kotamraju V. R., Sugahara K. N., Tammik O., Ruoslahti E., Battaglia G., Teesalu T. (2016) iRGD peptide conjugation potentiates intraperitoneal tumor delivery of paclitaxel with polymersomes. *Biomaterials* **104**, 247–257.

Sinijarv H. (2013) *Cellular uptake of ARC-based inhibitors of protein kinases*. University of Tartu.

Skålhegg B. S., Taskén K. (1997) Specificity in the cAMP/PKA signaling pathway. differential expression, regulation, and subcellular localization of subunits of PKA. *Front. Biosci. a J. virtual Libr.* **2**, 678–693.

Søberg K., Jahnsen T., Rognes T., Skålhegg B. S., Laerdahl J. K. (2013) Evolutionary Paths of the cAMP-Dependent Protein Kinase (PKA) Catalytic Subunits. *PLoS One* **8**, e60935.

Sudimack J., Lee R. J. (2000) Targeted drug delivery via the folate receptor. *Adv. Drug Deliv. Rev.* **41**, 147–162.

Sugahara K. N., Teesalu T., Karmali P. P., Kotamraju V. R., Agemy L., Girard O. M., Hanahan D., Mattrey R. F., Ruoslahti E. (2009) Tissue-Penetrating Delivery of Compounds and Nanoparticles into Tumors. *Cancer Cell* **16**, 510–520.

Tal-Gan Y., Freeman N. S., Klein S., Levitzki A., Gilon C. (2010) Synthesis and structure-activity relationship studies of peptidomimetic PKB/Akt inhibitors: The significance of backbone interactions. *Bioorganic Med. Chem.* **18**, 2976–2985.

Taylor S. S., Ilouz R., Zhang P., Kornev A. P. (2012) Assembly of allosteric macromolecular switches: lessons from PKA. *Nat. Rev. Mol. Cell Biol.* **13**, 646–658.

Teesalu T., Sugahara K. N., Ruoslahti E. (2013) Tumor-penetrating peptides. *Front. Oncol.* **3**, 1–8.

The GPCR Workgroup (Universtity of Tartu) *Aparecium software*.

Torchilin V. P. (2008) Tat peptide-mediated intracellular delivery of pharmaceutical nanocarriers. *Adv. Drug Deliv. Rev.* **60**, 548–558.

Trabulo S., Cardoso A. L., Mano M., Lima M. C. P. De (2010) Cell-Penetrating Peptides—Mechanisms of Cellular Uptake and Generation of Delivery Systems. *Pharmaceuticals* **3**, 961–993.

Trembley J. H., Kren B. T., Abedin M. J., Vogel R. I., Cannon C. M., Unger G. M., Ahmed K. (2017) CK2 molecular targeting-tumor cell-specific delivery of RNAi in various models of cancer. *Pharmaceuticals* **10**, 4–7.

Tünnemann G., Ter-Avetisyan G., Martin R. M., Stöckl M., Herrmann A., Cardoso M. C. (2008) Live-cell analysis of cell penetration ability and toxicity of oligo-arginines. *J. Pept. Sci.* **14**, 469–476.

Turowec J. P., Vilk G., Gabriel M., Litchfield D. W. (2013) Characterizing the convergence of protein kinase CK2 and caspase-3 reveals isoform-specific phosphorylation of caspase-3 by CK2α': implications for pathological roles of CK2 in promoting cancer cell survival. *Oncotarget* **4**, 560–571.

Tyagi S. (2016) Folate conjugates: a boon in the anti-cancer therapeutics. *Int. J. Pharm. Sci. Res.* **7**, 4278–4303.

Uri A., Raidaru G., Subbi J., Padari K., Pooga M. (2002) Identification of the ability of highly charged nanomolar inhibitors of protein kinases to cross plasma membranes and carry a protein into cells. *Bioorg. Med. Chem. Lett.* **12**, 2117–2120.

Vaasa A., Ligi K., Mohandessi S., Enkvist E., Uri A., Miller L. W. (2012) Time-gated luminescence microscopy with responsive nonmetal probes for mapping activity of protein kinases in living cells. *Chem. Commun.* **48**, 8595–8597.

Vaasa A., Lust M., Terrin A., Uri A., Zaccolo M. (2010) Small-molecule FRET probes for protein kinase activity monitoring in living cells. *Biochem. Biophys. Res. Commun.* **397**, 750–755.

Vaasa A., Viil I., Enkvist E., Viht K., Raidaru G., Lavogina D., Uri A. (2009) High-affinity bisubstrate probe for fluorescence anisotropy binding/displacement assays with protein kinases PKA and ROCK. *Anal. Biochem.* **385**, 85–93.

Vahter J. Manuscript in preparation.

Vahter J., Viht K., Uri A., Enkvist E. (2017) Oligo-aspartic acid conjugates with benzo[c][2,6]naphthyridine-8-carboxylic acid scaffold as picomolar inhibitors of CK2. *Bioorg. Med. Chem.* **25**, 2277–2284.

Vasconcelos L., Pärn K., Langel Ü. (2013) Therapeutic potential of cell-penetrating peptides. *Ther. Deliv.* **4**, 573–591.

Verdurmen W. P. R., Bovee-Geurts P. H., Wadhwani P., Ulrich A. S., Hällbrink M., Kuppevelt T. H. Van, Brock R. (2011) Preferential uptake of L-versus D-amino acid cell-penetrating peptides in a cell type-dependent manner. *Chem. Biol.* **18**, 1000–1010.

Viht K., Padari K., Raidaru G., Subbi J., Tammiste I., Pooga M., Uri A. (2003) Liquid-phase synthesis of a pegylated adenosine–oligoarginine conjugate, cell-permeable inhibitor of cAMP-dependent protein kinase. *Bioorg. Med. Chem. Lett.* **13**, 3035–3039.

Viht K., Saaver S., Vahter J., Enkvist E., Lavogina D., Sinijärv H., Raidaru G., Guerra B., Issinger O. G., Uri A. (2015) Acetoxymethyl Ester of Tetrabromobenzimidazole-

Peptoid Conjugate for Inhibition of Protein Kinase CK2 in Living Cells. *Bioconjug. Chem.* **26**, 2324–2335.

Viht K., Schweinsberg S., Lust M., Vaasa A., Raidaru G., Lavogina D., Uri A., Herberg F. W. (2007) Surface-plasmon-resonance-based biosensor with immobilized bisubstrate analog inhibitor for the determination of affinities of ATP- and protein-competitive ligands of cAMP-dependent protein kinase. *Anal. Biochem.* **362**, 268–277.

Vilk G., Weber J. E., Turowec J. P., Duncan J. S., Wu C., Derksen D. R., Zien P., et al. (2008) Protein kinase CK2 catalyzes tyrosine phosphorylation in mammalian cells. *Cell. Signal.* **20**, 1942–1951.

Vlahov I. R., Leamon C. P. (2012) Engineering folate-drug conjugates to target cancer: from chemistry to clinic. *Bioconjug. Chem.* **23**, 1357–1369.

Vlastaridis P., Kyriakidou P., Chaliotis A., Peer Y. Van de, Oliver S. G., Amoutzias G. D. (2017) Estimating the total number of phosphoproteins and phosphorylation sites in eukaryotic proteomes. *Gigascience* **6**, 1–11.

Wang H., Li M., Lin W., Wang W., Zhang Z., Rayburn E. R., Lu J., et al. (2007) Extracellular activity of cyclic AMP-dependent protein kinase as a biomarker for human cancer detection: distribution characteristics in a normal population and cancer patients. *Cancer Epidemiol. Biomarkers Prev.* **16**, 789–795.

Watkins C. L., Schmaljohann D., Futaki S., Jones A. T. (2009) Low concentration thresholds of plasma membranes for rapid energy-independent translocation of a cell-penetrating peptide. *Biochem. J.* **420**, 179–189.

Widmer N., Decosterd L. A., Csajka C., Leyvraz S., Duchosal M. A., Rosselet A., Rochat B., et al. (2006) Population pharmacokinetics of imatinib and the role of α1-acid glycoprotein. *Br. J. Clin. Pharmacol.* **62**, 97–112.

Wong W., Scott J. D. (2004) AKAP signalling complexes: Focal points in space and time. *Nat. Rev. Mol. Cell Biol.* **5**, 959–970.

Wu P., Nielsen T. E., Clausen M. H. (2015) FDA-approved small-molecule kinase inhibitors. *Trends Pharmacol. Sci.* **36**, 422–439.

Xu Z., Nagashima K., Sun D., Rush T., Northrup A., Andersen J. N., Kariv I., Bobkova E. V (2009) Development of high-throughput TR-FRET and AlphaScreen assays for identification of potent inhibitors of PDK1. *J. Biomol. Screen.* **14**, 1257–1262.

Yap T. A., Walton M. I., Grimshaw K. M., Poele R. H. Te, Eve P. D., Valenti M. R., Haven Brandon A. K. De, et al. (2012) AT13148 is a novel, oral multi-AGC kinase inhibitor with potent pharmacodynamic and antitumor activity. *Clin. Cancer Res.* **18**, 3912–3923.

Zhang J., Yang P. L., Gray N. S. (2009) Targeting cancer with small molecule kinase inhibitors. *Nat. Rev. Cancer* **9**, 28–39.

Zhao R., Min S. H., Wang Y., Campanella E., Low P. S., Goldman I. D. (2009) A role for the proton-coupled folate transporter (PCFT-SLC46A1) in folate receptor-mediated endocytosis. *J. Biol. Chem.* **284**, 4267–4274.

SUMMARY IN ESTONIAN

ARC-inhibiitorid: usaldusväärsetest biokeemilistest meetoditest rakkude füsioloogia reguleerimiseni

Inimrakk on keeruline süsteem, mis koosneb paljudest molekulidest ning rangelt reguleeritud molekulidevahelisest kommunikatsioonist. Ühed osalised raku elutegevuses on proteiinkinaaside (PKde) perekonna liikmed, mis koosneb ligikaudu 500 liikmest (Manning *et al.* 2002). PKde rolliks on katalüüsida fosforüülrühma ülekannet ATPlt sihtvalgule. Väike muudatus (fosforüülimine) sihtvalgu keemilises struktuuris mõjutab oluliselt sihtvalkude aktiivsust ning seetõttu ka raku elutegevuseks vajalikke protsesse.

Kuigi esimene PK avastati juba 1954. aastal (Burnett and Kennedy 1954), toimus PKde uurimises hüppeline areng alles 30 aastat hiljem. Aastate jooksul on kindlaks tehtud paljude PKde signaalradade eripärad ja ka PKde roll mitmete haiguste (nt neurodegeneratiivsete haiguste, vähkkasvajate, diabeedi, südame-veresoonkonna haiguste) tekkes. Tänaseks on vähiravimina USA terapeutiliste kaupade regulatsiooni (NDA) poolt kinnitatud üle 35 väikese molekulmassiga ühendi (Wu *et al.* 2015; Fabbro *et al.* 2015; Sharma *et al.* 2016; Rask-Andersen *et al.* 2014b). PKdega seotud arendusvaldkondades on oluline osakaal ka erinevatel biokeemilistel meetoditel nii uute ravimikandidaatide analüüsimiseks, PKde signaalradade uurimiseks kui ka PKde osaluse tuvastamiseks erinevate haiguste tekkes.

Käesoleva töö esimeses osas keskenduti analüüsimeetodite ning teises osas inhibiitorite arendusele ning rakendamisele. Mõlemal puhul kasutati biligandseid ühendeid, ARCe. Biligandne inhibiitor seostub kinaasi kahe substraaditaskuga korraga, mistõttu saavutatakse kõrge seostumisafiinsus ja selektiivsus sihtvalgu suhtes.

Esmalt analüüsiti unikaalsete fotoluminestsentsomadustega ARC-Lum(Fluo) sondi võimekust PK inhibiitorite dissotsiatsioonikonstantide (K_d) määramisel. Enamik inhibiitorite kiirsõeluuringu meetoditest kasutab antikeha ja fluorestsentsmarkeri kombinatsiooni. Antud töös kasutati vaid üht sondi, tänu millele on meetod võrreldes paljude teistega lihtsam, odavam ja täpsem. Leiti, et meetodi K_d määramispiir on 60 fM, mis on ligikaudu 300 korda madalam võrreldes senini enimkasutatud LanthaScreen™ Eu meetodiga. Meetodi tundlikkus on saavutatud peamiselt tänu uue meetodi kõrgele signaal-müra suhtele ja sondi afiinsusele (20 pM). Meetodi optimeerimisel pandi rõhku ka majanduslikele aspektidele. Töös tutvustati ka veebirakendust, mis toetab sobilike analüüsitingimuste valimist, mille juures on võimalik inhibiitorite seostumiskonstante määrata täpselt ning madalate kuludega.

Teisena arendati vedelikkromatograafiline meetod ARC-inhibiitorite ja -sondide rakusisese stabiilsuse ning kontsentratsiooni määramiseks. Näidati, et ühendite rakusisest kontsentratsiooni on võimalik reguleerida laias vahemikus (600 nM kuni 350 μM), varieerides rakkudele lisatud ainete kontsentratsioone ning inkubatsiooniaega. Samuti demonstreeriti, et basofiilseid PKsid sihtivad

ARC-ühendid sisenevad rakkudesse kiiresti (juba 10 min saavutatakse 30 µM kontsentratsioon) ning ained on rakkudes stabiilsed vähemalt 150 h jooksul. Selline paindlikkus võimaldab kasutada ARC-inhibiitoreid nii kiiretes sõeluuringutes kui ka katsetes, kus on vajalik jälgida inhibiitori mõju raku signaalradadele pikema aja jooksul. Kontsentratsiooni peenhäälestamine võimaldab vähendada rakkude ülekoormamist inhibiitoritega ning sealjuures minimiseerida ainete mittespetsiifilist seostumist valkudega.

Töö teine osa keskendus selliste biligandsete inhibiitorite arendusele, mis seonduvad PKde CK2 või PKA aktiivtsentrisse. PKA on alates selle avastamisest olnud enim uuritud PK ning seda kinaasi seostatakse erinevate südamehaiguste ja kasvajatega. Samuti on tuvastatud, et erinevate vähkkasvajatega patsientide veres on PKA kontsentratsioon kõrgem, mis teeb PKA ka oluliseks vähktõve biomarkeriks. Töögrupis oli varasemalt disainitud afiinne biligandne PKA inhibiitor ARC-904. Ühend sisenes rakkudesse väga efektiivselt (inkubeerides 1 h 10 µM ARC-904ga saavutati 100 µM rakusisene kontsentratsioon), kuid ei inhibeerinud PKAd raku tuumas vaatamata aine kõrgele kontsentratsioonile ning afiinsusele. Tõstmaks rakkudesse sisenemise efektiivsust, konjugeeriti ARC-904ga müristoüülrühm. Sellise struktuurilise muudatuse toel saavutati kolmekordne inhibiitori kontsentratsiooni tõus. Kuigi müristoüülitud ARC-1222 seostus PKAle ligi 10 korda madalama afiinsusega kui ARC-904 (K_d vastavalt 3,7 nM ja 0,4 nM), inhibeeris ARC-1222 PKAd rakkudes märgatavalt paremini. ARC-1222 inhibeerimisvõimekus oli võrreldes kommertsiaalse ATP-konkurentse inhibiitoriga H89 [K_d = 10 nM, (Davies *et al.* 2000)] ligikaudu kaks korda parem.

Teise kinaasina pakkus meile huvi CK2, mis katalüüsib hinnanguliselt ligi 20% kõigist valkude fosforüülimistest imetajate rakkudes. CK2 suurenenud aktiivsust on seostatud erinevate haigustega (sh vähktõve erinevad liigid ja tromboos), kusjuures arvatakse, et vähirakud vajavad oma elutegevuseks CK2 kõrget aktiivsust. Käesoleva töö käigus arendati seeria biligandseid CK2 inhibiitoreid. Parimale inhibiitorile oli omane nii kõrge afiinsus (40 pM) kui ka hea selektiivsus CK2 suhtes. CK2 sihtivate biligandsete inhibiitorite struktuuriliseks eripäraks on nende negatiivselt laetud peptiidne fragment, mis pärsib ainete suutlikkust läbida rakkude plasmamembraani. Töös katsetati erinevaid tehnoloogiaid ainete rakku sisenemise võimekuse tõstmiseks ning kõige tõhusamaks lahenduseks osutus karboksüülhapete esterdamine. Rakkudes estrid hüdrolüüsitakse, mille tulemusena avaldub inhibiitori funktsionaalsus CK2 suhtes. Ühendi ARC-772 (K_d = 0,3 nM) tõhusust CK2 inhibeerimisel illustreeris selektiivne apoptoosi aktiveerimine vähirakkudes juba aine mikromolaarsete kontsentratsioonide juures. Samadel tingimustel oli aine mõju normaalsetele rakkudele tühine. Vähirakkude selektiivsust tervete rakkude suhtes iseloomustas ARC-772 estri ligikaudu 50-kordne erinevus EC_{50} väärtustes. Kliinilistes katsetustes oleva ATP-konkurentse CK2 inhibiitori CX-4945 (K_d = 0,4 nM) puhul oli vastav erinevus vaid 5,5-kordne.

Kuna CK2 mängib olulist rolli ka tromboosi tekkes, testiti ARC-772 efektiivsust vereliistakute agregatsiooni vähendamisel. Saadud tulemused näitasid,

et ARC-772 vähendas võrreldes CX-4945ga märgatavalt efektiivsemalt ATP lisamisega esile kutsutud vereliistakute agregatsiooni.

Antud töö raames arendatud meetodid võimaldavad nii inhibiitorite afiinsuskonstantide täpsemat määramist kui ka ainete kontsentratsiooni määramist rakkudes. Uurimistöös arendatud selektiivsed, afiinsed ning hea raku plasmamembraani läbimisvõimega biligandsed inhibiitorid reguleerisid efektiivselt CK2 ja PKAga seotud signaalradasid. Doktoritöö tulemused toetavad biligandsete inhibiitorite rakendamist ravimiarenduses, haiguste diagnostikas ning biomeditsiinilistes uuringutes.

ACKNOWLEDGEMENTS

This research was supported by grants from the Estonian Science Foundation (8230, 8419, and 8055), Estonian Ministry of Education and Sciences (SF0180121s08), the Estonian Research Council (IUT20-17), and the Graduate School "Functional materials and technologies" (receiving funding from the European Regional Development Fund in University of Tartu, Estonia).

I would like to thank four of the most important people regarding the completion of this PhD thesis. Asko, your energetic attitude and good sense of (dark) humour have been just a bonus besides giving me all the support and advice one could wish from a supervisor. Angela, thank you for the patience and consistency; you were an inspiring example as there was so much in you I could relate to. Kaido, in addition to being one of the most interesting and funniest person I know, I would like to thank you for sharing your knowledge, broad experiences, and good ideas (both in science and in everyday topics). Taavi, thank you first, for bringing me to the laboratory, and second, for being such a kind, supportive, and caring scientific brother, but most importantly a good friend.

There are many other people who have been contributed to this thesis by instructing me (Darja, Marie, Kadri, Gerda), advising me (Erki, Marje, Ganesh, Katrin, Ago, Olga), helping me (Jürgen, Tõnis, Sergei, Maris, Reet, Anni), and laughing with me (all aforementioned) – I am sincerely thankful to you.

I would like to express my gratitude to my family for believing in my choice of studying chemistry (and me) despite not always understanding what it actually is that I am doing in the laboratory. Special thanks to my friends Iris, Liisa, Maarja, and Pirgit, for filling my need for good company, fun, and support. Thank you Maarja-Liisa, Ott, Jana, Siim, and Andi – I could not be happier for finding such remarkable friends from my course.

Thank you, Timo for your unquestionable love and support! These are sometimes the only things a person needs to carry on.

To finish, an apothegm from Taavi:

> "[…] I would like to thank the nature itself for being a complicated system. It seems that there will be no end in resolving some of the most intriguing tasks, and even simpler endeavours can be left without an answer. It is fascinating, really, and relatively frustrating simultaneously."

PUBLICATIONS

CURRICULUM VITAE

Name: Hedi Rahnel (Sinijärv)
Date of birth: August 28, 1989
Citizenship: Estonian
Address: University of Tartu, Institute of Chemistry
Ravila 14a, 50411 Tartu, Estonia
E-mail: hedi.rahnel@gmail.com

Education:

2013–…	University of Tartu, PhD student in chemistry
2011–2013	University of Tartu, MSc in applied measurement science
2008–2011	University of Tartu, BSc in chemistry

Professional employment:

2017–…	AS Kevelt, quality assurance specialist
2012–2015	University of Tartu, Institute of Chemistry, chemist
2012	Estonian Veterinary and Food Laboratory, trainee

Professional organization

2016–…	Member of Estonian Biochemical Society

Scientific publications

1. **H. Rahnel,** K. Viht, D. Lavogina, O. Mazina, T. Haljasorg, E. Enkvist, A. Uri, Selective Biligand Inhibitor of CK2 Increases Caspase-3 Activity in Cancerous Cells and Inhibits Platelet Aggregation, ChemMedChem. 12 (2017) 1723-1236. doi:10.1002/cmdc.201700457
2. T. Ivan, E. Enkvist, **H. Sinijarv**, A. Uri, Competitive ligands facilitate dissociation of the complex of bifunctional inhibitor and protein kinase, Biophys. Chem. 228 (2017) 17-24. doi:10.1016/j.bpc.2017.06.004.
3. **H. Sinijarv**, S. Wu, T. Ivan, T. Laasfeld, K. Viht, A. Uri, Binding assay for characterization of protein kinase inhibitors possessing sub-picomolar to sub-millimolar affinity, Anal. Biochem. 531 (2017) 67–77. doi:10.1016/j.ab. 2017.05.017.
4. K. Viht, S. Saaver, J. Vahter, E. Enkvist, D. Lavogina, **H. Sinijärv**, G. Raidaru, B. Guerra, O.G. Issinger, A. Uri, Acetoxymethyl Ester of Tetrabromobenzimidazole-Peptoid Conjugate for Inhibition of Protein Kinase CK2 in Living Cells, Bioconjug. Chem. 26 (2015) 2324–2335. doi:10.1021/ acs.bioconjchem.5b00383.
5. M. Kriisa, **H. Sinijärv**, A. Vaasa, E. Enkvist, S. Kostenko, U. Moens, A. Uri, Inhibition of CREB Phosphorylation by Conjugates of Adenosine Analogues and Arginine-Rich Peptides, Inhibitors of PKA Catalytic Subunit, ChemBioChem. 16 (2015) 312–319. doi:10.1002/cbic.201402526.

ELULOOKIRJELDUS

Nimi: Hedi Rahnel (Sinijärv)
Sünniaeg: 28. August, 1989
Kodakondsus: Eesti
Aadress: Tartu Ülikool, keemia instituut
Ravila 14 a, 50411 Tartu, Eesti
E-mail: hedi.rahnel@gmail.com

Haridus:

2013–…	Tartu Ülikool, doktoriõpe keemias
2011–2013	Tartu Ülikool, MSc rakenduslikus mõõteteaduses
2008–2011	Tartu Ülikool, BSc keemias

Erialane teenistuskäik:

2017–…	AS Kevelt, kvaliteeditagamise spetsialist
2012–2015	Tartu Ülikool, keemia instituut, keemik
2012	Eesti veterinaar- ja toidulaboratoorium, praktikant

Teadusorganisatsioonid:

2016–…	Eesti biokeemia seltsi liige

Teaduspublikatsioonid:

1. **H. Rahnel,** K. Viht, D. Lavogina, O. Mazina, T. Haljasorg, E. Enkvist, A. Uri, Selective Biligand Inhibitor of CK2 Increases Caspase-3 Activity in Cancerous Cells and Inhibits Platelet Aggregation, ChemMedChem. 12 (2017) 1723-1236. doi:10.1002/cmdc.201700457
2. T. Ivan, E. Enkvist, **H. Sinijarv**, A. Uri, Competitive ligands facilitate dissociation of the complex of bifunctional inhibitor and protein kinase, Biophys. Chem. 228 (2017) 17-24. doi:10.1016/j.bpc.2017.06.004.
3. **H. Sinijarv**, S. Wu, T. Ivan, T. Laasfeld, K. Viht, A. Uri, Binding assay for characterization of protein kinase inhibitors possessing sub-picomolar to sub-millimolar affinity, Anal. Biochem. 531 (2017) 67–77. doi:10.1016/j.ab. 2017.05.017.
4. K. Viht, S. Saaver, J. Vahter, E. Enkvist, D. Lavogina, **H. Sinijärv**, G. Raidaru, B. Guerra, O.G. Issinger, A. Uri, Acetoxymethyl Ester of Tetrabromobenzimidazole-Peptoid Conjugate for Inhibition of Protein Kinase CK2 in Living Cells, Bioconjug. Chem. 26 (2015) 2324–2335. doi:10.1021/acs. bioconjchem.5b00383.
5. M. Kriisa, **H. Sinijärv**, A. Vaasa, E. Enkvist, S. Kostenko, U. Moens, A. Uri, Inhibition of CREB Phosphorylation by Conjugates of Adenosine Analogues and Arginine-Rich Peptides, Inhibitors of PKA Catalytic Subunit, ChemBioChem. 16 (2015) 312–319. doi:10.1002/cbic.201402526.

DISSERTATIONES CHIMICAE UNIVERSITATIS TARTUENSIS

1. **Toomas Tamm.** Quantum-chemical simulation of solvent effects. Tartu, 1993, 110 p.
2. **Peeter Burk.** Theoretical study of gas-phase acid-base equilibria. Tartu, 1994, 96 p.
3. **Victor Lobanov.** Quantitative structure-property relationships in large descriptor spaces. Tartu, 1995, 135 p.
4. **Vahur Mäemets.** The ^{17}O and ^{1}H nuclear magnetic resonance study of H_2O in individual solvents and its charged clusters in aqueous solutions of electrolytes. Tartu, 1997, 140 p.
5. **Andrus Metsala.** Microcanonical rate constant in nonequilibrium distribution of vibrational energy and in restricted intramolecular vibrational energy redistribution on the basis of slater's theory of unimolecular reactions. Tartu, 1997, 150 p.
6. **Uko Maran.** Quantum-mechanical study of potential energy surfaces in different environments. Tartu, 1997, 137 p.
7. **Alar Jänes.** Adsorption of organic compounds on antimony, bismuth and cadmium electrodes. Tartu, 1998, 219 p.
8. **Kaido Tammeveski.** Oxygen electroreduction on thin platinum films and the electrochemical detection of superoxide anion. Tartu, 1998, 139 p.
9. **Ivo Leito.** Studies of Brønsted acid-base equilibria in water and non-aqueous media. Tartu, 1998, 101 p.
10. **Jaan Leis.** Conformational dynamics and equilibria in amides. Tartu, 1998, 131 p.
11. **Toonika Rinken.** The modelling of amperometric biosensors based on oxidoreductases. Tartu, 2000, 108 p.
12. **Dmitri Panov.** Partially solvated Grignard reagents. Tartu, 2000, 64 p.
13. **Kaja Orupõld.** Treatment and analysis of phenolic wastewater with microorganisms. Tartu, 2000, 123 p.
14. **Jüri Ivask.** Ion Chromatographic determination of major anions and cations in polar ice core. Tartu, 2000, 85 p.
15. **Lauri Vares.** Stereoselective Synthesis of Tetrahydrofuran and Tetrahydropyran Derivatives by Use of Asymmetric Horner-Wadsworth-Emmons and Ring Closure Reactions. Tartu, 2000, 184 p.
16. **Martin Lepiku.** Kinetic aspects of dopamine D_2 receptor interactions with specific ligands. Tartu, 2000, 81 p.
17. **Katrin Sak.** Some aspects of ligand specificity of P2Y receptors. Tartu, 2000, 106 p.
18. **Vello Pällin.** The role of solvation in the formation of iotsitch complexes. Tartu, 2001, 95 p.
19. **Katrin Kollist.** Interactions between polycyclic aromatic compounds and humic substances. Tartu, 2001, 93 p.

20. **Ivar Koppel.** Quantum chemical study of acidity of strong and superstrong Brønsted acids. Tartu, 2001, 104 p.
21. **Viljar Pihl.** The study of the substituent and solvent effects on the acidity of OH and CH acids. Tartu, 2001, 132 p.
22. **Natalia Palm.** Specification of the minimum, sufficient and significant set of descriptors for general description of solvent effects. Tartu, 2001, 134 p.
23. **Sulev Sild.** QSPR/QSAR approaches for complex molecular systems. Tartu, 2001, 134 p.
24. **Ruslan Petrukhin.** Industrial applications of the quantitative structure-property relationships. Tartu, 2001, 162 p.
25. **Boris V. Rogovoy.** Synthesis of (benzotriazolyl)carboximidamides and their application in relations with *N*- and *S*-nucleophyles. Tartu, 2002, 84 p.
26. **Koit Herodes.** Solvent effects on UV-vis absorption spectra of some solvatochromic substances in binary solvent mixtures: the preferential solvation model. Tartu, 2002, 102 p.
27. **Anti Perkson.** Synthesis and characterisation of nanostructured carbon. Tartu, 2002, 152 p.
28. **Ivari Kaljurand.** Self-consistent acidity scales of neutral and cationic Brønsted acids in acetonitrile and tetrahydrofuran. Tartu, 2003, 108 p.
29. **Karmen Lust.** Adsorption of anions on bismuth single crystal electrodes. Tartu, 2003, 128 p.
30. **Mare Piirsalu.** Substituent, temperature and solvent effects on the alkaline hydrolysis of substituted phenyl and alkyl esters of benzoic acid. Tartu, 2003, 156 p.
31. **Meeri Sassian.** Reactions of partially solvated Grignard reagents. Tartu, 2003, 78 p.
32. **Tarmo Tamm.** Quantum chemical modelling of polypyrrole. Tartu, 2003. 100 p.
33. **Erik Teinemaa.** The environmental fate of the particulate matter and organic pollutants from an oil shale power plant. Tartu, 2003. 102 p.
34. **Jaana Tammiku-Taul.** Quantum chemical study of the properties of Grignard reagents. Tartu, 2003. 120 p.
35. **Andre Lomaka.** Biomedical applications of predictive computational chemistry. Tartu, 2003. 132 p.
36. **Kostyantyn Kirichenko.** Benzotriazole – Mediated Carbon–Carbon Bond Formation. Tartu, 2003. 132 p.
37. **Gunnar Nurk.** Adsorption kinetics of some organic compounds on bismuth single crystal electrodes. Tartu, 2003, 170 p.
38. **Mati Arulepp.** Electrochemical characteristics of porous carbon materials and electrical double layer capacitors. Tartu, 2003, 196 p.
39. **Dan Cornel Fara.** QSPR modeling of complexation and distribution of organic compounds. Tartu, 2004, 126 p.
40. **Riina Mahlapuu.** Signalling of galanin and amyloid precursor protein through adenylate cyclase. Tartu, 2004, 124 p.

41. **Mihkel Kerikmäe.** Some luminescent materials for dosimetric applications and physical research. Tartu, 2004, 143 p.
42. **Jaanus Kruusma.** Determination of some important trace metal ions in human blood. Tartu, 2004, 115 p.
43. **Urmas Johanson.** Investigations of the electrochemical properties of polypyrrole modified electrodes. Tartu, 2004, 91 p.
44. **Kaido Sillar.** Computational study of the acid sites in zeolite ZSM-5. Tartu, 2004, 80 p.
45. **Aldo Oras.** Kinetic aspects of dATPαS interaction with $P2Y_1$ receptor. Tartu, 2004, 75 p.
46. **Erik Mölder.** Measurement of the oxygen mass transfer through the air-water interface. Tartu, 2005, 73 p.
47. **Thomas Thomberg.** The kinetics of electroreduction of peroxodisulfate anion on cadmium (0001) single crystal electrode. Tartu, 2005, 95 p.
48. **Olavi Loog.** Aspects of condensations of carbonyl compounds and their imine analogues. Tartu, 2005, 83 p.
49. **Siim Salmar.** Effect of ultrasound on ester hydrolysis in aqueous ethanol. Tartu, 2006, 73 p.
50. **Ain Uustare.** Modulation of signal transduction of heptahelical receptors by other receptors and G proteins. Tartu, 2006, 121 p.
51. **Sergei Yurchenko.** Determination of some carcinogenic contaminants in food. Tartu, 2006, 143 p.
52. **Kaido Tämm.** QSPR modeling of some properties of organic compounds. Tartu, 2006, 67 p.
53. **Olga Tšubrik.** New methods in the synthesis of multisubstituted hydrazines. Tartu. 2006, 183 p.
54. **Lilli Sooväli.** Spectrophotometric measurements and their uncertainty in chemical analysis and dissociation constant measurements. Tartu, 2006, 125 p.
55. **Eve Koort.** Uncertainty estimation of potentiometrically measured ph and pK_a values. Tartu, 2006, 139 p.
56. **Sergei Kopanchuk.** Regulation of ligand binding to melanocortin receptor subtypes. Tartu, 2006, 119 p.
57. **Silvar Kallip.** Surface structure of some bismuth and antimony single crystal electrodes. Tartu, 2006, 107 p.
58. **Kristjan Saal.** Surface silanization and its application in biomolecule coupling. Tartu, 2006, 77 p.
59. **Tanel Tätte.** High viscosity $Sn(OBu)_4$ oligomeric concentrates and their applications in technology. Tartu, 2006, 91 p.
60. **Dimitar Atanasov Dobchev**. Robust QSAR methods for the prediction of properties from molecular structure. Tartu, 2006, 118 p.
61. **Hannes Hagu**. Impact of ultrasound on hydrophobic interactions in solutions. Tartu, 2007, 81 p.
62. **Rutha Jäger.** Electroreduction of peroxodisulfate anion on bismuth electrodes. Tartu, 2007, 142 p.

63. **Kaido Viht.** Immobilizable bisubstrate-analogue inhibitors of basophilic protein kinases: development and application in biosensors. Tartu, 2007, 88 p.
64. **Eva-Ingrid Rõõm.** Acid-base equilibria in nonpolar media. Tartu, 2007, 156 p.
65. **Sven Tamp.** DFT study of the cesium cation containing complexes relevant to the cesium cation binding by the humic acids. Tartu, 2007, 102 p.
66. **Jaak Nerut.** Electroreduction of hexacyanoferrate(III) anion on Cadmium (0001) single crystal electrode. Tartu, 2007, 180 p.
67. **Lauri Jalukse.** Measurement uncertainty estimation in amperometric dissolved oxygen concentration measurement. Tartu, 2007, 112 p.
68. **Aime Lust.** Charge state of dopants and ordered clusters formation in CaF_2:Mn and CaF_2:Eu luminophors. Tartu, 2007, 100 p.
69. **Iiris Kahn**. Quantitative Structure-Activity Relationships of environmentally relevant properties. Tartu, 2007, 98 p.
70. **Mari Reinik.** Nitrates, nitrites, N-nitrosamines and polycyclic aromatic hydrocarbons in food: analytical methods, occurrence and dietary intake. Tartu, 2007, 172 p.
71. **Heili Kasuk.** Thermodynamic parameters and adsorption kinetics of organic compounds forming the compact adsorption layer at Bi single crystal electrodes. Tartu, 2007, 212 p.
72. **Erki Enkvist.** Synthesis of adenosine-peptide conjugates for biological applications. Tartu, 2007, 114 p.
73. **Svetoslav Hristov Slavov**. Biomedical applications of the QSAR approach. Tartu, 2007, 146 p.
74. **Eneli Härk.** Electroreduction of complex cations on electrochemically polished Bi(*hkl*) single crystal electrodes. Tartu, 2008, 158 p.
75. **Priit Möller.** Electrochemical characteristics of some cathodes for medium temperature solid oxide fuel cells, synthesized by solid state reaction technique. Tartu, 2008, 90 p.
76. **Signe Viggor.** Impact of biochemical parameters of genetically different pseudomonads at the degradation of phenolic compounds. Tartu, 2008, 122 p.
77. **Ave Sarapuu.** Electrochemical reduction of oxygen on quinone-modified carbon electrodes and on thin films of platinum and gold. Tartu, 2008, 134 p.
78. **Agnes Kütt.** Studies of acid-base equilibria in non-aqueous media. Tartu, 2008, 198 p.
79. **Rouvim Kadis.** Evaluation of measurement uncertainty in analytical chemistry: related concepts and some points of misinterpretation. Tartu, 2008, 118 p.
80. **Valter Reedo.** Elaboration of IVB group metal oxide structures and their possible applications. Tartu, 2008, 98 p.
81. **Aleksei Kuznetsov.** Allosteric effects in reactions catalyzed by the cAMP-dependent protein kinase catalytic subunit. Tartu, 2009, 133 p.

82. **Aleksei Bredihhin.** Use of mono- and polyanions in the synthesis of multisubstituted hydrazine derivatives. Tartu, 2009, 105 p.
83. **Anu Ploom.** Quantitative structure-reactivity analysis in organosilicon chemistry. Tartu, 2009, 99 p.
84. **Argo Vonk.** Determination of adenosine A_{2A}- and dopamine D_1 receptor-specific modulation of adenylate cyclase activity in rat striatum. Tartu, 2009, 129 p.
85. **Indrek Kivi.** Synthesis and electrochemical characterization of porous cathode materials for intermediate temperature solid oxide fuel cells. Tartu, 2009, 177 p.
86. **Jaanus Eskusson.** Synthesis and characterisation of diamond-like carbon thin films prepared by pulsed laser deposition method. Tartu, 2009, 117 p.
87. **Marko Lätt.** Carbide derived microporous carbon and electrical double layer capacitors. Tartu, 2009, 107 p.
88. **Vladimir Stepanov.** Slow conformational changes in dopamine transporter interaction with its ligands. Tartu, 2009, 103 p.
89. **Aleksander Trummal.** Computational Study of Structural and Solvent Effects on Acidities of Some Brønsted Acids. Tartu, 2009, 103 p.
90. **Eerold Vellemäe.** Applications of mischmetal in organic synthesis. Tartu, 2009, 93 p.
91. **Sven Parkel.** Ligand binding to 5-HT_{1A} receptors and its regulation by Mg^{2+} and Mn^{2+}. Tartu, 2010, 99 p.
92. **Signe Vahur.** Expanding the possibilities of ATR-FT-IR spectroscopy in determination of inorganic pigments. Tartu, 2010, 184 p.
93. **Tavo Romann**. Preparation and surface modification of bismuth thin film, porous, and microelectrodes. Tartu, 2010, 155 p.
94. **Nadežda Aleksejeva.** Electrocatalytic reduction of oxygen on carbon nanotube-based nanocomposite materials. Tartu, 2010, 147 p.
95. **Marko Kullapere.** Electrochemical properties of glassy carbon, nickel and gold electrodes modified with aryl groups. Tartu, 2010, 233 p.
96. **Liis Siinor.** Adsorption kinetics of ions at Bi single crystal planes from aqueous electrolyte solutions and room-temperature ionic liquids. Tartu, 2010, 101 p.
97. **Angela Vaasa.** Development of fluorescence-based kinetic and binding assays for characterization of protein kinases and their inhibitors. Tartu 2010, 101 p.
98. **Indrek Tulp.** Multivariate analysis of chemical and biological properties. Tartu 2010, 105 p.
99. **Aare Selberg.** Evaluation of environmental quality in Northern Estonia by the analysis of leachate. Tartu 2010, 117 p.
100. **Darja Lavõgina.** Development of protein kinase inhibitors based on adenosine analogue-oligoarginine conjugates. Tartu 2010, 248 p.
101. **Laura Herm.** Biochemistry of dopamine D_2 receptors and its association with motivated behaviour. Tartu 2010, 156 p.

102. **Terje Raudsepp.** Influence of dopant anions on the electrochemical properties of polypyrrole films. Tartu 2010, 112 p.
103. **Margus Marandi.** Electroformation of Polypyrrole Films: *In-situ* AFM and STM Study. Tartu 2011, 116 p.
104. **Kairi Kivirand.** Diamine oxidase-based biosensors: construction and working principles. Tartu, 2011, 140 p.
105. **Anneli Kruve.** Matrix effects in liquid-chromatography electrospray mass-spectrometry. Tartu, 2011, 156 p.
106. **Gary Urb.** Assessment of environmental impact of oil shale fly ash from PF and CFB combustion. Tartu, 2011, 108 p.
107. **Nikita Oskolkov.** A novel strategy for peptide-mediated cellular delivery and induction of endosomal escape. Tartu, 2011, 106 p.
108. **Dana Martin.** The QSPR/QSAR approach for the prediction of properties of fullerene derivatives. Tartu, 2011, 98 p.
109. **Säde Viirlaid.** Novel glutathione analogues and their antioxidant activity. Tartu, 2011, 106 p.
110. **Ülis Sõukand.** Simultaneous adsorption of Cd^{2+}, Ni^{2+}, and Pb^{2+} on peat. Tartu, 2011, 124 p.
111. **Lauri Lipping.** The acidity of strong and superstrong Brønsted acids, an outreach for the "limits of growth": a quantum chemical study. Tartu, 2011, 124 p.
112. **Heisi Kurig.** Electrical double-layer capacitors based on ionic liquids as electrolytes. Tartu, 2011, 146 p.
113. **Marje Kasari.** Bisubstrate luminescent probes, optical sensors and affinity adsorbents for measurement of active protein kinases in biological samples. Tartu, 2012, 126 p.
114. **Kalev Takkis.** Virtual screening of chemical databases for bioactive molecules. Tartu, 2012, 122 p.
115. **Ksenija Kisseljova**. Synthesis of aza-β^3-amino acid containing peptides and kinetic study of their phosphorylation by protein kinase A. Tartu, 2012, 104 p.
116. **Riin Rebane.** Advanced method development strategy for derivatization LC/ESI/MS. Tartu, 2012, 184 p.
117. **Vladislav Ivaništšev.** Double layer structure and adsorption kinetics of ions at metal electrodes in room temperature ionic liquids. Tartu, 2012, 128 p.
118. **Irja Helm.** High accuracy gravimetric Winkler method for determination of dissolved oxygen. Tartu, 2012, 139 p.
119. **Karin Kipper.** Fluoroalcohols as Components of LC-ESI-MS Eluents: Usage and Applications. Tartu, 2012, 164 p.
120. **Arno Ratas.** Energy storage and transfer in dosimetric luminescent materials. Tartu, 2012, 163 p.
121. **Reet Reinart-Okugbeni**. Assay systems for characterisation of subtype-selective binding and functional activity of ligands on dopamine receptors. Tartu, 2012, 159 p.

122. **Lauri Sikk.** Computational study of the Sonogashira cross-coupling reaction. Tartu, 2012, 81 p.
123. **Karita Raudkivi.** Neurochemical studies on inter-individual differences in affect-related behaviour of the laboratory rat. Tartu, 2012, 161 p.
124. **Indrek Saar.** Design of GalR2 subtype specific ligands: their role in depression-like behavior and feeding regulation. Tartu, 2013, 126 p.
125. **Ann Laheäär.** Electrochemical characterization of alkali metal salt based non-aqueous electrolytes for supercapacitors. Tartu, 2013, 127 p.
126. **Kerli Tõnurist.** Influence of electrospun separator materials properties on electrochemical performance of electrical double-layer capacitors. Tartu, 2013, 147 p.
127. **Kaija Põhako-Esko.** Novel organic and inorganic ionogels: preparation and characterization. Tartu, 2013, 124 p.
128. **Ivar Kruusenberg.** Electroreduction of oxygen on carbon nanomaterial-based catalysts. Tartu, 2013, 191 p.
129. **Sander Piiskop.** Kinetic effects of ultrasound in aqueous acetonitrile solutions. Tartu, 2013, 95 p.
130. **Ilona Faustova**. Regulatory role of L-type pyruvate kinase N-terminal domain. Tartu, 2013, 109 p.
131. **Kadi Tamm.** Synthesis and characterization of the micro-mesoporous anode materials and testing of the medium temperature solid oxide fuel cell single cells. Tartu, 2013, 138 p.
132. **Iva Bozhidarova Stoyanova-Slavova.** Validation of QSAR/QSPR for regulatory purposes. Tartu, 2013, 109 p.
133. **Vitali Grozovski**. Adsorption of organic molecules at single crystal electrodes studied by *in situ* STM method. Tartu, 2014, 146 p.
134. **Santa Veikšina**. Development of assay systems for characterisation of ligand binding properties to melanocortin 4 receptors. Tartu, 2014, 151 p.
135. **Jüri Liiv.** PVDF (polyvinylidene difluoride) as material for active element of twisting-ball displays. Tartu, 2014, 111 p.
136. **Kersti Vaarmets.** Electrochemical and physical characterization of pristine and activated molybdenum carbide-derived carbon electrodes for the oxygen electroreduction reaction. Tartu, 2014, 131 p.
137. **Lauri Tõntson**. Regulation of G-protein subtypes by receptors, guanine nucleotides and Mn^{2+}. Tartu, 2014, 105 p.
138. **Aiko Adamson.** Properties of amine-boranes and phosphorus analogues in the gas phase. Tartu, 2014, 78 p.
139. **Elo Kibena**. Electrochemical grafting of glassy carbon, gold, highly oriented pyrolytic graphite and chemical vapour deposition-grown graphene electrodes by diazonium reduction method. Tartu, 2014, 184 p.
140. **Teemu Näykki.** Novel Tools for Water Quality Monitoring – From Field to Laboratory. Tartu, 2014, 202 p.
141. **Karl Kaupmees.** Acidity and basicity in non-aqueous media: importance of solvent properties and purity. Tartu, 2014, 128 p.

142. **Oleg Lebedev**. Hydrazine polyanions: different strategies in the synthesis of heterocycles. Tartu, 2015, 118 p.
143. **Geven Piir.** Environmental risk assessment of chemicals using QSAR methods. Tartu, 2015, 123 p.
144. **Olga Mazina.** Development and application of the biosensor assay for measurements of cyclic adenosine monophosphate in studies of G protein-coupled receptor signalinga. Tartu, 2015, 116 p.
145. **Sandip Ashokrao Kadam.** Anion receptors: synthesis and accurate binding measurements. Tartu, 2015, 116 p.
146. **Indrek Tallo.** Synthesis and characterization of new micro-mesoporous carbide derived carbon materials for high energy and power density electrical double layer capacitors. Tartu, 2015, 148 p.
147. **Heiki Erikson.** Electrochemical reduction of oxygen on nanostructured palladium and gold catalysts. Tartu, 2015, 204 p.
148. **Erik Anderson.** *In situ* Scanning Tunnelling Microscopy studies of the interfacial structure between Bi(111) electrode and a room temperature ionic liquid. Tartu, 2015, 118 p.
149. **Girinath G. Pillai.** Computational Modelling of Diverse Chemical, Biochemical and Biomedical Properties. Tartu, 2015, 140 p.
150. **Piret Pikma.** Interfacial structure and adsorption of organic compounds at Cd(0001) and Sb(111) electrodes from ionic liquid and aqueous electrolytes: an *in situ* STM study. Tartu, 2015, 126 p.
151. **Ganesh babu Manoharan.** Combining chemical and genetic approaches for photoluminescence assays of protein kinases. Tartu, 2016, 126 p.
152. **Carolin Siimenson**. Electrochemical characterization of halide ion adsorption from liquid mixtures at Bi(111) and pyrolytic graphite electrode surface. Tartu, 2016, 110 p.
153. **Asko Laaniste.** Comparison and optimisation of novel mass spectrometry ionisation sources. Tartu, 2016, 156 p.
154. **Hanno Evard.** Estimating limit of detection for mass spectrometric analysis methods. Tartu, 2016, 224 p.
155. **Kadri Ligi.** Characterization and application of protein kinase-responsive organic probes with triplet-singlet energy transfer. Tartu, 2016, 122 p.
156. **Margarita Kagan.** Biosensing penicillins' residues in milk flows. Tartu, 2016, 130 p.
157. **Marie Kriisa.** Development of protein kinase-responsive photoluminescent probes and cellular regulators of protein phosphorylation. Tartu, 2016, 106 p.
158. **Mihkel Vestli.** Ultrasonic spray pyrolysis deposited electrolyte layers for intermediate temperature solid oxide fuel cells. Tartu, 2016, 156 p.
159. **Silver Sepp**. Influence of porosity of the carbide-derived carbon on the properties of the composite electrocatalysts and characteristics of polymer electrolyte fuel cells. Tartu, 2016, 137p.
160. **Kristjan Haav**. Quantitative relative equilibrium constant measurements in supramolecular chemistry. Tartu, 2017, 158 p.

161. **Anu Teearu**. Development of MALDI-FT-ICR-MS methodology for the analysis of resinous materials. Tartu, 2017, 205 p.
162. **Taavi Ivan**. Bifunctional inhibitors and photoluminescent probes for studies on protein complexes. Tartu, 2017, 140 p.
163. **Maarja-Liisa Oldekop**. Characterization of amino acid derivatization reagents for LC-MS analysis. Tartu, 2017, 147 p.
164. **Kristel Jukk**. Electrochemical reduction of oxygen on platinum- and palladium-based nanocatalysts. Tartu, 2017, 250 p.
165. **Siim Kukk**. Kinetic aspects of interaction between dopamine transporter and *N*-substituted nortropane derivatives. Tartu, 2017, 107 p.
166. **Birgit Viira**. Design and modelling in early drug development in targeting HIV-1 reverse transcriptase and Malaria. Tartu, 2017, 172 p.
167. **Rait Kivi**. Allostery in cAMP dependent protein kinase catalytic subunit. Tartu, 2017, 115 p.
168. **Agnes Heering**. Experimental realization and applications of the unified acidity scale. Tartu, 2017, 123 p.
169. **Delia Juronen**. Biosensing system for the rapid multiplex detection of mastitis-causing pathogens in milk. Tartu, 2018, 85 p.